Universidade Federal de Minas Gerais
Engineering School
Department of Sanitary and Environmental Engineering
Postgraduate Program in Sanitation, Environment and Water Resources.

APPLICATION OF MEMBRANE SEPARATION PROCESSES ON THE TREATMENT OF TEXTILE EFFLUENT FOR WATER AND DYE REUSE

Carolina Fonseca Couto

Belo Horizonte

2016

APPLICATION OF MEMBRANE SEPARATION PROCESSES ON THE TREATMENT OF TEXTILE EFFLUENT FOR WATER AND DYE REUSE

Carolina Fonseca Couto

Carolina Fonseca Couto

APPLICATION OF MEMBRANES SEPARATION PROCESSES ON THE TREATMENT OF TEXTILE EFFLUENT FOR WATER AND DYE REUSE

Dissertation presented to the Postgraduate Program in Sanitation, Environment and Water Resources of Federal University of Minas Gerais as a partial requirement to obtain the title of Master in Sanitation, Environment and Water Resources.

Concentration area: Environmental Studies

Research Line: Characterization, prevention and control of pollution

Supervisor: D. Sc. Míriam Cristina Santos Amaral Moravia

Belo Horizonte
Escola de Engenharia da UFMG

2016

Carolina Fonseca Couto

APPLICATION OF MEMBRANES SEPARATION PROCESSES ON THE TREATMENT OF TEXTILE EFFLUENT FOR WATER AND DYE REUSE

Dissertação apresentada ao Programa de Pós-graduação em Saneamento, Meio Ambiente e Recursos Hídricos da Universidade Federal de Minas Gerais, como requisito parcial à obtenção do título de Mestre em Saneamento, Meio Ambiente e Recursos Hídricos.

Área de concentração: Meio Ambiente

Linha de pesquisa: Caracterização, prevenção e controle da poluição

Orientador: D. Sc. Míriam Cristina Santos Amaral Moravia

Belo Horizonte

Escola de Engenharia da UFMG

2016

C871a

Couto, Carolina Fonseca.
Application of membrane separation processes on the treatment of textile effluent for water and dye reuse [manuscrito] / Carolina Fonseca Couto.- 2016.
xiv, 104 f, enc.: il.

Orientadora: Míriam Cristina Santos Amaral Moravia.

Mestrado (dissertação) - Universidade Federal de Minas Gerais, Escola de Engenharia.

Inclui bibliografia.

1. Engenharia sanitária - Teses. 2. Meio ambiente - Teses. 3. Biorreatores - Teses. 4. Indústria têxtil - Teses. 5. Água - Reutilização - Teses. I. Moravia, Míriam Cristina Santos Amaral. II. Universidade Federal de Minas Gerais. Escola de Engenharia. III. Título.

CDU: 628(043)

Página com as assinaturas dos membros da banca examinadora, fornecida pelo Colegiado do Programa

AGRADECIMENTOS

First of all, I would like to express my gratitude to God, the one who gives us the opportunity of life, of being someone better and empowers us in all work.

Over the past year and a half I have received support and encouragement from a great number of people who was by my side encouraging me to keep going.

I would like to thank my parents, José and Josinalva, my sister, Luiza, for their constant support, patience, for believing in me and encouraging me to follow my dreams, filled with love and strong dedication, for being my number 1 fans. Also, I would like to thank my little ones, Morgana, Melão and Minduim, for keeping me sane, and making me smile in the bad days.

I would like express my infinite gratitude to Miriam, my supervisor, for her dedication, patience, availability and, specially, trust, for accepting me, for opening many opportunities; for teaching me and showing me the way, and for frequently encouraging me in a special way, making me believe in my potential.

I would like to thank my relatives, in special, my grandmother, aunt Lúcia, Dinda, uncle Nando, aunt Socorro, Dulce, Aurinha, who helped countless time, supporting me in a foreign state.

In memorium, I would like to express my gratitude to Grandmother Anita and my grandfathers João and Gracindo. This work is dedicated to them.

I thank Vinícius and his family that welcomed me with wide open arms and hearts. Thank you, so so much!

For their collaboration, support and encouragement, I would like to thank DESA professors.

For his collaboration, I would like to thank professor Arne Verliefde.

I would like to thank Larissa, Janine and Andreza for helping me with all the tests I did, for contributing so much with this work. Without you, I wouldn't be able to do accomplish so much in such a short time.

I would like to thank all my co-workers from the 4544 and 4542 lab, who always helped me in the doing little favours that made a huge difference. In special, I would like to thank Priscila, Rose and Tati. I found in them a friendship for life.

I thank my friend Bárbara for helping me countless times, Lucilaine and Mirna who has always been available to help me, sharing her knowledge and support.

I thank the Department of Chemistry Cefet-MG, especially Professor Luzia Sergina, by infrared spectrophotometric analysis.

I thank the textile industry Tear Textil, by providing the effluent.

I thank CAPES, for the scholarship granted. CNPq for the financing the project "Beneficiamento do efluente do tingimento empregando processos de separação por membranas: recuperação do índigo blue e geração de água de reuso" and FAPEMIG for always fouding the many researchers developed by the group.

I thank my postgraduate classmates and GEAPS coworkers, who have always been at my side.

Finally, thanks to my relatives, friends and all who were not mentioned here but have contributed to the fulfillment of this project.

ABSTRACT

Textile industry consumes large amount of water as well as dyes and various processing chemicals during the many stages of textile processing generating substantial quantity of wastewater potentially polluting. Thus, in this context, this work aims to investigate the application of a membrane separation process applied to the treatment of textile effluent containing indigo blue, in order to generate industrial water as well as promote dye reuse. Two treatment routs was assessed. The first one consisted in microfiltration (MF), followed by membrane bioreactor (MBR) and then nanofiltration (NF). The second rout was MF followed by NF. Raw textile effluent is not biodegradable due to dye chemical complexity, however MF permeate is much more biodegradable since the molecules weight are much smaller, being readily assimilated by the microorganisms. The indigo blue dye was efficiently retained by the MF membrane (100%), which allows its recovery from the concentrate stream. The MBR resulted in COD and ammonia removal of 73% and 100%, respectively. This process already enables the water in a few textile processes, such as, floor and equipment washing. However, it is still needed a polishing step to apply this water in more noble using. NF technology was successfully applied to polish textile effluent. The best NF filtration performances were provided under a pressure of 12 bar and a cross-flow velocity of 0.63 cm s^{-1} for both studied treatment routs. The NF performance, in terms of COD, conductivity, colour, nitrogen removal was not influenced by pH; however, higher pH values of the NF feed resulted in increased membrane fouling. High temperature and pH also reduces the NF rejection even the worst case evaluated (37.5 ºC and pH 11), NF90 is still able to attend the manufactory quality requirement. The principal cause of flux decline was determined to be concentration polarization in all studied cases, but chemical cleaning of the membrane was sufficient to regain the initial permeability. The maximum water recovery rate obtained for a single MF-NF step in the treatment of microfiltered textile effluent is 40% resulting in a total capital cost (CapEx) of the MF-NF treatment system estimated at US$ 58,362.50, and the total operational cost (OpEx) was 0.31 US$/$m^3$ of effluent. Since both studied routs showed similar results, the MF-NF hybred system was chosen considering area requirements, energy and equipment consumption, as well as system complexity. The NF permeate meets the quality requirements for all processes within the textile industry, while the NF concentrate can be used to wash equipment, screens in the printworks, print paste containers, and floors.

RESUMO

A indústria têxtil consome grandes quantidades de água, bem como corantes e produtos químicos auxiliares durante os vários estágios de processamento têxtil, gerando quantidade substancial de efluentes potencialmente poluidores. Assim, neste contexto, este trabalho destina-se a investigar a aplicação de processos de separação por membranas aplicadas ao tratamento de efluentes têxteis contendo azul índigo, a fim de gerar água de reuso industrial, assim como promover a reutilização do corante. Duas rotas tratamento foram avaliadas. A primeira consistiu em microfiltração (MF), seguido por biorreator com membrana (MBR) e, em seguida, nanofiltração (NF). A segunda rota foi MF seguido de NF. O efluente bruto não é biodegradável devido à complexidade química do corante, no entanto, o permeado da MF apresenta ser biodegradável. O corante índigo blue foi eficientemente retido pela membrana de MF (100%), o que permite a sua recuperação a partir da corrente de concentrado. O BRM promoveu a remoção de COD e de amônia de 73% e 100%, respectivamente. Este processo já permite a aplicação do seu permeado em alguns processos têxteis, tais como, lavagem de piso e equipamentos. No entanto, ainda é necessária uma etapa de polimento para possibilitar a aplicação da água em usos de mais nobres. A NF foi aplicada com sucesso para este fim. Os melhores desempenhos da NF foram obtidos sob uma pressão de 12 bar e uma velocidade de escoamento de 0,63 cm s^{-1}. O desempenho da NF em termos de COD, condutividade, cor, remoção de nitrogênio não foi influenciada pelo pH; No entanto, os valores de pH da alimentação mais elevados resultou num aumento da incrustação da membrana. Alta temperatura e pH reduz a rejeição do processo. Mesmo o pior caso avaliado, NF90 ainda é capaz de atender a exigência de qualidade de água da indústria. A principal causa da redução de fluxo foi atribuída à concentração de polarização. A limpeza química da membrana foi suficiente para recuperar a permeabilidade inicial. A taxa máxima de recuperação de água obtida por um único passo MF-NF no tratamento de efluente têxtil foi de 40%, resultando em um custo de capital total (CapEx) do sistema de tratamento MF-NF estimado em US$ 58.362,50, e o custo operacional total (OpEx) foi de 0,31 US$/$m^3$ de efluentes. Uma vez que ambas as rotas estudadas apresentaram resultados semelhantes, o sistema híbrido MF-NF foi escolhido considerando requisitos de área, consumo de energia e equipamentos, bem como a complexidade do sistema. NF atende aos requisitos de qualidade para todos os processos dentro da indústria têxtil, enquanto o concentrado da NF pode ser aplicado a usos mais grosseiros.

SUMMARY

LIST OF FIGURES

LIST OF TABLES

LIST OF SYMBOLS AND ABREVIATIONS

A	Filtration area
ATR-FTIR	Fourier transform coupled total attenuated reflectance system
CP	Concentration polarization
COD	Chemical oxygen demand
Cr	Chrome
Cu	Copper
D_h	Cell hydraulic diameter
D_i	Diffusion coefficient
EC	Electrical conductivity
EDX	Energy dispersive X-ray spectroscopy
F_{df}	flux decline due to fouling
Fe	Iron
R_{cc}	hydraulic resistance after chemical cleaning
R_f	Hydraulic resistance of the fouling layer
R_{fr}	Reversible fouling layer
R_{fir}	Irreversible fouling layer
J_{sd}	Effluent flux
J_w	Water flux
MBR	Membrane bioreactor
MF	Microfiltration
Mn	Manganese
MWCO	Molecular weight cut-off
NF	Nanofiltration

Q	feed flow rate
Re	Reynolds number
r_{int}	logarithmic mean radius difference
R	Rejection
R_m	Hydraulic resistance of the membrane
SEC	Specific energy consumption
SEM	Scanning electron microscopy
S_c	Schmidt number
S_h	Sherwood number
TMP	Transmembrane pressure
UF	Ultrafiltration
TS	Total solids
TVS	Total volatile solids
TDS	Total dissolved solids
T_{fd}	Total flux decline
WP	Water permeability
$\Delta\Pi$	Trans-membrane osmotic pressure difference
μ_w	Water viscosity

1. INTRODUCTION

1.1. Contextualization and problem

The textile industry is one of the longest industrial chains in the manufacturing industry, being directly intertwined with many sectors, such as the agricultural sector when it needs inputs in the form of natural fibres and a few types of dyes as well as with the chemical industry when it comes to the wide range of man-made fibres and auxiliary chemicals used in the dyeing processes. It is a very diverse and heterogeneous industry, with its products being used by virtually everybody – private households and businesses alike. Thus, textile industry is expected to grow along with the population growth, being characterized by being one of the largest industries in the world (VALH, *et al.*, 2011).

Denim is one of the most popular types of fabric used by men and women of all ages and social classes. Much of its popularity is mainly due to the attractiveness of its blue colour and the finishing effects that develop when the fabric is laundered repeatedly. Thus, this kind of production deserves attention by its production, environmental and economic impact.

The application of indigo as colouring matter for textile materials can be observed in several fabrics dated to ancient times when only natural stuff, such as plants and animal derivatives were the known sources of dyes. It can be traced back to 2400BC, where fine indigo dyed borders were used and it was found in the Egyptian tombs (PAUL, 2015).

The textile chains, specifically the ones that produce denim using indigo blue, starts with the production or harvest of raw fibre, followed by the dyeing process, the fabric production, and then, the final product is made. Fibres can be classified in two main categories: man-made and natural such as cotton. The basic chain production is schematically represented in Figure 1.

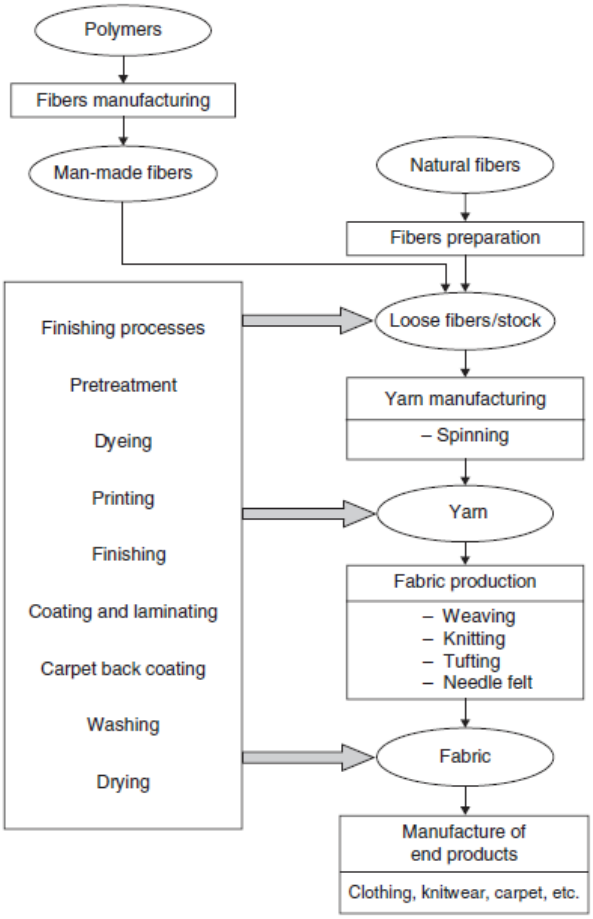

Figure 1: Schematically draw of the basic chain production (Source: VALH, et al., 2011)

Fibre pre-treatment has to guarantee the removal of any other material other than the fibres in order to improve the uniformity and affinity with dye stuffs as well as finishing treatments. Then a process of stock is taken place in order to open the fibre and help the following steps, thus the fibre will look more evenly. The yarn manufacturing is basically the production of yarn, which is taken in several steps in order to thickening the yarn and making it more resistant. Then, either it is preceded to the fabric production or the dyeing process, depending on the type of fabric and dye which is intended to be made. For denim fabrics, the dyeing process is taken before the fabric production.

Dyeing processes is taken in a multi dip/nip padding technique with intermediate air oxidation (CHAKRABORTY, 2010). Indigo blue does not have natural affinity with cotton, thus, it needs to be reduced to its soluble form (leuco form), to develop a chemical affinity with the cellulose fiber. To occur indigo blue reduction, the dye bath happens in alkaline solutions (pH ranging from 10.5-11.5) using a strong reducing agent, such as sodium dithionite (SHAW *et al.*, 2002). The dye penetrates and adheres into the pores of the cotton fibre when it is immersed in the dyeing bath; after the fibre is exposed to air, the indigo is oxidized to its

insoluble form and getting stuck definitely between the fibres of the fabric (PASCHOAL, 2005; SULLINS *et al.*, 1978). Industries usually have separate units destined for dyeing with indigo that combines sizing-precise pre-treatment-cum-wrap dyeing section. The colouring method chosen (Slasher, Rope and Loop) is followed by dyeing of the cotton, after that, white cotton is interlaced with dyed cotton to produce fabric with blue front and white background.

Textile industries are an intensive water consumer. Water is mainly used in dyeing process and other minor usages around the industry facility, such as equipment and floor washing. According to Valh *et al.* (2011), processes using water are desizing, scouring or kiering, bleaching, mercerizing, dyeing, washing, neutralization, and salt bath. The consumption of water ranges about 281-784 l kg^{-1} of cotton, where the dyeing processes can consume 8-300 l kg^{-1} of cotton, depending on the kind of dye (CORREIA *et al.*, 1994).

Textile industries not only need plenty of available water but also with a high quality in order to meet the dyeing criteria. However it has been reported that no guidelines for process water quality in the textile finishing industry exist (BRUGGEN *et al.*, 2004). Therefore, requirements for the processes which ones involve the usage of water in the textile industry will mainly depend on individual companies standards and applied techniques. However a few authors point some requirements, for instance, chemical oxygen demand (COD) the maximum recommended level is 200 mg L^{-1}, no visible colour, total hardness of 100 ppm $CaCO_3$ and a neutral pH (VALH *et al.*, 2011). Also, textile industries not only consume large volumes of water but lots of chemicals (ROBINSON *et al.*, 2001).

Textile industry is considered as one of the most polluting industries. Many different processes in fabric manufacturing use water and generate substantial quantities of wastewater, mostly consisting of spent or unutilized resources (DASGUPTA *et al.*, 2015). The amount and the composition of wastewater vary and depend on different factors, such as the nature of the processed fabric, applied dye, or special finishing. A few authors affirm that this amount ranges about 21 to 377 m^3 of wastewater per ton of produced product (BUSCIO *et al.*, 2015).

The wastewater originated from the textile industry is usually rich in colour, chemical oxygen demand (COD), complex chemicals, inorganic salts, total dissolved solids (TDS), pH ranging from acid to basic, high temperature, turbidity and salinity (VERMA *et al.*, 2012). Dyes are considered as the most peremptory source of contamination due to their high molecular weight, complex structures and show very low biodegradability (KIM *et al.*, 2004). The

presence of dye even at a very low concentration is highly visible and harmful to aquatic life (CHEN *et al.*, 2015).

The most applied treatment technique to this kind of effluent is activated sludge, and, although it provides good COD removal, it has low efficiency in salt removal and discolouration due to chemical stability and resistance to microbiological attack of the dyes (BUSCIO *et al.*, 2015). It would be necessary large areas and a residence time to promote the decolourization-fermentation process (ROBINSON *et al.*, 2001).

Coagulation/flocculation, although it is possible to meet the discharging requirements, it not only generates large amounts of sludge that need further treatment which increases the treatment costs, but also can be a source of secondary pollutants due to the generation of by-products (BUSCIO *et al.*, 2015; DASGUPTA *et al.*, 2015). Also, fluctuations compounds concentrations can compromise the efficiency of these conventional processes (AOUNI *et al.*, 2012). Adsorptive processes have similar drawbacks as the coagulation/flocculation processes. Disposal of the spent adsorbents is costly, associated with fast reduction of the efficiency and difficulty in regeneration of spent adsorbent make this process not so attractive (ROBINSON *et al.*, 2001). Advantage oxidation processes, such as, ozonation can be quite costly making this process not economically viable and may produce toxic by-products (ONG *et al.*, 2014).

Despite the growing need for preservation of water resources because of environmental, financial and public health issues, it is known of only a few studies about the assessment of the recovery and reuse of water used in the textile industry and the dye in question. The reuse of textile wastewater and its chemical auxiliary spent in the throughout the many process existent in the fabric manufacturing are quite a challenge. The already stated drawbacks can be satisfactory overcome using membrane based technology, which includes microfiltration, ultrafiltration, nanofiltration, reverse osmosis or a combination of two or more of these processes.

It is also possible to highlight the good performances in textile wastewater treatment using membrane allowing high removal of colour, COD and ions, besides the possibility to produce recycled water and provide recovery of the dye, reflecting an increase in business profit and preservation of water resources (AOUNI *et al.*, 2012, CHEN *et al.*, 2015, GOZÁLVEZ-ZAFILLA *et al.*, 2008).

Furthermore, the start-up cost with implementation of the process is offset by the express saved in terms of water consumption and reuse of the recovered salts and dye (KURT *et al.*, 2012; TANG & CHEN, 2002). The short payback period associated with this type of technology make membrane treatment based process more attractive and cost efficient than others treatment (DASGUPTA *et al.*, 2015).

Microfiltration and membrane bioreactor are mostly applied as a pre-treatment to hybrid systems in order to reduce fouling and membrane deterioration in nanofiltration (NF) and reverse osmoses (RO) as well as concentrate the target dye to promote reuse (BUSCIO *et al.*, 2015).

Since 1980, many studies have been studying the use of NF in the treatment of the textile effluent *(*AMAR *et al.*, 2012), some have already dealt with the reuse of the products process: water (Chen *et al.*, 2015) and dye (BUSCIO *et al.*, 2015), however, studies are still needed focusing on the wastewater originated from dyeing baths of textile industries containing indigo in order to improve the treatment efficiency of nanofiltration process in terms of reducing membrane fooling and energy requirements.

1.2. Justification

The Brazilian textile industry, one of the oldest sectors installed in Brazil, is passing through a hard time due to economic pressure, in terms of high taxes and the strong Chinese competition, taking the space where once was occupied by the Brazilians products, reducing considerably the industry income and therefore turning a thriving industry into an obsolete industrial park.

All these factors combined together, associated with the water crisis and thus, an increase on the environmental pressure, press the textile industry to taking a new environmental approach in terms of reducing water consumption and a more environmentally friendly waste handling, considering the high pollution potential associated to textile effluents.

Membrane separation processes (MSP) come into this scenario in order to provide a more efficient effluent treatment. Membranes allow the potential to reuse water and dye reuse from the wastewater, reducing economic losses in the dyeing processes, as well as reducing the costs with waste treatment and water acquisition. This could help this industrial sector in

regaining economic credibility and commercial space. In a global view, it also helps the Brazilian economy in helping a needing sector.

However, to achieve this all, a good understanding of membrane-foulant interaction mechanisms is necessary in order to reduce fouling and flux decline problems, known as the main draw backs of industrial membrane application.

So, more studies on this subject are essential to provide the necessary knowledge about all the interactions between the foulants in the effluents and the membrane surface. Chemicals occurring in this wastewater range from dies to auxiliary chemicals, occurring in different concentrations, and thus an extended study is required in order to cover all the large problems that may appear.

1.3. Objectives

1.3.1. General

This study aims to investigate the application of membrane separation processes on the treatment of industrial textile wastewater containing indigo blue in order to achieve industrial water reuse and the recovery of the dye of effluent from the dyeing stage.

1.3.2. Specifics

- Evaluate the effect of pressure and pH on the MF performance and their effect in concentrating indigo blue;
- Evaluate the performance of MBR to remove organic matter and nutrients from textile effluent after MF;
- Evaluate the effect of pressure, pH and cross flow velocities, on the NF performance when used MBR permeate;
- Evaluate the effect of pressure, pH, cross flow velocities, temperature and indigo concentration in the effluent on the NF performance when used MF permeate.

1.4. Structural form

Besides this introduction (Chapter 1) and the final considerations (Chapter 5), this dissertation is structured in three chapters in an article format. The choice of an article format indicates that the chapters are interdependent and can be read separately. Each specific objective relates to one chapter. Chapter 2, which relates to the first and second specific objectives, assess the

performance of the microfiltration in the clarification of the raw textile wastewater and the possibility of indigo concentration and reuse, in order to come back to the dyeing process and the performance of submerged membrane bioreactor (MBR), in treating MF permeate, in terms of nutrients and organic matter removal and fouling investigation in conditions of shock load. Chapter 3, attending the third specific objective, assess the first treatment route, which consists in microfiltration, followed by MBR and finally followed by NF (Figure 2). It was assessed the effect of pressure, pH and cross flow velocities in the effluent on the NF performance, in order to achieve water reuse in the dyeing process, as well as investigate flux decline, membrane fouling and its causes. Chapter 4 attends the fourth specific objective, addressing the second treatment route, which consists in microfiltration, followed by NF (Figure 2). It aims to assess the some parameters, such as the ones from the chapter 3 plus temperature and indigo concentration in the feed effluent as well as incorporating an economic viability study.

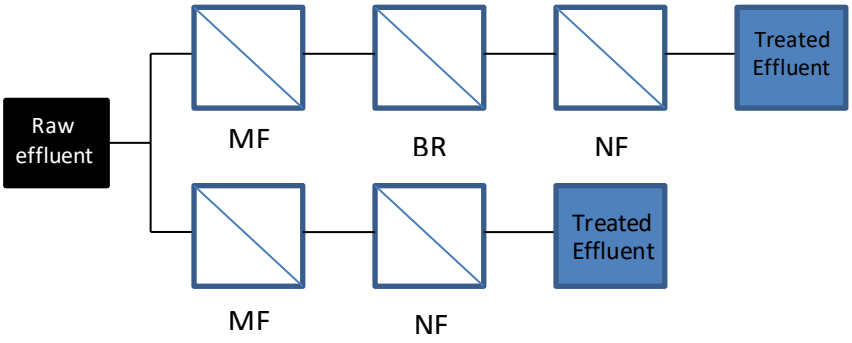

Figure 2 - Schematic draw of the treatment routs

1.5. References

AMAR, N. B. KECHAOU, N.; PALMERI, J.; DERATANI, A.; SGHAIER, A. Comparison of tertiary treatment by nanofiltration and reverse osmosis for water reuse in denim textile industry. *Journal of Hazardous Materials*, v. 170, p. 111–117, 2009.

AOUNI, A.; FERSI, C; CUARTAS-URIBE, B; BES-PÍA, A.; ALCAINA-MIRANDA, M. I.; DHAHBI, M. Reactive dyes rejection and textile effluent treatment study using ultrafiltration and nanofiltration processes. *Desalinization*, v. 297, p. 87-96, 2012.

BUSCIO, V.; MARÍN, M. J.; CRESPI, M.; GUTIÉRREZ-BOUZÁN, C.. Reuse of textile wastewater after homogenization–decantation treatment coupled to PVDF ultrafiltration membranes. *Chemical Engineering Journal*, v. 265,p. 122–128, 2015.

CHAKRABORTY, J. N. *Fundamentals and practices in colouration of textiles*. 1. ed. India: Woodhead Publishing, 2009. 400p.

CHEN, V.; YANGA, Y.; ZHOUA, M.;LIUA, M.; YUA,S.; GAOL, G. Comparative study on the treatment of raw and biological treated textile effluents through submerged nanofiltration. *Journal of Environmental Management*, v. 284, p. 121-129, 2015.

Correia VM, Stephenson T, and Judd SJ. Characterisation of textile wastewaters – a review. *Environmental Technology*, v. 15, p. 917 - 929, 1994.

DASGUPTA, J.; SIKDER, J.; CHAKRABORTY, S.; CURCIO, S.; DRIOLI, E. Remediation of textile effluents by membrane based treatment techniques: A state of the art review. *Journal of Environmental Management*, v. 147, p. 55-72, 2015.

GOZÁLVEZ-ZAFRILLA, J. M.; SANZ-ESCRIBANO, D.; LORA-GARCÍA, J.; LEÓN HIDALGO; M. C. Nanofiltration of secondary effluent for wastewater reuse in the textile industry. *Desalination*, v. 222, p. 272–279, 2008.

KIM, T.; PARK, C.; YANG, J.; KIM, S. Comparison of disperse and reactive dye removals by chemical coagulation and Fenton oxidation. *Journal of Hazardous Materials*, v. B112 p. 95–103, 2004.

KURT, E.; KOSEOGLU-IMER, D. Y.; DIZGE, N.; CHELLAM, S. ; KOYUNCU, I. Pilot-scale evaluation of nanofiltration and reverse osmosis for process reuse of segregated textile dyewash wastewater. *Desalination*, v. 302, p. 24–32, 2012.

ONG, Y. K.; LI, F. L.; SUN, S.; ZHAO, B.; LIANG, C.; CHUNG, T. Nanofiltration hollow fiber membranes for textile wastewater treatment: Lab-scale and pilot-scale studies. *Chemical Engineering Science*, v. 114, p. 51–57, 2014.

PASCHOAL, F. M. M.; TREMILIOSI-FILHO, G. Aplicação da tecnologia de eletrofloculação na recuperação do corante índigo blue a partir de efluentes industriais. *Quími. Nova*, v. 28, p. 766-772, 2005.

ROBINSON, T.; MCMULLAN, G.; MARCHANT, R.; NIGAM, P. Remediation of dyes in textile effluent: a critical review on current treatment technologies with a proposed alternative. *Bioresource Technology*, v. 77, p. 247-255, 2001.

SHAW, C. B.; CARLIELL, C. M.; WHEATLEY, A. D. Anaerobic/aerobic treatment of colored textile effluents using sequencing batch reactors. *Water Res.*, v. 36, p. 1993-2001, 2002.

SULLINS, J. K.; KINGSPORT, T. Method of recovering oxidized dye from dye wash water. *United States Patent*. Nº 4.092.105, 1978.

VALH, J. V.; MARECHAL, A. M. L.; VAJNHANDL, S.; JERIC, T.; SIMON, E. *Treatise on Water Science:* Volume 4: Water-Quality Engineering. 1. ed. Slovenia: Elsevier, 2011. 22p.

VERMA, A.K.; DASH, R.R.; BHUNIA, P. A review on chemical coagulation/flocculation technologies for removal of colour from textile wastewaters. *Journal of Environmental Management*, v. 93, p. 154-168, 2012.

TANG, C.; CHEN,V. Nanofiltration of textile wastewater for water reuse. *Desalination*, v. 143, p. 11-20, 2002.

2. MF AND MEMBRANE BIOREACTOR INTEGRATED SYSTEM APPLIED TOWARD WATER AND INDIGO REUSE FROM DENIM TEXTILE EFFLUENT

2.1. Introduction

Textile industries depends directly to the availability of high-quality water, which is a key factor in many processes, such as washing, bleaching, printing and coating of textile products. According to the literature, the water consumption in textile industries is reported to range 3-932 L/kg product depending on fibre type, applied techniques and technologies (BRIK *et al.*, 2006), generating 21 to 377 m^3 of wastewater per ton of produced product (BUSCIO *et al.*, 2015). Also, this industrial sector consumes large amounts of dyes and a variety of processing chemicals which ones are employed in different stages of textile processing (DASGUPTA *et al.*, 2015). Moreover, it is estimated that about 50% of the auxiliary chemicals are wasted in the processes depending on the ratios of fixation in textile production processes (KHATRI *et al.*, 2015), and also, 15% of the dye is lost during the dyeing process (VEDRENNE *et al.*, 2012), converted not only in environmental impacts, but also in economic damage.

Textile effluents are characterized by high colour, chemical oxygen demand (COD), inorganic salts, total dissolved solids (TDS), salinity, temperature and complex chemicals. It is reported that COD loads of textile wastewaters range between 13 and 390 g COD/kg product (OZTURK *et al.*, 2016). The constant variety of the effluent characteristics due to the batch wise nature of the dyeing process makes treatment a challenge.

Indigo blue ($C_{16}H_{10}N_2O_2$), a dye belonging to the vat group, is a synthetic organic dye and due to its complex chemical structure it is considered as a persistent substance (MANU *et al.*, 2007; SANROMAN *et al.*, 2005). It is one of the oldest known dyes and a very important kind of dye because it is applied to dyeing of denim, which popularity has increased throughout the time.

The most used type of treatment for this kind of effluent is activated sludge, however, due to the large amounts of toxic, non-biodegradable organic compounds, salts and heavy metals, traditional biological treatment is not efficient (BLANCO *et al.*, 2012), large amount of areas as well as a long hydraulic retention time should be necessary to archive sufficient efficiency to meet discharge criteria (ROBINSON *et al.*, 2001). Inefficient treatment may cause severe

environmental damage, such as flora and fauna losses due to the chemicals toxicity and increase in water colour and turbidity (DASGUPTA *et al.*, 2015).

In the past few years, membrane separation processes are becoming a popular kind of treatment process and have been replacing the conventional biological processes (FRIHA *et al.*, 2015), mostly because it provides not only a viable pollution control and in order to meet the increasingly strict discharged limits, but also, it provides a possibility of water reuse and recycling valuable components from the effluent (LIU *et al.*, 2011; ELLOUZE *et al.*, 2012; ZHENG *et al.*, 2013) increasing the industry profit.

Microfiltration (MF), due to its pore sizes ranging from 0.1-10 μm, can be applied as a pre-treatment to remove suspended solids, polysaccharides, cellular debris and other materials present in the solution, which usually cannot be removed by conventional filtration (SANTOS *et al.*, 2016). Because indigo blue oxidized is insoluble in aqueous solution, MF process can be applied in order to separate the dye and concentrate it, opening a possibility of returning the dye to the dyeing process. Due to its pore sizes, microfiltration allows unconsumed auxiliary chemicals, dissolved organic pollutants, ions and other soluble contaminants to pass through the membrane with permeate (JUANG *et al.*, 2013). The MF permeate can be treated by biological process once the indigo blue, persistent substance, is retained by the MF membrane.

Membrane bioreactor (MBR) technology is a hybrid process that combines the conventional biological sludge process, with a microfiltration or ultrafiltration membrane system (LUONG *et al.*, 2016). MBR enables the employment of high sludge ages, due to solids retention, eliminating the use of secondary decanters being replaced by a membrane which typically has a pore diameter from 0.01 to 0.08μm, facilitating the growth of specialised microorganisms in the reactor in such a way that promotes improved degradation of refractory organics (BRIK *et al.*, 2006).

MBR has several advantages associated to this process such as small footprint, low maintenance, consistency in final treated water quality independent of sludge conditions in the bioreactor, lower sludge production, and higher removal of nutrients, organic and persistent organic pollutants (POP) over conventional activated sludge processes (JEGATHEESAN *et al.*, 2016). MBRs processes have been used for the treatment of textile effluents in several studies with encouraging results. Yigit *et al.* (2009) have assessed the application of aerobic

submerged hollow fibre MBR with 0.04 mm pore membrane for treating denim textile wastewater. It was obtained COD and colour removals of 97% and 98%, respectively. Badani *et al*. (2005) investigated the treatment of textile wastewater by side stream aerobic ultrafiltration MBR with average colour removal of 70% and COD removal up to 97%. It is noteworthy that these studies evaluated the use of MBR to treat the raw effluent.

In the present study, the performance of the conjugation of MF and aerobic submerged MBR system for the treatment of textile wastewater was evaluated in terms of clarification and reduction of organic load in the textile effluent in order to obtain water reuse for coarse uses in the dye processes, such as floor and equipment washing, as well as promoting indigo concentration and reuse. Many studies have focused on the treatment of synthetic textile wastewater, applying one or another treatment. Application of a hybrid system to the treatment of real effluent in order to recover not only the water but also the dye, as far as it is known by the Authors haven't being addressed so far yet.

2.2. Materials and methods

2.2.1. Effluent Source

The present study was conduct with a textile wastewater sample supplied from a Tear Textil Ind. e Com. LTDA (Paraopeba, Brasil). In short, the dyeing process is taken in 4 steps: (1) the fibre is cleaned in order to remove any remaining dirty and then, (2) it is taken to the treatment process so it is prepared to be dyed. (3) The next step consists of the dyeing process where the fibre is immersed in a dye bath in alkaline conditions, and then, after that, (4) the fibre is washed to remove any unfixed dye. The wastewater contains indigo blue and other auxiliaries chemicals, which amounts depend on the type of jeans that are producing. The effluent used in this study was collected fortnightly for about one year on the rinsing stage of the dyeing process. The main characteristics of the raw effluent are shown on the Table 1.

Table 1:Main characteristics of the raw effluent

Parameter	Raw effluent
pH	7.64±3.91
EC (μS cm^{-1})	3275±1980
Colour (HZ)	7129±3186
Indigo Blue (g L^{-1})	0.74±0.19
COD (mg L^{-1})	3050±1524
Ammonia(mg L^{-1})	10.16±9.33
Phosphorus (mg L^{-1})	<2
Alkalinity (mg L^{-1})	530.33
Calcium (mg L^{-1})	37.79±4.24
Magnesium (mg L^{-1})	<1.25
Hardness (mg L^{-1})	38.19±6.81
Sulphate (mg L^{-1})	178.67±2.02
Total solids (g L^{-1})	4.87±3.53
Total volatile solids (g L^{-1})	1.10±0.29

2.2.2. Experimental set-up and methods

Figure 3 shows a schematic of the laboratory-scale MF-MBR hybrid system. The effluents were treated by MF in order to recovery the dye in the concentrated. MF was conducted on a commercial membrane module (PAM Membranas LTDA), polyetherimide-based polymer composition with average pore diameter of 0.4 μm, and a filtration area of 1 m^2. In all experiments, the pressure was measured by a manometer and was adjusted by a needle-type valve. MF was performed at concentrated mode filtration, where the permeates were collected in a separated tank and concentrates were returned to feed tank, constant pressure of 1 bar, cross flow rate of 2.4 L min^{-1} and up to a recovery rate of 80%. The permeate MF was treated in the MBR. Figure 4 presents the schematic of the submerged MBR system used. The biological tank volume was 6 L. The system possessed five process currents: (1) MBR feeding line, containing raw effluent to be treated, (2) compressed air line for bioreactor aeration, (3) biologically degraded and micro filtered effluent line, (4) vacuum line connected to vacuum tank, and (5) permeated backwash line. A submerged polyetherimide hollow fibre module was utilized up to 294th monitoring day, consisting of an average pore size of 0.5 μm, membrane area of 0.044 m², packing density of 500 m²/m³). After that a submerged PVDF hollow fibre module (GE) (average pore size of 0.04 μm, membrane area of 0.047 m², a non-ionic and hydrophilic surface) was used.

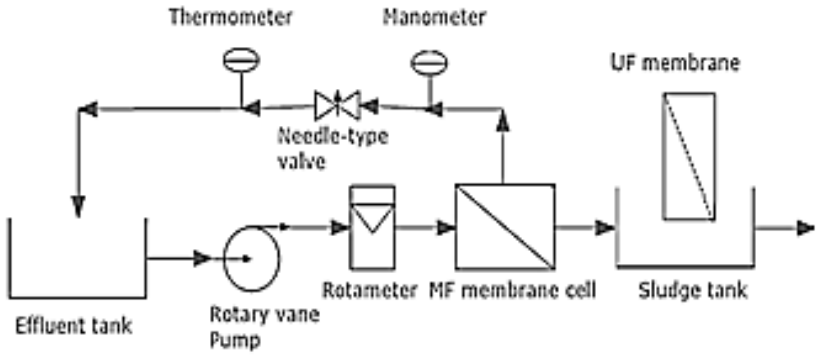

Figure 3: Schematic of the MF-MBR bench-scale units

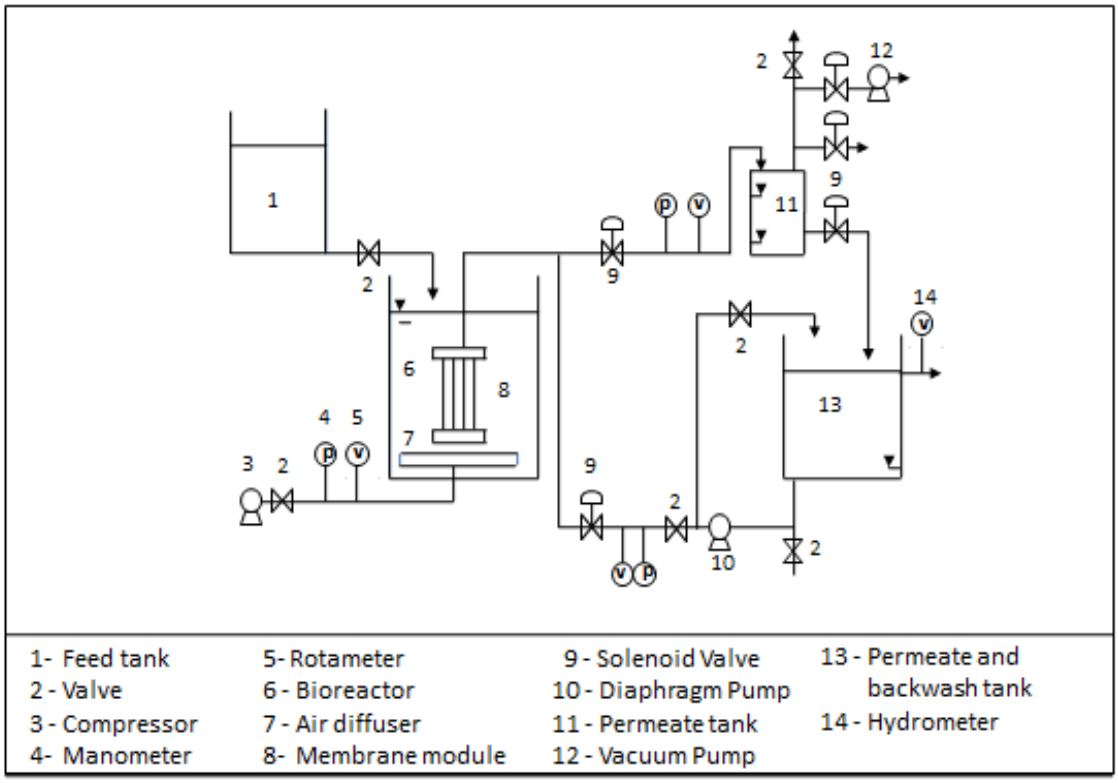

Figure 4: Scheme of the MBR used

The feed was stored in the feed tank and unloaded by gravity to the biological tank where a float valve controlled the level.

2.2.3. Experimental procedure

The microfiltration experiments were carried out with raw effluent under different pressure and pH and a fixed flow rate (2.4 L min^{-1}) and recovery rate of 90%. The pressure was

controlled at 0.5, 0.8, 1.0 and 1.3 bar. Feed pH was adjusted at 7, 8, 9, 10 and 11 using 1 M NaOH and 1:1 H_2SO_4 solutions. In each operating condition, the following procedure was adopted: (1) filtration of de-ionized water under three different TMP (0.5, 0.8 and 1 bar) until a constant flux was obtained to each pressure; (2) filtration of raw effluent under the selected condition (3) washing the fouled membrane module with flowing de-ionized water for 2 minutes with concentrated flow rate of 1.2 L min^{-1} to remove the foulants that loosely deposited on the membrane surface; (4) filtration of de-ionized water under for 10 minutes under the TMP of 1 bar; (5) chemical cleaning of membrane (sodium hypochlorite (0.4% m/m)); (6) filtration of de-ionized water under three different TMP (0.5, 0.8 and 1 bar) until a constant flux was obtained to each pressure. All tests were conduct in duplicates. The flux rate was measured at every 2 minutes in the 10 first minutes into the tests and then at every 5 minutes throughout the test and permeate samples were collected at every 10% of recovery.

The MBR was initially inoculated with sludge from the activated sludge reactor of the actual company providing the effluent. After an initial acclimatization stage of the microorganisms to the conditions of the MBR and of the effluent, which lasted 29 days, the hydraulic retention time was established as 8 hours (value defined having as basis the literature and previous tests) and SRT as 60 days. The useful sludge volume in the MBR was kept at 4 L, the operational flow was of 0.5 L/h . A 0.5 Nm^3/h air flow to the biological tank was used. The backwash was activated for 15 seconds at every 15 minutes of permeation.

During the MBR operation, the pressure was recorded daily. Samples of feed (MF permeate), permeate and biological sludge were collected three times a week for physicochemical characterization.

The maintenance chemical cleaning was carried out weekly using a 500 ppm solution of sodium hypochlorite for 20 min. The recovery chemical cleaning of the membrane was performed when the operational pressure achieved the value of 0.55 bar. The recovery chemical cleaning of the membrane was done using a 2.000 ppm solution of sodium hypochlorite for 20 min in an ultrasound bath.

2.2.4. Fouling investigation

To investigate fouling, it was evaluated the evolution of permeability and membrane resistance. Resistance to filtration was assessed in accordance with the serial resistance model proposed by Choo and Lee (1998). With that model, total resistance of the fouling and the

resistances of each parcel of the total resistance (membrane resistance (R_m), static adsorption (R_a), pore blockage (R_p) and cake (R_c)) were calculated. In order to do so, it was necessary to determine the J_i, J_a, J_f and J_v flux. The Ji flux was determined for permeation of pure water into the clean membrane. The J_a flux was determined for microfiltered or ultrafiltered water after static adsorption of the sludge onto the membrane for 2 h with no pressurization. The J_v flux was determined by the permeation of the sludge, and the J_f flux was determined by the permeation of microfiltered water after sludge permeation and washing of the module with running water to remove the tort. The flows were measured at a determined pressure. With the value of the J_i, J_a, J_f and J_v flux, the R_m, R_a, R_p and R_t resistances were calculated using eqs 1–3.

$$R_a = \left(\frac{J_i}{J_a} - 1\right) R_m \qquad \text{Eq. (1)}$$

$$R_p = \left(\frac{J_i}{J_f} - 1\right) R_m - R_a \qquad \text{Eq. (2)}$$

$$R_t = \left(\frac{J_i}{J_v} - 1\right) R_m - R_a - R_p \qquad \text{Eq. (3)}$$

To compare if the resistance values obtained using the resistance-in-series model proposed by Choo and Lee (1998) are equivalent to the operational resistance values, the total resistance obtained by the test (R_m+R_a+R_{bp}+R_c) was compared with the values of operational resistance. In order to calculate operational resistance, eq 4 was employed.

$$R_{Operacional} = \left(\frac{P_i}{P_v} - 1\right) x R_m + R_m \qquad \text{Eq. (4)}$$

In which:

P_i = pressure applied to the permeation of microfitered or ultrafiltered water through clean membrane; P_v = pressure applied to the permeation of MBR liquid before the interruption of the operation for membrane cleaning; and R_m = membrane resistance.

2.2.5. Analytical Methods

The colour, COD, ammonia, and TDS contents of the effluent were analysed following methods 2120 C, 5220 D, 4500-NH3 B C, and 2540 B E, respectively, in accordance with the recommendations of Standard Methods for the Examination of Water and Wastewater

(APHA, 2005). pH was measured according to the method 4500 H B a digital calibrated pH-meter. TOC was analysed using TOC Shimadzu TOC-V CNP. Conductivity was determined following the method 2510 B with a calibrated conductivity meter (Condutivímetro Hach 44600) and indigo was determined by colourimetry test. Concentration of Cl^-, SO_4^{2-}, PO_4^{3-}, Mg and Ca will be measure by ion chromatography (ICS-1000 ion chromatograph equipped with the Dionex AS-22 column and ICS 12a). Samples was also characterized by Fourier transform coupled total attenuated reflectance system (ATR-FTIR) using a spectrophotometer Shimadzu FTIR IRPrestige-21. The spectra were recorded in the range 4000-400 cm^{-1} with resolution of 4 cm^{-1}.

To assess the aerobic biodegradability performed by the adapted Zahn-Wellens Method (OECD, 1995), it was used 2 l reactors, fed with raw effluent, MF permeate and glucose, 2 ml of nutrient solution ($CaCl_2$, $FeCl_3.7H_2O$, $MgSO_4$, and phosphate buffer) prepared according to the DBO method (APHA, 2012), and inoculum at a concentration of 100 mg L^{-1} of SSV (sludge collected in the activated sludge reactors used to treat domestic sewage). The reactors were subjected to aeration by electric compressors, and substrate depletion was monitored by means of soluble COD analysis (filtered) for 28 days, with intervals of about 2 days. The biodegradability was determined by the percentage of removed COD.

The characterization of different molecular weight fractions using membranes of 10 and 100 kDa using an Amicon ultrafiltration cell (8000 series and 8200 model).

The molecular weight distribution of raw effluent, MF permeate and MBR permeate was performed using an ultrafiltration cell (Series 8000, Model 8200, Amicon®) and membranes with molecular weight cut of 1, 10 and 100 kDa, in accordance with the procedure described by Amaral *et al*. (2009). To conduct this test, all samples were previously filtered through standard AP40 filter with opening 0.45 uM pore. Fractions were analyzed for COD concentration.

2.2.6. Calculations

The volumetric permeate flux (*J*) in terms of litres per square meter per hour (L m^{-2} h^{-1}) was calculated using Eq. (1), as follows:

$$J = \frac{V}{A \times \Delta t}, \quad (1)$$

where A is the effective area of the membrane module for permeation and V is the volume of permeate collected over a time interval of Δt.

Flux normalization to 25 °C was accomplished by means of a correction factor related to the fluid viscosity, according to Eq. (2):

$$J = \frac{V}{A \cdot t} \cdot \frac{\mu(T)}{\mu(25°C)} \quad (2)$$

where J is the normalized permeate flux at 25 °C, $\mu(T)$ is the water viscosity at the process temperature, and $\mu(25\,°C)$ is the water temperature at 25 °C.

The membrane water permeability (K) for each test was obtained from the linearization of the ratio of normalized permeate flux of pure water (J) by applied pressure (ΔP) at 12.0, 10.0, 8.0, and 6.0 bar.

The observed rejection was calculated using Eq. (2), as follows:

$$R(\%) = \frac{C_f - C_p}{C_f} \times 100, \quad (3)$$

where C_f and C_p represent the solute content on the feed and permeate streams, respectively.

According to the simplified resistance-in-series model, the total filtration resistance could be divided into membrane resistance and fouling resistance. The membrane resistance to filtration (R_M) was determined from Eq. (4):

$$R_M = \frac{1}{K \cdot \mu(25°C)} \quad (4)$$

The total fouling resistance to filtration (R_f) was calculated based on the values of the normalized effluent permeate flux (J_{sd}) obtained near the end of each experiment (Eq. 5). This resistance includes the concentration polarization, the adsorption of components on the membrane surface and scaling.

$$R_f = \frac{\Delta P - \Delta\pi}{\mu(25°C) \cdot J_{sd}} - R_M \quad (5)$$

where ($\Delta P - \Delta\pi$) is the process effective pressure, i.e., applied pressure minus osmotic pressure. The osmotic pressure difference was calculated using the van't Hoff equation (Eq. 6):

$$\Delta\pi = \sum_{i=0}^{n} (C_r - C_p) \cdot R \cdot T \quad (6)$$

where C_r and C_p are the concentrations of solute "i" on the retentate and permeate, respectively, R is the universal gas constant, and T is the temperature in Kelvin.

The fouling resistance (R_f) is a combination of the resistance of the reversible fouling (R_{fr}) and irreversible fouling layer (R_{fir}), as follows [19]. R_{fr} is mostly due to the deposition of a cake layer on the membrane surface, which can be removed through physical cleaning, such as water washing; thus, it can be controlled by adjusting the feed flow conditions. R_{fir} is due to materials that adsorb onto the membrane surface and into the pores that can be removed by chemical cleaning.

The total flux decline (FD) was also calculated, as follows:

$$FD = \frac{(J_w - J_{sd})}{J_w}. \quad (7)$$

where J_w is the volumetric permeate flux of pure water of the membrane before effluent filtration.

Flux decline can be attributed to concentration polarization (CP) and fouling (F); thus, the flux decline due to CP was obtained using Eq. (8), as follows:

$$CP = \frac{(J_{pc} - J_{sd})}{J_{wc}}, \quad (8)$$

where J_{pc} is the volumetric water flux of the physically cleaned membrane after effluent filtration.

The flux decline due to fouling (F) was obtained using Eq. (9), as follows:

$$F = \frac{(J_w - J_{pc})}{J_w}. \quad (9)$$

The specific energy consumption (SEC) was calculated from the relation between the rate of work done by the pump (W_{pump}) and permeate flow rate (Q_p) using Eq. (10) [29], as follows:

$$SEC = \frac{W_{pump}}{Q_p}, \quad (10)$$

where

$$W_{Pump} = \Delta p \times Q_f, \quad (11)$$

where Q_f is the volumetric feed flow rate and Δp is assumed to be equivalent to the permeate pressure.

The permeate product water recovery for NF processes (Y) can be defined using Eq. (12), as follows:

$$Y = \frac{Q_p}{Q_f}. \quad (12)$$

By combining Eqs. (7), (8), and (9), the equation to determine SEC can be rewritten as follows:

$$SEC = \frac{\Delta P}{Y}. \quad (13)$$

2.2.7. Statistic Evaluation

Nonparametric behavior in a high number of samples were verified. Thus, the nonparametric Spearman rank correlation coefficient, which is based on the ranks of the samples instead of their value, was preferred over the other tests and used in this study. Mann Whitney' and Kruskal Wallis' test was used to check for the existing significant differences between the evaluated parameters (α = 5%). Kruskal Wallis' tests were followed by nonparametric multiple comparisons among groups (α = 5%).

The correlation calculations and testing were performed using Statistic® software. The values of the correlation coefficients were tested for their statistical significance, which is the probability p of occurring by chance. Therefore, relationships were considered relevant for the Spearman correlation coefficient at the 95% significance level (P=0.05).

2.3. Results and discussion

2.3.1. MF performance

2.3.1.1. Effect of TMP on MF flux and permeate characteristics

As expected, it is noted an increase in the flux values with the increase in TMP values (0.5 to 1.3 bar) (Figure 5). For every evaluated pressure conditions, the permeate flux decreased gradually with the increasing recovery rate due to fouling and concentration polarization phenomena. The resistance due to membrane fouling increase from $5.34x10^{12}$ m^{-1} to $7.07x10^{12}$ m^{-1} bar with increasing TMP from 0.5 to 1.0 bar, respectively. The same profile was observed to contribution of irreversible membrane fouling. However, the increase of the TMP from 1.0 to 1.3 bar led to a decrease of membrane fouling resistance to $6.33x10^{12}$ m^{-1} and the irreversible membrane fouling contribution (Table 2). These results suggest that the high permeate flux at 1.3 bar resulted in a rapid cake formation that prevent fouling due to pore blockage reducing the irreversible fouling and consequently the total membrane fouling. This hypothesis is supported by lower chemical cleaning efficiency values observed in the assays carried out at 0.8 and 1.0 bar that showed higher irreversible fouling contribution.

Specific energy consumption (SEC) relates the permeate flux by area of membrane to the required energy. This factor is directly associated to operational costs. This analysis was also carried out to each test in order to archive the energy-optimal process operation. It is observed a decrease in SEC with a decrease on TMP, with a subtle difference in the TMP of 0.8, 1 and 1.3 bar (Table 2).

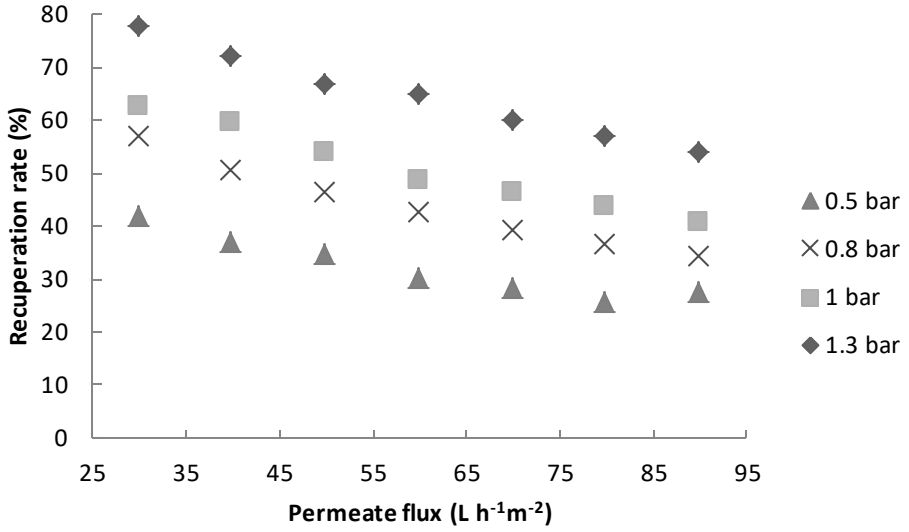

Figure 5: Permeate flux as a function of the recuperation rate, under different TMP

Table 2: Water and Permeate flux, hydraulic resistance (R_m, R_f, R_{fr}, R_{fir}, R_{cc}) and specific energy consumption when applied MF system, under 20ºC, natural pH, flow rate of 2.4 $L.min^{-1}$, permeate recovery rate of 90% and different TMP

TMP (bar)	Jw ($L/m^2.h$)	Jsd_0 [a] ($L/m^2.h$)	Jsd_f [b] ($L/m^2.h$)	Jw_{fc} [c] ($L/m^2.h$)	Jw_{cc} [d] (L/m2.h)	Hydraulic Resistance ($x10^{12}$ m^{-1})					Chemical Cleaning	SEC ($kWh\ m^{-3}m^{-2}$)
						R_m	R_f	R_{fr}	R_{fir}	R_{cc}	Efficiency (%)	
0.5	94.36	64.86	24.82	90.00	94.36	1.90	5.34	5.24	0.09	0.00	100.00	805.84
0.8	144.71	104.90	33.82	129.60	136.57	1.99	6.51	6.28	0.23	0.12	92.65	946.24
1	171.24	108.08	39.20	144.00	153.60	2.10	7.07	6.67	0.40	0.24	86.64	1020.46
1.3	198.32	138.98	53.80	193.05	201.17	2.36	6.33	6.26	0.06	0.00	101.97	1003.83

Table 3: MF permeate characteristics in filtration of raw effluent, under 20ºC and different TMPs

Parameter	Raw effluent	Permeate concentration								Observed rejection (%)			
		0.5 bar		0.8 bar		1 bar		1.3 bar		0.5 bar	0.8 bar	1 bar	1.3 bar
COD (mg/L)	3100	2635.3±	248.9	2538.6±	198.1	2527.5±	263.4	2457.9±	247.8	15	22	22	24
pH	9.63	9.6±	0	9.7±	0	9.6±	0	9.7±	0	-	-	-	-
EC (mS/cm)	10.59	9.7±	1	9.7±	1.1	9.8±	0.9	9.9±	1	8.5	8.5	7.5	6.3
TOC (mg/L)	696.8	513.5		510.2		510.6		509.8		26.3	26.8	26.7	26.8
Colour (HZ)	7940	441±	80.9	455.9±	44.2	479.6±	59.3	495.9±	99.9	99.5	99.5	99.4	99.4
Indigo Blue (g/L)	0.57	0	-	0	-	0	-	0	-	100	100	100	100

Table 3 shows the MF membrane rejection at different TMP conditions. According to Kruskal Wallis' test, there is no significant difference in COD, EC and colour in the permeate between the applied TMP for a p-value=0.05.

Nonetheless, aiming the dye recovery, the indigo concentration in the concentrated stream was measured. The dye concentration increased with the TMP applied (4.76 to 8.61 g/L from 0.5 to 1.3 bar, respectively).

Considering the MF performance in terms of permeate flux, membrane fouling, rejection and energy requirements, the operating pressure of 1.3 bar was selected for textile effluent MF.

2.3.1.2. Effect of pH on MF flux and permeate characteristics

Taking in consideration the variability of the raw effluent, it was assessed MF performance at pHs of 7, 8, 9, 10 and 11. The permeate flux decrease with increasing the effluent pH (Figure 6). It was probably caused by membrane fouling due to the presence of dye and auxiliary chemicals in the raw effluent. At higher pH, indigo blue becomes soluble in aqueous solution, taking the mono-phenolate form (Figure 7), which may fouled the membrane by adsorption contributing for the irreversible fouling resistance increasing and chemical cleaning efficiency decreasing (Table 4). At pH 9, it is observed the higher fouling resistance. At this pH, indigo is mostly present in the acid leuco form and a small amount of mono-phenolate form, which may explain the obtained result. It is a mixture of soluble and insoluble indigo forms that can compromise the filtration efficiency.

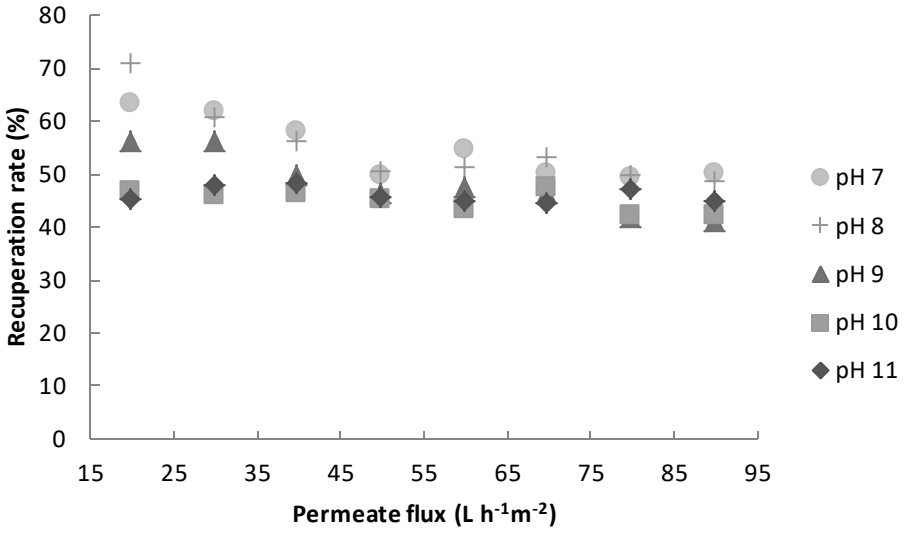

Figure 6: Permeate flux as a function of the recuperation rate, under different pH

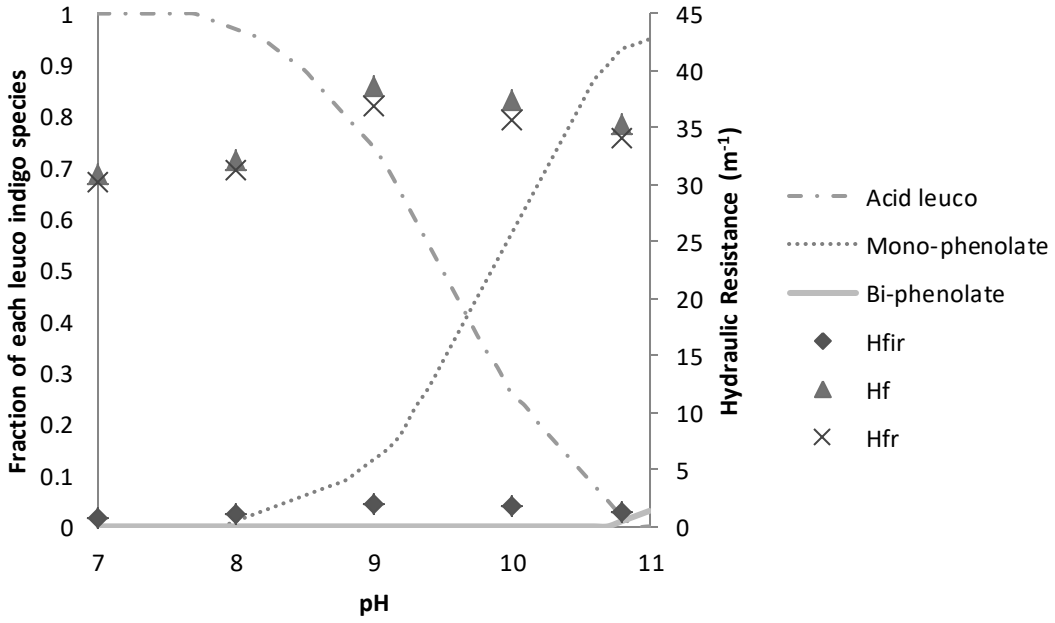

Figure 7: Fractional form of each reduced species of indigo and hydraulic resistance as function of pH (source: adapted from CHAKRABORTY, 2009)

Table 4: Water and Permeate flux, hydraulic resistance (R_m, R_f, R_{fr}, R_{fir}, R_{cc}) and specific energy consumption when applied MF system, under 20ºC, 1.3 bar, flow rate of 2.4 $L.min^{-1}$, permeate recovery rate of 90% and different pH

pH	Jw ($L/m^2.h$)	Jsd_0 [a] ($L/m^2.h$)	Jsd_f [b] ($L/m^2.h$)	Jw_{fc} [c] ($L/m^2.h$)	Jw_{cc} [d] (L/m2.h)	Hydraulic Resistance ($x10^{12}$ m^{-1})					Chemical Cleaning	SEC ($kWh\ m^{-3}m^{-2}$)
						R_m	R_f	R_{fr}	R_{fir}	R_{cc}	Efficiency (%)	
7	85.92	72.62	50.00	81.90	87.81	5.44	3.91	3.64	0.27	0.0	100	1040.01
8	87.81	71.83	48.18	85.80	88.05	5.32	4.38	4.25	0.12	0.0	100	1079.39
9	88.05	59.17	40.93	74.10	85.80	5.31	6.11	5.11	1.00	0.14	95.22	1270.50
10	85.80	58.02	42.00	71.76	82.35	5.45	5.68	4.61	1.07	0.23	92.13	1238.10
11	82.35	58.38	44.03	64.74	79.06	5.67	4.94	3.39	1.54	0.24	91.42	1223.08

Table 5: MF permeate characteristics in filtration of raw effluent, under 20ºC, 1.3 bar and different pH

Parameter	Raw effluent	Permeate concentration										Observed rejection (%)				
		pH7		pH8		pH9		pH10		pH 11		pH 7	pH 8	pH 9	pH 10	pH 11
COD (mg/L)	1172.3	553.1	±84.26	553.8	±84.15	555.7	±78.33	611.6	±86.35	614.0	±88.21	52.8	52.8	52.6	47.8	47.6
pH	9.42	7.58	±0.08	8.14	±0.11	8.971	±0.09	9.65	±0.05	10.6	±0.05	-	-	-	-	-
EC (mS/cm)	2645	2076.4	±277.41	2078	±203.23	2070	±232.67	2029	±292.04	2339	±298.85	21.5	21.4	21.7	23.28	11.58
COT (mg/L)	265.5	41.65		42.28		79.14		140.4		144.8		84.3	84.1	70.2	47.12	45.46
Colour (HZ)	1344	73.259	±19.72	82.89	±34.75	83.26	±30.46	85.11	±19.49	86.96	±30.29	99.5	99.4	99.4	99.4	99.4
Indigo Blue (g/L)	2.44	0	-	0	-	0	-	0	-	0	-	100	100	100	100	100

Table 5 shows the MF membrane rejection at different effluent pH conditions. According to Kruskal Wallis' test, there is no significant difference in COD, indigo blue concnetratrion and colour values in the permeate between the evaluated effluent pH for a p-value=0.05, except for EC values. Applying Kruskal Wallis' test, it is noted statistical difference in EC in the permeate for a p-value=0.05, and multiple comparisons among groups identified the difference in pH 11 from the other tests (Table 5). This difference can be associated to increasing of ions in solution due to pH correction.

Also, analysing the MF concentrate (Table 6), the pH 8, where indigo takes the reduced non-ionic form, was the most efficient pH in indigo retention and concentration reaching 8.18 g/L.

Table 6: Dye concentration in the concentrated stream as a function of pH

pH	Dye concentration (g/L)
7	6.79
8	8.18
9	5.62
10	6.12
11	5.25

These results show that MF can be applied in a wide pH range of activities without loss of quality permeate supporting possible variations of the pH of the effluent due to changes in dyeing conditions. Considering the monitoring time (2 years), the effluent pH has neutral nature with values range from 815 to 4571 mg L^{-1} and average of 3050±1524 mg L^{-1}. The neutral nature of effluent pH is important for the sustainatibilty of the process, since in this condition it was observed the higher permeate flux, low fouling e low energy demand.

2.3.1.3. Potential of reuse of the Indigo Blue in the concentrate and the permeate as a water reuse

The indigo blue dye was efficiently retained by the MF membrane (100%) resulting in a concentrate stream with indigo blue concentration of 6.13±1.44 g/L (Table 7). It is important to highlight that indigo blue concentration in the permeate depends of the indigo blue concentration in the raw effluent. During the 2 years of monitoring, the indigo blue concentration in the raw effluent

ranged from 0.39 to 0.95 g/l with average value of 0.74±0.19 g/L and consequently the concentration of indigo blue in the concentrate ranged from 4.01 to 8.23 g/L with average value of 6.34±0.96 g/L. It has been reposted on the literature that the indigo blue concentration required to for automated dyeing process, in its reduced form (i.e. mono-phenolate), ranges about 2-3 g L^{-1} (CHAKRABORTY, 2009), thus all MF process is efficient enough to promote dye concentration to be reused. In any case, it is possible to mixture the concentrate and more commercial indigo in order to meet up the bath volume requirement. For the reuse of concentrate in the dyeing process, it is necessary to ensure the concentration of important interferents of the dyeing process is below the maximum allowed value, such as Ca^{+} and Mg^{+} content, Fe^{+} Cu^{+} and Cl^{-}. According to Chakraborty (2009), it is important to control the concentration of indigo around 2-3 g/L, above that value, there is no gain in colour, and also the pH of the dyeing bath has to be controlled since the dye uptake depends on it.

ATR-FTIR analysis was conducted for raw effluent, MF permeate, MF concentrate and indigo blue commercial standard. In the spectrum of dry raw effluent, MF concentrate and commercial indigo blue dye it can observed absorptions at 3290.5601 cm^{-1} (ν N-H) characteristic stretch of aromatic amine, 2976.1631 cm^{-1} (ν C-H), 1546.9104 cm^{-1} (ν C=O), 1404.1780 cm^{-1} (ν C=C) stretch aromatic ring, 1068.5641 cm^{-1} (δ C-H), 837.1061 and 752 cm^{-1} (δ C-H) angular deformation of the aromatic ring, that are described in the literature for indigo blue dye (PASCHOAL *et al.*, 2005) (Figure 8 and 9). It can also be seen the presence of some contaminants. Absorptions at 1296.1644 cm^{-1} (ν S=O), stretching characteristic of sulfonate groups, indicate a possible contaminant (Figure 7). According to Chakraborty (2009), the dyeing process can be carried out with a mixture of sulphur and indigo which may explain the existence of sulfonate groups. However, the functional groups associated to contaminants were also found in the commercial dye. Thus the IR data confirm that the concentrate has the potential to be reused.

By overlapping the bands of raw effluent, MF permeate and MF concentrate, it is possible to verify the efficiency of the microfiltration process to concentrate indigo blue in its insoluble form, since it is not observed all bands correspondent to indigo blue in the MF permeate, and the efficiency of MF process in reducing the contamination load in the permeate stream.

Table 7: Physicochemical characteristics of the raw effluent and MF permeates (MF operational conditions: pressure 1.3 bar, 2.4 L min-1, 20°C, and recovery rate of 90%)

Parameter	MF Concentrate	MF Permeate	% MF efficiency	Washing-off[a]	Equipment Washdown[a]	Dyeing[b]
pH	8.22±.3.91	8.68±0.29	-	7.0–8.0	6.5–8.0	3.0-10.0
EC (μS cm^{-1})	16375±1980	2433±979	25.71	-	-	-
Colour (HZ)	35644±3186	0	100	nv[c]	nv[c]	5
Indigo Blue (g L^{-1})	6.34±0.96	0	100	-	-	-
COD (mg L^{-1})	6407±396	612±170	65.44	200	500–2000	-
Ammonia (mg L^{-1})	24.37±9.33	6.60±9.76		-	-	-
Phosphorus (mg L^{-1})	<2	<2	-	-	-	-
Alkalinity (mg L^{-1})	430	573.33		-	-	-
Calcium (mg L^{-1})	25.69±6.81	32.69±1.53	13.48	-	-	-
Magnesium (mg L^{-1})	<1.25	<1.25	-	-	-	-
Hardness (mg L^{-1})	50.29±4.24	30.1±2.29	21.18	100	100	25
Sulphate (mg L^{-1})	223.56±0.47	259.32±84.82	6.87	-	-	-
Total solids (g L^{-1})	15.76±0.54	3.62±2.09	25.68	-	-	5
Total volatile solids (g L^{-1})	5.2±0.12	0.99±1.21	9.37	-	-	100

-Not identified; *[a]VALH et al. 2011; [b]FIESP 2014; [c] None visible*

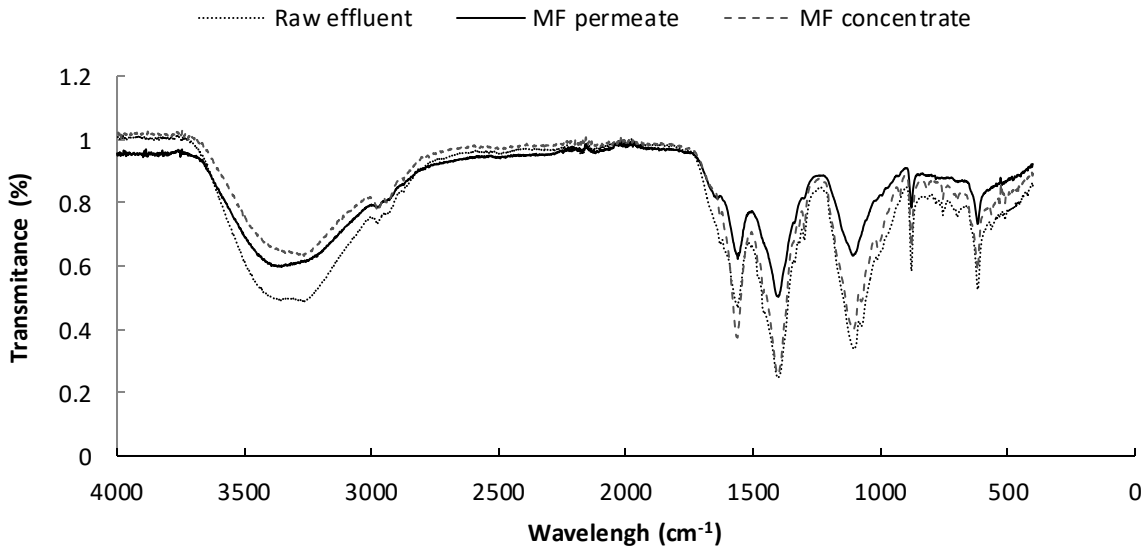

Figure 8: ATR-FTIR of the raw effluent, MF and NF permeate

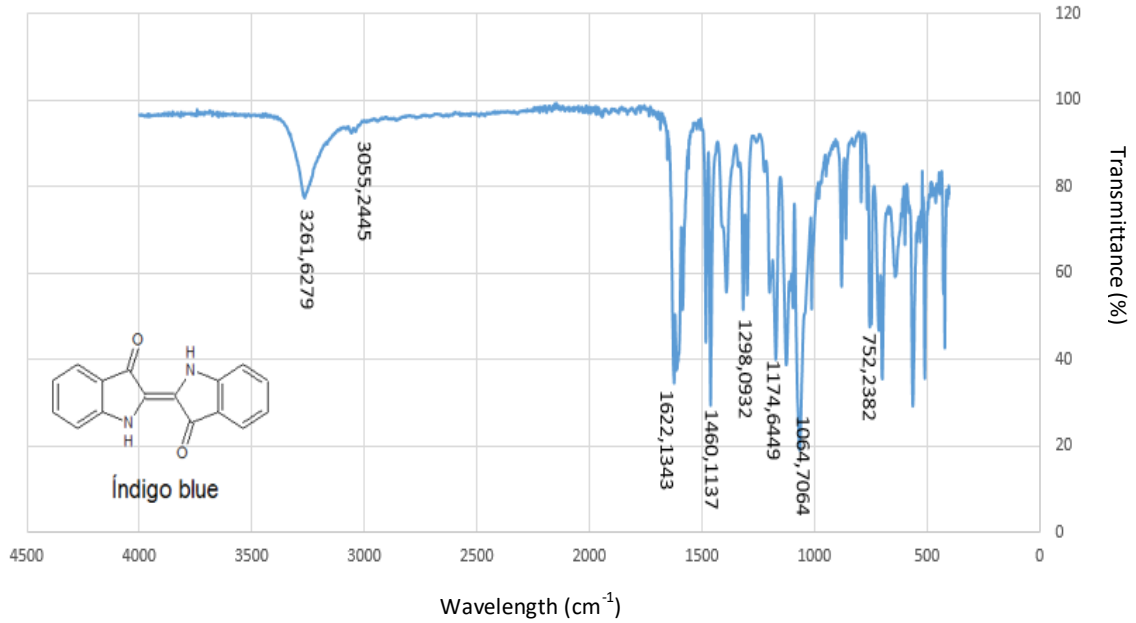

Figure 9: ATR-FTIR of commercial indigo blue

As can also be seen in Table 7, it was possible to obtain approximately 100% of colour removal and reduce the COD and conductivity by about 65% and 25%, respectively, using the MF process.

The requirements for water quantity in the textile industry vary according to the process, i.e. the yarn and technology applied; for example, dyeing, desizing, and bleaching processes use 8–300, 3–9, and 3–124 L kg^{-1} of cotton, respectively (VALH *et al.*, 2011). The water quality required is also dependent on the process, and the dyeing step (i.e. fabric wash-off) has the highest quality restrictions. The MF permeate has enough quality to attend certain activities in the textile industry, such as equipment and floor washing (Table 7). However, it is needed a polishing step to reuse this effluent in more quality restringing steps, for instance, dye baths.

Raw effluent showed maximal aerobic biodegradability around 69%, whereas, MF permeate presented to have a higher biodegradability, around 84% (Figure 10). Since glucose is a biodegradable substrate, high biodegradation percentage of glucose confirm activity of the microbial of the sludge used as a inoculum. Increase in biodegradability is attributed to the removal of the dye in the MF process. According to Manu *et al*. (2007) and SANROMAN *et al*., (2005), indigo blue is considered as a persistent substance due to its complex chemical structure inducing greater difficulty in microbiological degradation. This results show the importance of MF as pre-treatment. MF promotes complete retention of the dye and increases the biodegradability of the effluent enabling both the reuse of indigo blue in the concentrate and application of biological process to removal the organic matter of permeate.

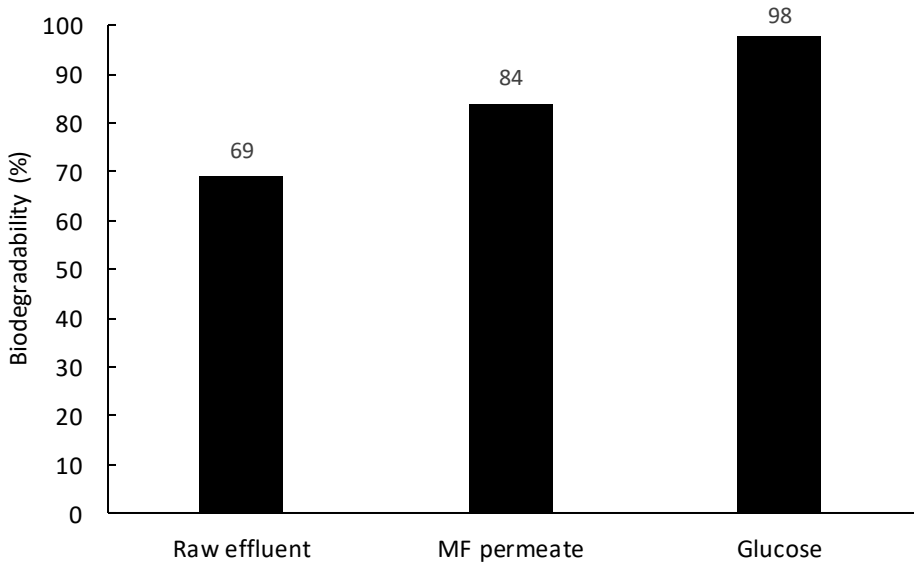

Figure 10: Aerobic biodegradation of raw effluent and MF permeate

2.3.2. MBR performance

2.3.2.1. COD removal performance of the MBR

Figure 10 shows the performance of MBR system with respect to the COD removal during the two experimental stages. During the first stage (MBR operated with microfiltration membrane (from the 1st to 294th day)), the raw effluent COD concentration ranged between 815 and 4,571 mg/L with an average value of 3,603 mg/L and standard deviation of 1,555 mg/L. The MF applied as pretreatment reduced the effluent COD to 1100 ±578 mg/L. The average value of the corresponding MBR permeate COD was 227.4±89 mg/L which gives an average removal efficiency of 77±7 %. During the second stage (MBR operated with ultrafiltration membrane (from the 295th to 539th day)), the raw effluent COD concentration ranged between 1,087 and 4,571 mg/L with an average value of 2,583 mg/L and standard deviation of 1,327 mg/L. The MF applied as pretreatment reduced the effluent COD to 721±316 mg/L. The average value of the corresponding MBR permeate COD was 157±62 mg/L which gives an average removal efficiency of 78±6 %. The significant differences of MBR permeate COD concentration in both stages was confirmed by statistical analyses based on Mann Whitney test method with p value < 0,05. However this difference cannot be directly associated to the use of ultrafiltration in comparison to microfiltration in the MBR because the COD of raw effluent and MF permeate in both stages were significantly different according to Mann Whitney test method with p value < 0,05. Besides that, the use of UF instead of MF in the MBR does not contribute to reduction of variations in the MBR permeate COD. The MBR-MF permeate and MBR-UF COD value show a variation coefficient of 38.9 and 39.1 % respectively.

It is evident the importance of the microfiltration or ultrafiltration as pretreatment for ensure the good MBR performance. The MF act reducing the fluctuations on organic load feeding the MBR. The raw effluent COD values show a variation coefficient of 49.9%, and this value was reduced to 39.9% after the MF process.

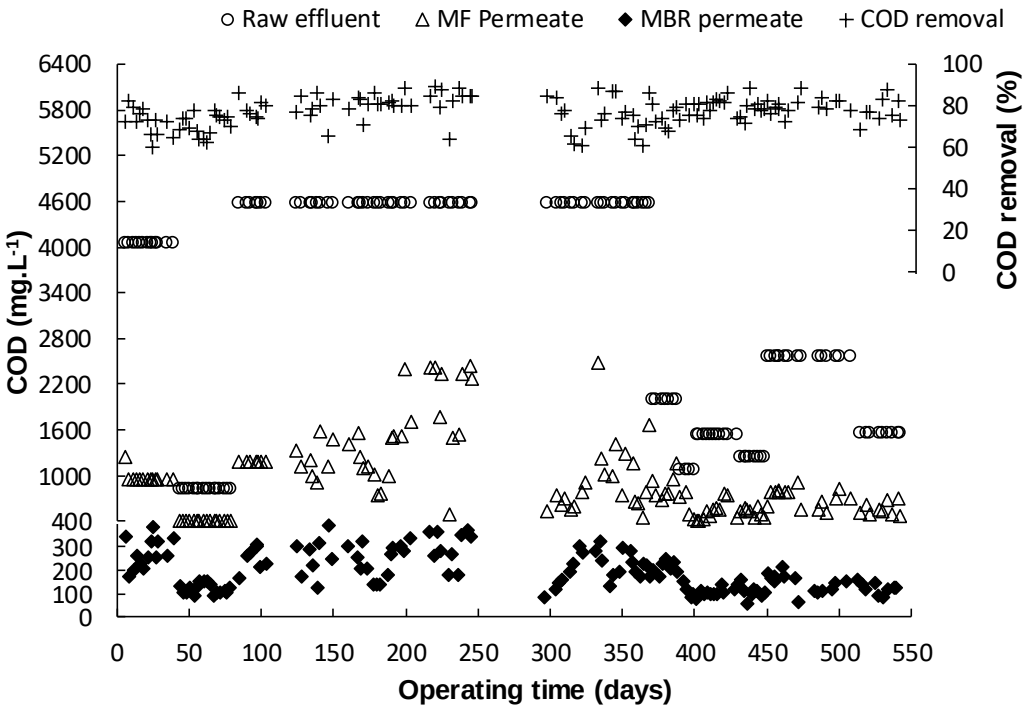

Figure 11: Raw effluent, MF and MBR permeate COD content and MBR COD removal efficiency

The MBR efficiency of COD removal (78±6 mg/L) was calculated considering the total COD feeding the MBR (MF permeate COD content). However, as can be seen in the figure 11 the MF permeate showed maximal aerobic biodegradability 89%. Then, the average real MBR efficiency calculated considering only the COD biodeagrable fraction content in the MF permeate is 78±6 %. It is noteworthy that the residual organic matter in the MBR permeate does not comprise only biodegradable, non-biodegradable or slowly biodegradable compounds, but also intermediate and final compounds, complex organic compounds formed during condensation reactions of organic compounds affluent and intermediate and final products degradation such as soluble microbial products (SMP) and extracellular polymer substances (EPS) (Barker *et al.*, 1999).

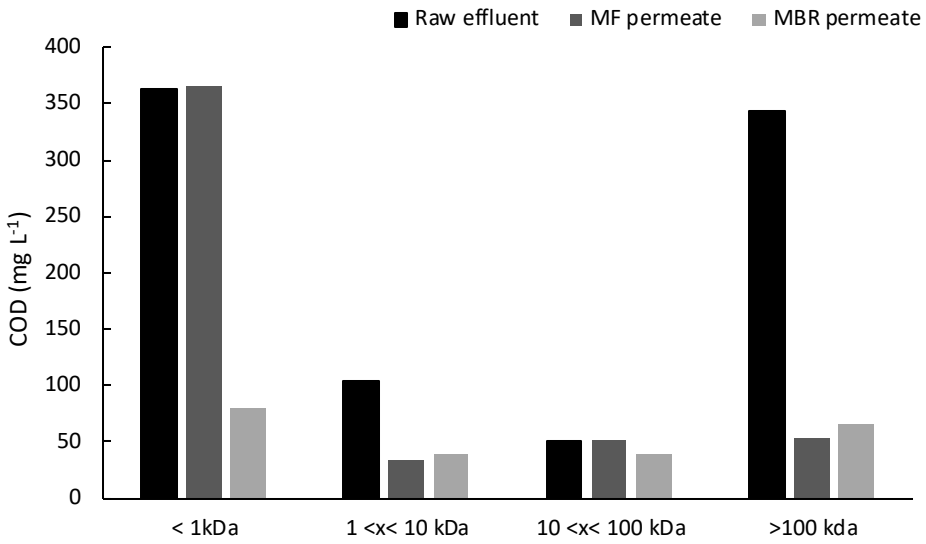

(a)

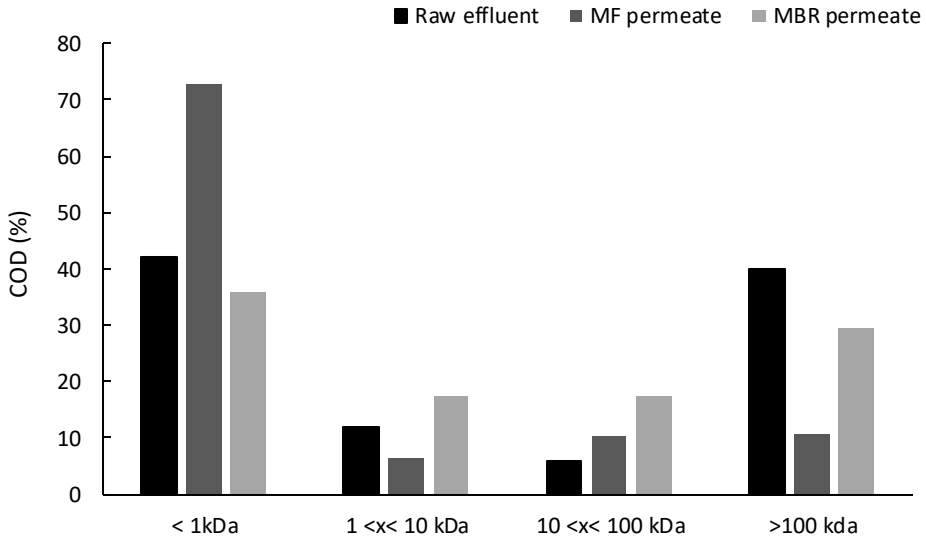

(b)

Figure 12: Comparison between the COD content in biological degradation and MBR

It is observed that for raw effluent (Figure 12), about 42% has low molecular weight (<1 kDa), and approximately 40% has high molecular weight (> 100 KDa). It is believed that molecules with high molecular weight are mainly constituted by indigo blue and auxiliary chemicals that give relatively low biodegradability characteristics for the raw effluent. MF process removed a significant portion of the molecules with high molecular weight (greater than 1 kDa) showing once again the efficiency of this technology in retaining indigo blue and some auxiliary chemicals. However it is not efficient in retaining low molecular weight

compounds. These results corroborate the increase of the biodegradability of the effluent after MF process. Several authors have noted that the COD relative to low molecular weight compounds (<1kDa) is more readily degraded compared with the fraction of high molecular weight (> 1 kDa) (Barker *et al.*, 1999).

MBR exhibited high efficiency to remove low molecular weight compounds (<1 Kda), but it is not effective in the removal of high molecular weight compounds (>100 kDa). Moreover it is noted an increase in the concentration of compounds with high molecular weight (>100 KDa), that can be attributed to the microbial products such as EPS and SMP.

2.3.2.2. Variations of MLVSS and filtration performance in the MBR

Figure 13 shows the MLVSS concentration, the feed to micro-organism rate (F/M) and the MBR organic load throughout the operation time.

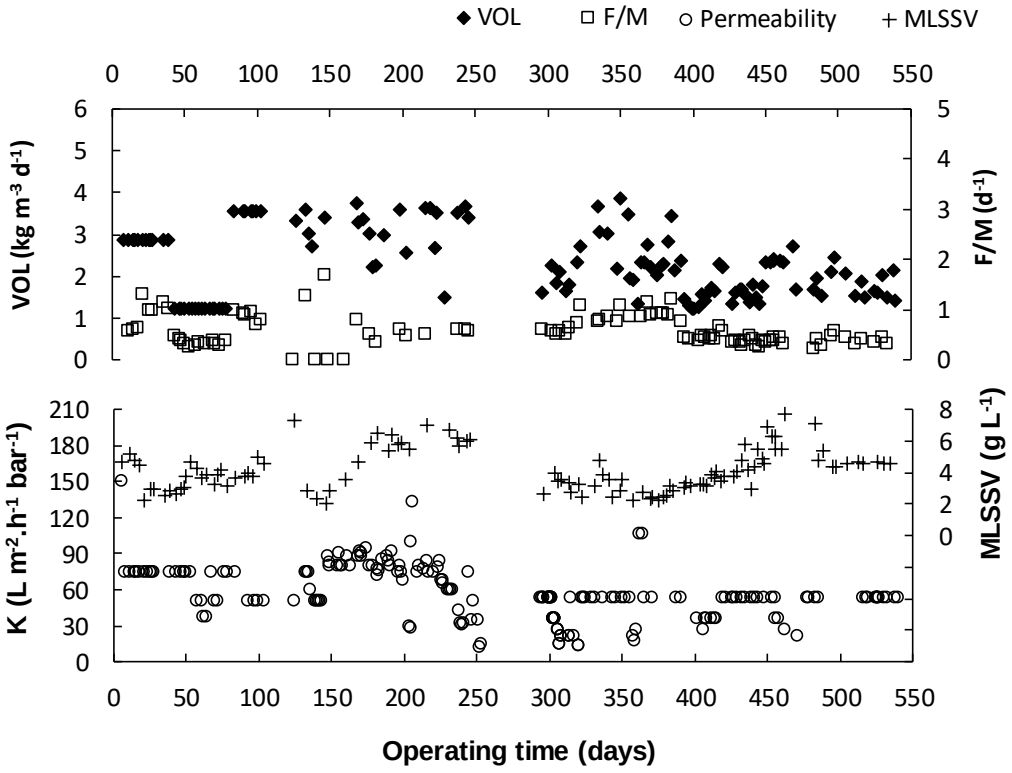

Figure 13: COV, F/M, MLSSV and membrane permeability during the operation time

The MLVSS concentration in the MBR ranged between 2.2 and 7.7 g/L with an average value of 4.2 g/L and standard deviation of 1.3 g/L. The decrease in the MLVSS occurred in the 130

and 300th monitoring day was due operational problem that resulted in the sludge loss. According to statistical analyses based on Mann Whitney test method with 5% of significant level, there is no significant difference between the MLVSS concentration in the first and second stage, that is, there is no influence of MLVSS concentration on MBR-MF and MBR-UF performance.

The average volumetric organic load (VOL) and feed/microorganism ratio was 2.3±0.8 kg/m^3.d and 0.6 ± 0.3 d^{-1} respectively. However, the operation under unstable F/M and COV conditions did not influenced the MBR performance since the MBR presented high organic matter removal capacity, which can be justified by the high biodegradability of the effluent (JANCZUKOWICZ *et al.*, 2008) and by the MBR robustness to operate in load variation conditions (JUDD, 2006). According to Spearman correlation test there are no correlation between VOL and MLVSS and MBR performance for a p-value=0.05.

The membrane of MBR shown good filtration performance since only a few permeability decay episodes was observed. These results suggest the biological sludge treating this type of effluent has low fouling potential and/or the chemical cleaning procedure was efficient to control the membrane fouling. The MF and UF membrane used in the MBR exhibited average permeability values of 68 ± 21 and 45 ± 15 L/m^2.h.bar. The significant differences of MF and UF membrane permeability was confirmed by statistical analyses based on Mann Whitney test method with p value=0.05. The membrane permeability variation can be associated to a MLVSS concentration. In this study it was found a negative correlation between permeability values and MLVSS concentration (Spearman R =-0.244, p-level=0.05).

2.3.2.3. MBR permeate quality

In addition to high organic matter removal, an efficient removal of ammonia and solids may also be noted. The high sludge retention time usually applied in MBRs contribute to the occurrence of nitrification in these systems, since nitrifying bacteria, which are responsible for the conversion of ammonium into nitrate, are notoriously slow growing micro-organisms (JUDD, 2006). The effluent became more coloured, which can be attributed to the microorganism byproducts; similar results were reported by Yigit *et al.* (2009) and Spagni *et al.* (2012). The sulphate concentrations of the MF and MBR permeates were 1762±113 and 2281±14 mg L^{-1}, respectively. The increase in the sulphate concentration after MBR

treatment was attributed to biodegradation of sulfonated organic compounds, such as indigo carmim, which is a possible contaminant in commercial indigo blue dye. Additionally, calcium and magnesium were retained in the MBR; this is associated with the interactions of the membrane with soluble microbial products and extracellular polymeric substance (EPSs), which have chelating properties (ARABI and NAKHLA 2010).

After MBR treatment, the effluent was already sufficiently pure for reuse in certain textile processes such as washing-off (Table 8).

Table 8: Permeate and concentrate physicochemical characteristics

Parameter	**MBR Permeate**	**Washing-off[a]**	**Equipment Washdown[a]**	**Dyeing[b]**
pH	8±0.26	7.0–8.0	6.5–8.0	3.0-10.0
EC (μS cm^{-1})	2461±504	-	-	-
Colour (HZ)	288±96	nv[c]	nv[c]	5
Indigo Blue (g L^{-1})	0	-	-	-
COD (mg L^{-1})	157±62	200	500–2000	-
Ammonia (mg L^{-1})	0.11±0.18	-	-	-
Phosphorus (mg L^{-1})	<2	-	-	-
Alkalinity (mg L^{-1})	498.52	-	-	-
Calcium (mg L^{-1})	25.21±1.15	-	-	-
Magnesium (mg L^{-1})	<1.25	-	-	-
Sulphate (mg L^{-1})	228.13±1.45	-	-	-
Hardness (mg L^{-1})	26.46±3.03	100	100	25
TS[a] (g L^{-1})	2.48±0.93	-	-	5
TVS[b] (g L^{-1})	0.73±1.02	-	-	100
Iron (mg L^{-1})	nm[e]	0.1	0.1	0.1
Manganese (mg L^{-1})	nm[e]	-	-	0.01
TSS[c] (g L^{-1})	nd[d]	-	-	5

-Not identified; *[a]VALH et al. 2011; [b]FIESP 2014; [c] None visble ; [d]not detected; [e]not measured*

2.4. Conclusion

Treatment of textile effluent with a combination of MF and MBR processes is sufficient to meet the reuse criteria for some industry activities, such as floor cleaning; however, further polishing is required to achieve the quality needed for other steps in the dyeing process.

The best operation condition in terms of applied pressure and pH, provided almost 60% and 99.5% of COD and colour removal, respectively. Also, the flux decline was mostly attributed to concentration polarization and the chemical cleaning was efficient enough to recover initial hydraulic resistance.

MF process showed to be completely efficient in separating and concentrating indigo blue.

MBR process provides a stable process, muffling such impacts, maintaining its permeate COD concentration and COD removal efficiency mostly constant throughout the time. Also, showing good efficiency in ammonia removal.

Raw textile effluent is not biodegradable due to dye chemical complexity, however MF permeate is much more biodegradable since the molecules weight are much smaller, being readily assimilated by the microorganisms.

2.5. References

AMARAL, M. C. S. Caracterização de Lixiviados Empregando Parâmetros Coletivos e Identificação de Compostos. 2007. 270p. Dissertação (Mestrado em Saneamento, Meio Ambiente e Recursos Hídricos). Escola de Engenharia da Universidade Federal de Minas Gerais (EE/UFMG), Belo Horizonte, 2007.

AMARAL, M.C.; FERREIRA, C.F.; LANGE, L.C.; AQUINO, S.F. (2009) Characterization of landfill leachates by molecular size distribution, biodegradability, and inert chemical oxygen demand. *Water Environment Research*, v. 81, n. 5, p. 499-505

ANDRADE, L.; MOTTA, G.; AMARAL, M. Treatment of dairy wastewater with a membrane bioreactor. *Brazinlian Journal Chemestry Engineering*, v. 30, p. 759–770, 2013.

ARABI, S. & NAKHLA, G. Impact of molecular weight distribution of soluble microbial products on fouling in membrane bioreactors. *Separation and Purification Technology*. v. 73, n. 3, p. 391-396, 2010.

BADANIA, Z.; AIT-AMARA, H.; SI-SALAH, A.; BRIK, M.; FUCHS, W. Treatment of textile waste water by membrane bioreactor and reuse. *Desalination*, v. 185, p. 411–417, 2005.

BAKER, R.W. *Membrane technology and applications*, 2. Ed. John Wiley & Sons Ltd, England, 2004.

BARKER D. J.; MANNUCCHI G. A.; SALVI S. M. L. e STUCKEY D. C. Characterization of soluble residual chemical oxygen demand (COD) in anaerobic wastewater treatment effluents. *Water Research*, v.33, n.11, p.2499-2510, 1999.

BARKER, J. R.; MILKE, M. W.; MIHELCIC, J. R. Relationship Between Chemical and Theorical Oxygen Demand for Specific Classes of Organic Chemicals. Water Research, v. 33, n. 2, p. 327-334, 1999.

BLANCO, J.; TORRADES, F.; MORÓN, M.; BROUTA-AGNÉSA, M.; GARCÍA-MONTAÑO, J. Photo-Fenton and sequencing batch reactor coupled to photo-Fenton processes for textile wastewater reclamation: feasibility of reuse in dyeing processes. *Chem. Eng*, v. 240, p. 469-475, 2014.

BRIK, M.; SCHOEBERL, P.; CHAMAM, B.; BRAUN, R., FUCHS; W. Advanced treatment of textile wastewater towards reuse using a membrane bioreactor. *Process Biochemistry*, v. 41, p. 1751–1757, 2006.

CHAKRABORTY, J. N. *Fundamentals and practices in colouration of textiles*. 1. ed. India: Woodhead Publishing, 2009. 400p.

CHEN, V.; YANGA, Y.; ZHOUA, M.;LIUA, M.; YUA,S.; GAOL, G. Comparative study on the treatment of raw and biological treated textile effluents through submerged nanofiltration. *Journal of Environmental Management*, v. 284, p. 121-129, 2015.

DASGUPTA, J.; SIKDER, J.; CHAKRABORTY, S.; CURCIO, S.; DRIOLI, E. Remediation of textile effluents by membrane based treatment techniques: A state of the art review. *Journal of Environmental Management*, v. 147, p. 55-72, 2015.

ELLOUZE, E.; TAHRI, N.; AMAR, R. B. Enhancement of textile wastewater treatment process using Nanofiltration. *Desalination*, v. 286, p. 16–23, 2012.

FRIHA, I.; BRADAI, M.; JOHNSON, D.; HILAL, N.; LOUKIL, S.; AMOR, F. B.; FEKI, F.; HAN, J.; ISODA, H.; SAYADI, S. Treatment of textile wastewater by submerged membrane bioreactor: *In vitro* bioassays for the assessment of stress response elicited by raw and reclaimed wastewater. *Journal of Environmental Management*, v. 160, p. 184-192, 2015.

GOZÁLVEZ-ZAFRILLA, J. M.; SANZ-ESCRIBANO, D.; LORA-GARCÍA, J.; LEÓN HIDALGO; M. C. Nanofiltration of secondary effluent for wastewater reuse in the textile industry. *Desalination*, v. 222, p. 272–279, 2008.

JANCZUKOWICZ, W.; ZIELINSKI, M.; DE˛BOWSKI, M. Biodegradability evaluation of dairy effluents originated in selected sections of dairy production. *Bioresource Technology*, v. 99, p. 4199–4205, 2008.

JEGATHEESAN, V.; PRAMANIK, B, K.; CHEN, J.; NAVARATNA, D.; CHANG, C.; SHU, L. Treatment of textile wastewater with membrane bioreactor: A critical review. *Bioresource Technology*, v. 204, p. 202-212, 2016.

JUDD, S. *The MBR Book*. Principles and Applications of Membrane Bioreactors in Water and Wastewater Treatment, Elsevier, Oxford, 2006.

LIU, M.; LÜ, Z.; CHEN, Z.; YU, S.; GAO, C. Comparison of reverse osmosis and nanofiltration membranes in the treatment of biologically treated textile effluent for water reuse. *Desalination*, v. 281, p. 372–378, 2011.

LUONG, T.V.; SCHMIDT, S.; DEOWAN, S.A.; HOINKIS, J.; FIGOLI, A.; GALIANO, F. Membrane bioreactor and promising application for textile industry in Vietnam. In: 13th Global Conference on Sustainable Manufacturing - Decoupling Growth from Resource Use, 2016, Bình Dương New City, Vietnam.

KHELIFI, E.; GANNOUN, H.; TOUHAMI, Y.; BOUALLAGUI, H.; HAMDI, M. Aerobic decolourization of the indigo dye-containing textile wastewater using continuous combined bioreactors. *Journal of Hazardous Materials*, v. 152, p. 683–689, 2008.

MANU, B. Physico-chemical treatment of indigo dye wate-water. *Color. Technol.*, v. 123, p. 197-202, 2007.

MONDAL, M.; DE, S. Treatment of textile plant effluent by hollow fiber nanofiltration membrane and multi-component steady state modelling. *Chemical Engineering Journal*, v.285, p. 304-3018, 2016

OECD. *Detailed review paper on biodegradability testing environment monograph*, n.98, 1995.

ROBINSON, T.; MCMULLAN, G.; MARCHANT, R.; NIGAM, P. Remediation of dyes in textile effluent: a critical review on current treatment technologies with a proposed alternative. *Bioresource Technology*, v. 77, p. 247-255, 2001.

SANROMAN, M. A.; PAZOS, M.; RICART, M. T.; CAMESELLE, C. Decolorization of textile indigo dye by DC electric current. *Eng. Geol.*, v. 77, p. 253-261, 2005.

SANTOS, C.D.; SCHERER, R.K.; CASSINI, A. S.; MARCZAK, L.D.F.; TESSARO, I.C. Clarification of red beet stalks extract by microfiltration combined with ultrafiltration. *Journal of Food Engineering*, v. 185, p. 35-41, 2016.

SPAGNI, A.; CASU, S.; GRILLI, S. Decolourisation of textile wastewater in a submerged anaerobic membrane bioreactor. *Bioresource Technology*, v. 117, p. 180–185, 2012.

SHAW, C. B.; CARLIELL, C. M.; WHEATLEY, A. D. Anaerobic/aerobic treatment of colored textile effluents using sequencing batch reactors. *Water Res.*, v. 36, p. 1993-2001, 2002.

VALH, J. V.; MARECHAL, A. M. L.; VAJNHANDL, S.; JERIC, T.; SIMON, E. *Treatise on Water Science:* Volume 4: Water-Quality Engineering. 1. ed. Slovenia: Elsevier, 2011. 22p.

VON SPERLING, M. *Lodos Ativados* (Activated sludge). Princípios do Tratamento Biológico de Aguas Residuárias (Principles of Biological Wastewater Treatment), Segrac, Belo Horizonte, 2005.

YIGIT, N. O.; UZAL, N.; KOSEOGLU, H.; HARMAN, I.; YUKSELER, H.; YETIS, U.; CIVELEKOGLU, G.; KITIS, M. Treatment of a denim producing textile industry wastewater using pilot-scale membrane bioreactor. *Desalination*, v. 240, p. 143-150, 2009.

UNLU, M.; YUKSELER, H.; YETIS, U. Indigo dyeing wastewater reclamation by membrane-based filtration and coagulation processes. *Desalination*, v. 240, p. 178-185, 2009.

ZHENG, Y.; YU, S.; SHUAI, S.; ZHOU, Q.; CHENG, Q.; LIU, M; GA, C. Color removal and COD reduction of biologically treated textile effluent through submerged filtration using hollow fiber nanofiltration membrane. *Desalination*, v. 314, p. 89–95, 2013.

3. INTEGRATION OF MICROFILTRATION AND A MEMBRANE BIOREACTOR AS A PRE-TREATMENT FOR NANOFILTRATION TO PROMOTE TEXTILE EFFLUENT REUSE

3.1. Introduction

A large variety of industries have arisen because of rapid socio-economic changes. However, the progress in these sectors has increased the pressure on natural resources, resulting in severe environmental degradation. Thus, environmental protection, which is attained through the use of sustainable processes, has become necessary for technological development.

Textile effluent characteristics may vary significantly because the dyeing process is carried out in batches; generally, the effluent has high chemical oxygen demand (COD), pH, turbidity, and salinity, contains significant amounts of inorganic salts and total dissolved solids (TDS), and is highly coloured (ASGHAR *et al.*, 2014, DASGUPTA *et al.*, 2015). These factors, which are associated with the remnant or spent resources of the dyeing process, impede the further application of the effluent. Also, these effluents are likely to have negative environmental impacts if discharged without appropriate treatment.

Indigo blue ($C_{16}H_{10}N_2O_2$) is a synthetic organic dye that is considered to be a persistent substance because of its complex chemical structure (MANU, 2007; SANROMAN *et al.*, 2005). Indigo blue is common in many commercial dyes because of the popularity of denim and is widely used in the textile industry, specifically for the production of jeans. Figure 14 shows the reaction for the oxidation/reduction of indigo blue.

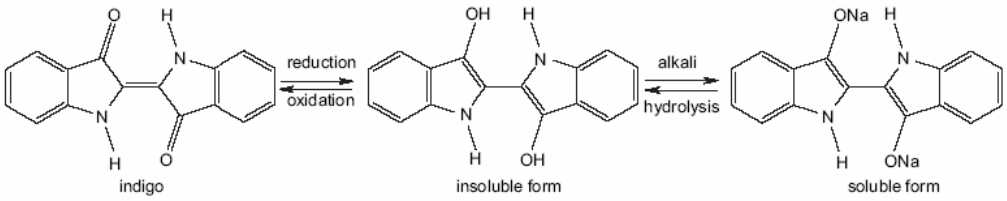

Figure 14: Oxidation/reduction of indigo blue

The stated drawbacks can be satisfactory overcome using membrane-based technologies, which include microfiltration, ultrafiltration, nanofiltration, reverse osmosis, or a combination of two or more of these processes. Membrane-based technologies are promising for the treatment of indigo blue–containing effluent, because they enable simultaneous

recovery of the dye and reduction of the colour and organic and inorganic load of the effluent.

Filtration processes that involve microfiltration (MF) or ultrafiltration (UF) also enable recovery of the indigo blue because the dye molecules are stable and insoluble in aqueous media; thus, MF and UF processes may be used to recover the pigment for reuse in the dyeing process. However, MF and UF produce a permeate which can still contain other chemical products used in the dyeing process, such as auxiliary chemicals.

Promising results with respect to water reuse have been reported using a membrane bioreactor (MBR). The use of MBR has resulted in a removal efficiency greater than 95% for COD and biological oxygen demand (BOD) and 99% for colour from a highly concentrated mixed wastewater obtained from the wet processes of denim production (YIGIT *et al.*, 2009; SPAGNI *et al.*, 2012). However, the inorganic dissolved solids could not be removed using MF or UF, which prevents water reuse. However, the product generated by the MBR can be directly used for other applications such as washing and rinsing the tanks in the production line and on-site irrigation. The MBR effluents require further purification for reuse for the dyeing process (BRIK *et al.*, 2005; FRIHA *et al.*, 2015).

Among pressure-driven membrane processes, nanofiltration (NF) has been found to be the most efficient for the treatment of textile wastewater because of its unique separation characteristics, which include size exclusion, electrostatic repulsion, and lower energy consumption; in addition, the resultant effluent has potential for reuse (CHEN *et al.*, 2015; LIN *et al.*, 2015).

Permeate flux is one of the most important factors for the assessment of membrane performance and economic feasibility because it reflects the amount of solute and solvent that pass through the membrane (LIU *et al.*, 2011). The reduction of permeate flux with time is known to be a major issue for pressure-driven membranes; this is mainly due to membrane fouling caused by the deposition of organic and inorganic compounds, colloids, suspended solids, and bacteria onto the membrane surface (ELLOUZE *et al.*, 2012)

Within this context, this study aims to investigate the viability of the integration of MF, an MBR, and NF for the recovery of dye and production of high-quality, reusable water from a textile effluent, specifically, from dyeing processes involving indigo blue.

3.2. Experimental

3.2.1. Effluent Source

Effluent source was carried out accordingly to section 2.2.1.

3.2.2. Analytical Methods

The colour, COD, ammonia, and TDS contents of the effluent were analysed following methods 2120 C, 5220 D, 4500-NH_3 B C, and 2540 B E, respectively, of the Standard Methods for the Examination of Water and Wastewater (APHA, 2005). The pH was measured according to method 4500 H B using a digital, calibrated pH meter. The TOC was analysed using a TOC Shimadzu TOC-V CNP instrument. The conductivity was determined following method 2510 B using a calibrated conductivity meter (Condutivímetro Hach 44600), and the indigo blue content was determined using a colourimetry test. Concentration of Cl^-, SO_4^{2-}, PO_4^{3-}, Mg and Ca will be measure by ion chromatography (ICS-1000 ion chromatograph equipped with the Dionex AS-22 column and ICS 12a).

3.2.3. Experimental Apparatus

The feed temperature was maintained at 20±5°C using an immersed coil.

Figure 15 shows a schematic of the laboratory-scale MF-MBR-NF hybrid system. The effluents were treated by MF to recover the dye in a concentrated stream. MF was conducted using a commercial membrane module (PAM Membranas LTDA) containing a polyetherimide-based polymer with an average pore diameter of 0.4 μm and filtration area of 1.0 m^2. In all the experiments, the pressure was measured using a manometer and adjusted via a needle-type valve. MF was performed under concentrated-mode filtration, which involved collection of the permeates in a separate tank and return of the concentrates to a feed tank at a constant pressure of 1 bar, cross-flow rate of 2.4 L min^{-1}, and maximum recovery rate of 80%. The permeate MF was treated in the MBR (bioreactor volume: 4 L; hydraulic retention time: 8 h; sludge retention time: 30 d), and the MBR permeate was further treated using NF

membranes. The MBR was equipped with a commercial submerged membrane module (ZeeWeed) with a polyvinylidene fluoride (PVDF)-based polymer with an average pore diameter of 0.04 µm and filtration area of 0.047 m^2. The MBR was operated for 357 days, under continuous aeration and intermittent permeation (15 min of suction and 15 s of backwashing) to reduce membrane fouling. Nanofiltration was carried out using an NF90 membrane (Dow Filmtec). This membrane has a molar weight cut-off of 100 Da (ZULAIKHA *et al.*, 2014), average membrane hydraulic resistance of 5.8 × 10^{13} m^{-1}, and rejection rates of NaCl (2000 mg L^{-0}) and $MgSO_4$ (2000 mg L^{-1}) of 85–95% and 97%, respectively (DOWFILMTEC™). The NF unit had a maximum operating pressure of 15 bar, which was obtained using a rotary vane pump equipped with a speed controller at a maximum flow of 530 L h^{-1}. A needle-type valve was used to adjust the feed flow rate and trans-membrane pressure. The pressure was measured using a manometer. NF was conducted using a stainless-steel membrane cell with a diameter of 9 cm and filtration area of 63.6 cm^2. The flat-sheet commercial membranes were cut to fit the membrane cell, and a 28 mil (25.4 µm) feed spacer was placed over the membrane to promote flow distribution. The feed temperature was maintained at 20±5°C using an immersed coil.

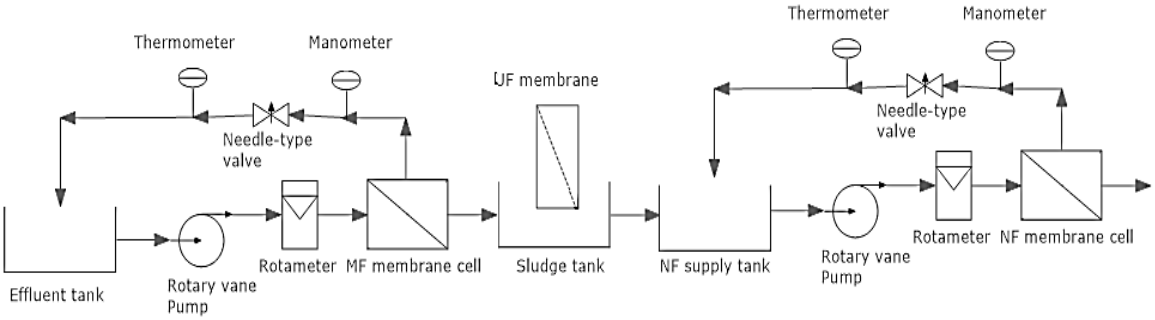

Figure 15: Schematic of the MF-MBR-NF bench-scale units

3.2.4. Experimental Procedure

The NF experiments were carried out on the MBR permeate at various TMPs, pH values, flow rates, and recovery rates. The TMP was controlled at 8, 10, 12, or 15 bar, and the feed pH was adjusted to be 7, 8, 9, or 11 using 1 M NaOH and 1:1 H_2SO_4 solutions. The flow rate was adjusted to be 0.8, 1.6, 2.4, or 3.2 L min^{-1} by changing the pump speed. Under each set of operating conditions, the following procedure was used: (1) De-ionized water was filtered at three different TMPs (i.e. 10, 12, and 15 bar) until a constant flux was obtained at each

pressure, (2) the MBR permeate was filtered under the selected conditions, (3) the fouled membrane module was washed with flowing de-ionized water for two minutes under a flow rate of 1.2 L min^{-1} to remove the foulants that were loosely deposited on the membrane surface, (4) de-ionized water was filtered for 20 minutes at a TMP of 10 bar, (5) the membrane was chemically cleaned using citric acid (pH 2) followed by NaOH (0.4% m/m), and (6) de-ionized water was filtered at three different TMPs (i.e. 10, 12, and 15 bar) until a constant flux was obtained at each pressure. All tests were conducted in duplicate. The flux rate was measured every 10 min, and 50 ml of the permeate samples were collected every 20 min.

3.2.5. Calculations

The volumetric permeate flux (J) in terms of litres per square meter per hour (L m^{-2} h^{-1}) was calculated using Eq. (1), as follows:

$$J = \frac{V}{A \times \Delta t}, \quad (1)$$

where A is the effective area of the membrane module for permeation and V is the volume of permeate collected over a time interval of Δt.

Flux normalization to 25 °C was accomplished by means of a correction factor related to the fluid viscosity, according to Eq. (2):

$$J = \frac{V}{A \cdot t} \cdot \frac{\mu(T)}{\mu(25°C)} \quad (2)$$

where J is the normalized permeate flux at 25 °C, $\mu(T)$ is the water viscosity at the process temperature, and $\mu(25\,°C)$ is the water temperature at 25 °C.

The membrane water permeability (K) for each test was obtained from the linearization of the ratio of normalized permeate flux of pure water (J) by applied pressure (ΔP) at 12.0, 10.0, 8.0, and 6.0 bar.

The observed rejection was calculated using Eq. (2), as follows:

$$R(\%) = \frac{C_f - C_p}{C_f} \times 100, \quad (3)$$

where C_f and C_p represent the solute content on the feed and permeate streams, respectively.

According to the simplified resistance-in-series model, the total filtration resistance could be divided into membrane resistance and fouling resistance. The membrane resistance to filtration (R_M) was determined from Eq. (4):

$$R_M = \frac{1}{K \cdot \mu(25°C)} \quad (4)$$

The total fouling resistance to filtration (R_f) was calculated based on the values of the normalized effluent permeate flux (J_{sd}) obtained near the end of each experiment (Eq. 5). This resistance includes the concentration polarization, the adsorption of components on the membrane surface and scaling.

$$R_f = \frac{\Delta P - \Delta\pi}{\mu(25°C) \cdot J_{sd}} - R_M \quad (5)$$

where ($\Delta P - \Delta\pi$) is the process effective pressure, i.e., applied pressure minus osmotic pressure. The osmotic pressure difference was calculated using the van't Hoff equation (Eq. 6):

$$\Delta\pi = \sum_{i=0}^{n} (C_r - C_p) \cdot R \cdot T \quad (6)$$

where C_r and C_p are the concentrations of solute "i" on the retentate and permeate, respectively, R is the universal gas constant, and T is the temperature in Kelvin.

The fouling resistance (R_f) is a combination of the resistance of the reversible fouling (R_{fr}) and irreversible fouling layer (R_{fir}), as follows [19]. R_{fr} is mostly due to the deposition of a cake layer on the membrane surface, which can be removed through physical cleaning, such as water washing; thus, it can be controlled by adjusting the feed flow conditions. R_{fir} is due to materials that adsorb onto the membrane surface and into the pores that can be removed by chemical cleaning.

The total flux decline (FD) was also calculated, as follows:

$$FD = \frac{(J_w - J_{sd})}{J_w}. \quad (7)$$

where J_w is the volumetric permeate flux of pure water of the membrane before effluent filtration.

Flux decline can be attributed to concentration polarization (CP) and fouling (F); thus, the flux decline due to CP was obtained using Eq. (8), as follows:

$$CP = \frac{(J_{pc} - J_{sd})}{J_{wc}}, \quad (8)$$

where J_{pc} is the volumetric water flux of the physically cleaned membrane after effluent filtration.

The flux decline due to fouling (F) was obtained using Eq. (9), as follows:

$$F = \frac{(J_w - J_{pc})}{J_w}. \quad (9)$$

The specific energy consumption (SEC) was calculated from the relation between the rate of work done by the pump (W_{pump}) and permeate flow rate (Q_p) using Eq. (10) [29], as follows:

$$SEC = \frac{W_{pump}}{Q_p}, \quad (10)$$

where

$$W_{Pump} = \Delta p \times Q_f, \quad (11)$$

where Q_f is the volumetric feed flow rate and Δp is assumed to be equivalent to the permeate pressure.

The permeate product water recovery for NF processes (Y) can be defined using Eq. (12), as follows:

$$Y = \frac{Q_p}{Q_f}. \quad (12)$$

By combining Eqs. (7), (8), and (9), the equation to determine SEC can be rewritten as follows:

$$SEC = \frac{\Delta P}{Y}. \quad (13)$$

3.2.6. Statistical Evaluation

Due to the small quantity of data (i.e. seven data points per NF test), a non-parametric statistical test was used. Kruskal Wallis' test was used to check for significant differences between the evaluated parameters, and then non-parametric multiple comparisons were investigated among the groups (α = 5%). STATISTICA 8.0 software was used for all statistical analyses.

3.3. Results and Discussion

3.3.1. MF and MBR Performance

Textile wastewater has highly variable salinity (expressed here in terms of electrical conductivity (EC)) and colour because it comprises a complex mixture of chemicals that depends on the colour of the jeans and the fibres used in the processes (Table 9). Although the dyeing processes that use indigo blue occur in the pH range of 10.5 to 11.5, the raw effluent could be neutral, as supported by the literature (CHEN *et al.*, 2015; GOZALVEZ-ZAFRILLA *et al.*, 2008). Also, the effluent is highly coloured and has high COD.

It was possible to obtain approximately 100% colour removal and reduce the COD and conductivity by about 65% and 26%, respectively, using the MF process. The indigo blue dye

was efficiently retained by the MF membrane (100%), which allows its recovery from the concentrate stream.

MBR was applied as a second-stage treatment process to improve the effluent characteristics. The MBR resulted in COD and ammonia removal of 73% and 100%, respectively. After MBR treatment, the effluent became more coloured, which was attributed to the byproducts of the microorganisms; similar results were reported by Yigit *et al.* (2009) and Spagni *et al.* (2012). The sulphate concentrations of the MF and MBR permeates were 1762±113 and 2281±14 mg L^{-1}, respectively. The increase in the sulphate concentration after MBR treatment was attributed to biodegradation of sulfonated organic compounds, such as indigo carmim, which is a possible contaminant in commercial indigo blue dye. Additionally, calcium and magnesium were retained in the MBR; this is associated with the interactions of the membrane with soluble microbial products and extracellular polymeric substance (EPSs), which have chelating properties (ARABI and NAKHLA 2010).

The MBR was operated for 370 days. During this period, the performance of the MBR system was not adversely affected by variations in the influent characteristics.

The requirements for water quantity in the textile industry vary according to the process, i.e. the yarn and technology applied; for example, dyeing, desizing, and bleaching processes use 8–300, 3–9, and 3–124 L kg^{-1} of cotton, respectively (VALH *et al.*, 2011). The water quality required is also dependent on the process, and the dyeing step (i.e. fabric wash-off) has the highest quality restrictions (Table 10). Thus, it is necessary to produce high quality water from industrial effluent for reuse.

After MBR treatment, the effluent was already sufficiently pure for reuse in certain textile processes such as equipment and floor washing. However, an additional polishing step, such as nanofiltration, is required to obtain the quality necessary for reuse in processes with higher quality requirements such as in the dye baths (Table 10).

Table 9: Physicochemical characteristics of the MF and MBR permeates

Parameter	Raw effluent	MF Concentrate	MF Permeate	MBR Permeate	% MF efficiency	% BRM Efficiency
pH	7.64±3.91	8.22±.3.91	8.68±0.29	8±0.26	-	-
EC ($\mu S\ cm^{-1}$)	3275±1980	16375±1980	2433±979	2461±504	25.71	-1.150
Colour (HZ)	7129±3186	35644±3186	0	288±96	100	-288
Indigo Blue ($g\ L^{-1}$)	0.48±0.09	2.4±0.09	0	0	100	-
COD ($mg\ L^{-1}$)	1771±396	6407±396	612±170	164±54	65.44	73.20
Ammonia ($mg\ L^{-1}$)	10.16±9.33	24.37±9.33	6.60±9.76	0.11±0.18		100
Phosphorus ($mg\ L^{-1}$)	<2	<2	<2	<2	-	-
Alkalinity	530.33	430	473.33	458.52	10.75	3.13
Calcium ($mg\ L^{-1}$)	37.79±4.24	25.69±6.81	32.69±1.53	25.21±1.15	13.48	20.40
Magnesium ($mg\ L^{-1}$)	<1.25	<1.25	<1.25	<1.25	-	-
Sulphate ($mg\ L^{-1}$)	178.67±2.02	223.56±0.47	259.32±84.82	228.13±1.45	6.87	-37.10
Total solids ($g\ L^{-1}$)	4.87±3.53	15.76±0.54	3.62±2.09	2.48±0.93	25.68	31.57
Total volatile solids ($g\ L^{-1}$)	1.10±0.29	5.2±0.12	0.99±1.21	0.73±1.02	9.37	26.91

-Not identified

Table 10: Water quality requirements for each process in the textile industry

Parameter	Recycled Effluent[a]	Washing-off[a]	Equipment Washdown[a]	Starching[b]	Washing[b]	Bleaching[b]	Dyeing[b]
Colour (Hazen)	nv[c]	nv[c]	nv[c]	5	5	5	5
EC (µs cm^{-1})	-	-	-	-	-	-	-
COD (mg L^{-1} O_2)	20–50	200	500–2000	-	-	-	-
pH	6.5–7.5	7.0–8.0	6.5–8.0	6.5–10	3.0–10.5	2.0–10.5	3.5–10
Total hardness (mg L^{-1})	90	100	100	25	25	25	25
Chloride (mg L^{-1})	500	500–200	3000–4000	-	-	-	-
Sulfate (mg L^{-1})	-	-	-	-	-	-	-
Fe (mg L^{-1})	0.1	0.1	0.1	0.3	0.1	0.1	0.1
Cu (mg L^{-1})	0.005	0.05	0.05	-	-	-	-
Cr (mg L^{-1})	0.01	0.1	0.1	-	-	-	-
Al (mg L^{-1})	0.02	-	-	-	-	-	-
Mn (mg L^{-1})	-	-	-	0.05	0.01	0.01	0.01
Zn (mg L^{-1})	-	-	-	-	-	-	-
TDS (mg L^{-1})	-	-	-	-	-	-	-
TSS (mg L^{-1})	-	-	-	5	5	5	5
TVS (mg L^{-1})	-	-	-	100	100	100	100

[a]VALH et al. 2011; [b]FIESP 2014; [c] None visble

3.3.2. Effect of TMP on the NF Flux and Permeate Characteristics

The applied pressure is one of the most critical factors in a membrane process. At each applied TMP, the permeate flux decreased gradually with increased operating time because of concentration polarization and/or fouling (Figure 16).

Although the permeate flux increased with increasing TMP (from 8 to 15 bar) (Figure 15), higher TMPs led to higher flux declines (Table 11); this phenomenon was also noted by Chen *et al.* (2015) and Amar *et al.* (2009). The initial and final permeate flux reached values of 52.83, 50.93, 42.83, and 34.03 and 45.46, 46.95, 39.61, and 32.70 L m^{-2} h^{-1} at 8, 10, 12, and 15 bar, respectively. The flux decline is mainly associated with fouling and CP phenomena, which increase the osmotic pressure at the membrane–effluent interface, thereby increasing the osmotic pressure across the membrane and reducing the driving force and flux (AOUNI *et al.*, 2012, CHIDAMBARAM *et al.*, 2015). For TMP values ranging from 8–12 bar, the majority of the flux decline was attributed to CP, which increases with increasing TMP. The flux decline due to CP reached 4, 5%, and 7% at 8, 10, and 12 bar, respectively. According to Chen *et al.* (2015), a rise in osmotic pressure due to concentration polarization has more impact than an increase in the resistance to mass transfer, known as cake formation and pore blocking, which generally increase the resistance to permeation. An increase in applied TMP leads to a rise in the initial flux values based on Darcy's law. However, the driving force was greater at higher pressures; therefore, there was an increase in the movement of both solvent and solutes towards the membrane surface resulting in greater accumulation of pollutants. This led to augmented concentration polarization and fouling resulting in a sharp flux decline (MUKHERJEE *et al.*, 2016). The high contribution of fouling to flux decline at a TMP of 15 bar suggests that the increase in the concentration polarization with increasing TMP (12 to 15 bar) implies that solute precipitation onto the membrane surface contributes to membrane fouling.

Cake formation and pore blocking are the most predominant mechanisms of NF membrane fouling; they increase the resistance to the permeation via both external fouling (cake layer) and internal fouling (adsorption and pore blocking) (CHEN *et al.*, 2015).

The increase in fouling resistance with increasing TMP correlated with flux decline (Table 11). This phenomenon was also observed by Chen *et al.* (2015). At TMPs of 8 to 12 bar, R_{fr} is greater than the R_{fir}, indicating that the cake layer contributes more significantly to the

fouling resistance than adsorption of materials onto the membrane surface and pore blocking. At 15 bar, the higher R_{fir} supports the hypothesis of solute precipitation onto the membrane surface.

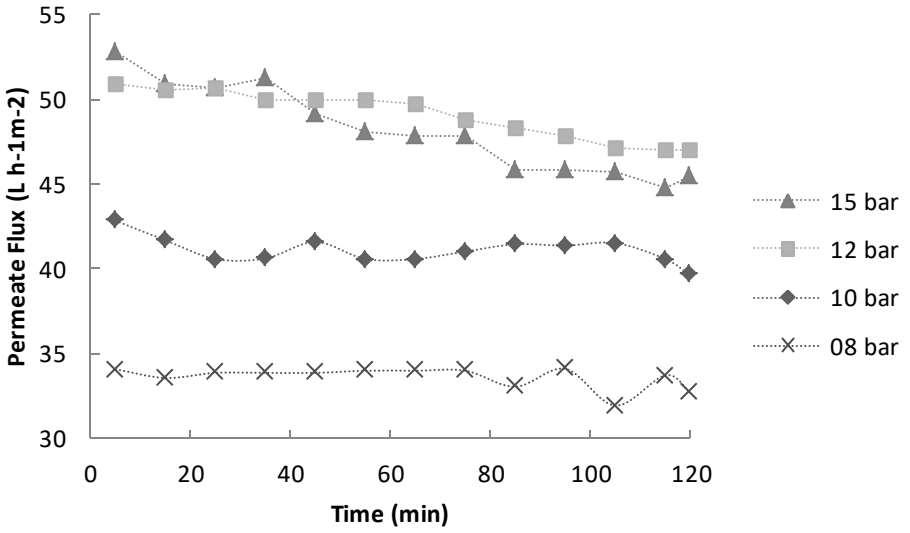

Figure 16: Time dependent flux decline as a function of TMP

Also, calculating the membrane hydraulic resistance (Table 11) after membrane chemical cleaning (R_{cc}) for each TMP test using Eq. (22) revealed that a higher TMP leads to a lower chemical cleaning efficiency. In fact, chemical cleaning was only efficient when applied to membranes operated at 10 and 8 bar. These results suggest that the high concentration polarization and fouling that occurs at high TMP values results in the precipitation of salts onto the membrane surface. Accordingly, it is important to optimize the chemical cleaning for membrane operation at high TMPs to ensure membrane permeability and the sustainability of the process.

The specific energy consumption, which directly affects the operational costs, was also calculated for each test in order to optimize the process. The results showed that the SEC decreased with decreasing TMP (Table 11) for the MBR permeate with slight differences as the TMP was increased from 8 to 10 bar and 10 to 12 bar.

The quality of the composite permeates obtained from experiments at 8, 16, 24, and 32 bar were compared with the corresponding feed values in Table 12. As is evident from the table, the NF rejection capacity for COD decreases with increasing TMP: As the TMP increases from 8 to 15 bar, the average COD concentration increased from about 28.9 to 41.2 mg L^{-1}.

The higher CP causes an increase in the solute concentration at the membrane surface; therefore, because the intrinsic retention of the membrane remains unchanged, the amount of solute transferred to the permeate increases. The results also indicated that the NF membrane effectively retains the solution and removes indigo blue and ammonia. The EC and TOC were independent of the TMP. It is important to note that, even at the highest TMP of 15 bar, which resulted in the lowest quality water, the quality of the permeate is sufficient for the most stringent processes of the textile industry.

Table 11:Water and permeate flux, flux decline, and hydraulic resistance (i.e. R_m, R_f, R_{fr}, R_{fir}, and R_{cc}) and specific energy consumption when applying NF at 20°C, 7.86 pH, a flow rate of 2.4 L min^{-1}, and various TMPs

TMP (bar)	Jw (L m^{-2} h^{-1})	Jsd_0[a] (L m^{-2} h^{-1})	Jsd_f[b] (L m^{-2} h^{-1})	Jw_{fc}[c] (L m^{-2} h^{-1})	Jw_{cc}[d] (L m^{-2} h^{-1})	Flux decline type			Hydraulic Resistance (x10^{13} m^{-1})					Chemical Cleaning Efficiency (%)	SEC (kWh $m^{-3}m^{-2}$)
						Total (%)	Fouling (%)	CP[e] (%)	R_m	R_f	R_{fr}	R_{fir}	R_{cc}		
15	72.81	52.83	45.46	55.28	71.20	37	24	13	6.65	5.21	2.11	3.10	0.10	96.75	13197
12	62.34	50.93	46.95	57,95	57.08	25	7	18	6.75	2.44	1.74	0.70	0.76	61.83	10223
10	47.87	42.82	39.61	45,27	48.29	17	5	12	7.51	1.57	1.13	0.43	0	105.05	10097
8	38.63	34.03	32.70	36.97	39.77	15	4	11	7.44	1.35	1.02	0.33	0	119.19	9787

[a]initial effluent permeate flux; [b]final effluent permeate flux; [c]water permeate flux after physical cleaning; [d]water permeate flux after chemical cleaning; [e]concentration polarization

Table 12: NF permeate characteristics

Parameter	MBR permeate	Permeate concentration				Observed rejection (%)			
		15 bar	12 bar	10 bar	8 bar	15 bar	12 bar	10 bar	8 bar
COD (mg L^{-1})	129.350	41.18±5.89	35.73±4.06	30.30±2.55	28.89±6.73	68.17±4.55	72.38±3.14	76.58±1.97	77.66±5.20
pH	7.86	8.39±0.31	8.22±0.22	7.11±0.05	8.23±0.14	-	-	-	-
EC (µS cm^{-1})	1855.09	34.89±1.79	35.23±7.05	33.46±3.13	35. 46±2.25	98.12±0.09	98.10±0.38	97.42±0.67	97.55±0.12
Colour (HZ)	274.56	0	0	0	0	100	100	100	100
NH_3 (mg L^{-1})	0	0	0	0	0	-	-	-	-

-Not identified

Thus, considering the flux decline, energy consumption, permeate production, permeate characteristics, and operational conditions, the optimal TMP was determined to be 12 bar because TMPs below 15 bar require finicky operational conditions and greater energy. Also, according to the Kruskal Wallis' test, there is no statistical difference between the characteristics of the permeates obtained at 12 bar and those obtained at 8 and 10 bar in terms of COD removal, being statistically different to results obtained at 15 bar (p-value=5%).

3.3.3. Effect of pH on the Flux and Permeate Characteristics

One of the factors that has a significant effect on the denim dyeing process is the pH of the indigo bath. The ideal dyeing pH is from 10.5 to 11.5 at which the performance of the dye is optimized (CHAKRABORTY, 2009). During biological processes, the pH was monitored and controlled to be close to neutral. However, eventually a shock load in the effluent can occur resulting in high MBR permeate pH values. According to the membrane supplier, NF90 should not be constantly operated at pH values greater than 10.0 (DOWFILMTEC™). Furthermore, the effluent pH can affect the membrane surface charge and, therefore, membrane separation performance. To examine the effects of the effluent pH on membrane performance, filtration procedures were performed at pH values of 7, 8, 9, and 11 (Table 13).

The results showed a decrease in permeate flux with increasing pH (from 7 to 11) (Figure 17). The final permeate flux were 57.95, 52.14, 48.10, and 45.20 L m^{-2} h^{-1} at pH values of 7, 8, 9, and 11, respectively. The charge of the membrane is an important parameter with respect to flux decline and the retention values at different pH values. The electrical charges of the functional groups of the membrane are dependent on the effluent pH. The membranes are positively and negatively charged at pH values below and above the isoelectric point, respectively (ERNST *et al.*, 2000). The isoelectric point of the NF90 membrane is pH 4 (BELLONA and DREWES, 2005). In general, the dissolved components in the raw effluent and EPSs produced during biological degradation are negatively charged. The increased electrostatic repulsion between the membrane and solutes promotes an increase in the flux decline and CP with increasing pH.

For feed pH values of 7 to 8, the highest flux decline occurred due to CP. Increasing the pH from 8 to 9 resulted in an increase in the flux decline; this is likely due to fouling (i.e. salt precipitates on the membrane surface) rather than CP. However, upon increasing the pH of

the feed from 9 to 11, the flux decline due to fouling decreased (13% (pH 9) to 7% (pH 11)) and the contribution of CP increased (9% (pH 9) to 14% (pH 11)). The reduction of flux decline due to membrane fouling is associated with the lower conductivity and COD rejection during filtration at pH 11 (Table 14).

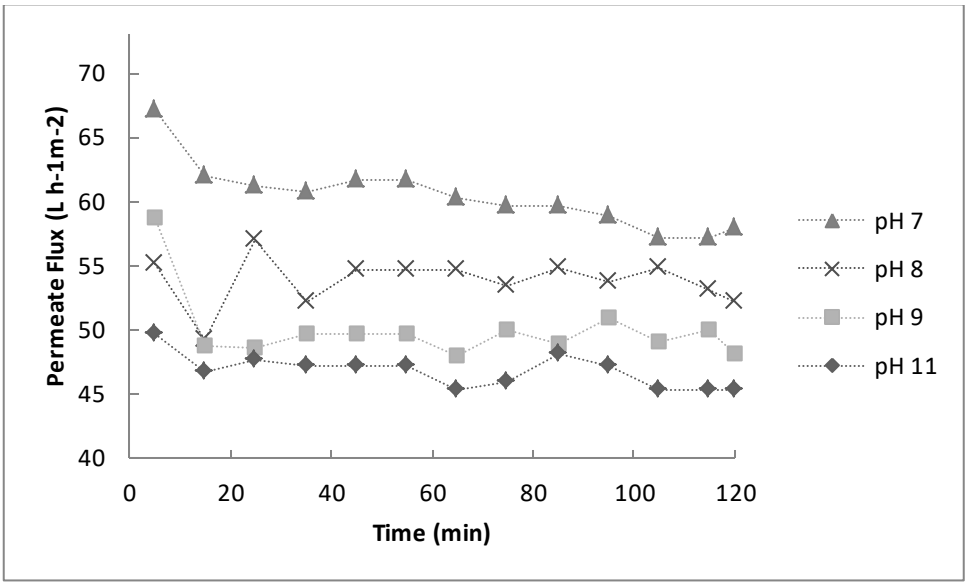

Figure 17: Time dependent flux decline as a function of pH

By studying a thin-film composite NF membrane, Dalwani *et al.* (2011) determined that the molecular weight cut-off of the membrane remained practically constant under acidic and neutral conditions. Conversely, under extremely alkaline conditions (pH 11) the molecular weight cut-off and effective average pore size increased. At pH 11, the zeta potential of the pore walls is highly negative; therefore, the electrostatic repulsion may cause pore enlargement, which would explain the results of this study.

Upon calculating the hydraulic resistance after membrane chemical cleaning (R_{cc}) for each test at various pH values, we noted that chemical cleaning was less efficient for recovery of the membrane permeability after filtration of pH 9 feed, which generated the highest membrane fouling.

According to the Kruskal Wallis' test, there is no statistical difference in the quality of the permeate obtained using feed with pH values ranging from 7 to 11 (p-value=0.05) (Table 14). These results suggest that the quality of the permeate is not affected by changes in the pH values of the effluent due to changing operating conditions during the dyeing and washing processes.

Table 13: Water and permeate flux, flux decline, and hydraulic resistance (i.e. R_m, R_f, R_{fr}, R_{fir}, and R_{cc}) when applying NF at 20°C and 12 bar with a flow rate of 2.4 L min^{-1} at various pH values

pH	Jw ($L\ m^{-2}\ h^{-1}$)	Jsd_0[a] ($L\ m^{-2}\ h^{-1}$)	Jsd_f[b] ($L\ m^{-2}\ h^{-1}$)	Jw_{fc}[c] ($L\ m^{-2}\ h^{-1}$)	Jw_{cc}[d] ($L\ m^{-2}\ h^{-1}$)	Flux decline type			Hydraulic Resistance ($x10^{13} m^{-1}$)				
						Total	Fouling	CP[e]	R_m	R_f	R_{fr}	R_{fir}	R_{cc}
7	61.20	61.98	57.95	60.73	60.23	5	1	5	6.96	0.48	0.57	0.00	0.22
8	60.23	55.17	52.14	56.89	61.68	13	6	8	7.18	1.09	0.69	0.40	0.00
9	61.68	58.62	48.10	53.50	54.44	22	13	9	6.80	2.16	0.91	1.26	1.00
11	56.7	49.61	45.20	53.03	54.13	21	7	14	7.81	1.72	1.39	0.33	0.30

[a]*initial effluent permeate flux;* [b]*final effluent permeate flux;* [c]*water permeate flux after physical cleaning;* [d]*water permeate flux after chemical cleaning;* [e]*concentration polarization*

Table 14: NF permeate characteristics

Parameter	MBR permeate	Permeate concentration				Observed rejection (%)			
		pH 7	pH 8	pH 9	pH 11	pH 7	pH 8	pH 9	pH 11
COD ($mg\ L^{-1}$)	114.72	46.2±0.9	38.9±1.4	43.4±3.9	43.5±3.0	72.9±1.7	77.2±0.8	74.6±2.3	74.0±1.3
pH	8.31	6.87±0.08	8.04±0.13	8.89±0.09	10.36±0.07	-	-	-	-
EC ($\mu S\ cm^{-1}$)	2378.06	31.16±1.73	30.90±4.24	37.04±7.20	125.61±9.80	98.68±0.07	98.70±0.18	98.44±0.30	94.72±0.41
Colour (HZ)	157.30	0	0	0	0	100	100	100	100
NH_3 ($mg\ L^{-1}$)	0	0	0	0	0	-	-	-	-

-Not identified

3.3.4. Effect of Flow Rate on the Flux and Permeate Characteristics

By increasing the feed flow rate, the cross-flow velocity increases and, consequently, the Reynolds number increases. This leads to a more turbulent flow, which improves the mass transfer conditions by facilitating the back diffusion of solutes retained by the membrane into the bulk solution and reducing CP. Consequently, the permeate flux increases for the following two reasons: Reduction of membrane fouling and reduction of osmotic pressure on the membrane surface, which increases the effective filtration pressure. Four cross-flow velocities of 0.21, 0.42, 0.63 and 0.84 cm s^{-1} were measured; these correspond to Reynolds numbers of 280, 559, 839, and 1118, respectively. According to Geraldes *et al.* (2002), for rectangular channels, the transition between laminar and turbulent flow occurs at a Reynolds number between 150 and 300 in the presence of spacers. Therefore, one of the sets of conditions in this study involved laminar flow while the others involved turbulent flow.

The total flux decline decreasesd with increasing cross-flow velocity from 0.21 to 0.63 cm s^{-1} (Figure 17); however, a further increase from 0.63 to 0.84 cm s^{-1} did not result in further fouling mitigation, which indicates that increasing the flow rate above 0.63 cm s^{-1} does not affect the permeate flux (Table 15). It was also observed that the majority of the flux decline was caused by concentration polarization. However, the improved hydrodynamic conditions mainly mitigated fouling, especially irreversible fouling: The flux decline due to fouling reduced from 9 to 1 and the irreversible fouling resistance reduced from 4.75 to 3.08 × 10^{13} m^{-1} upon increasing the cross-flow velocity from 0.21 to 0.84 cm s^{-1}.

Higher cross-flow velocities result in greater back transport from the membrane surface to the solution bulk; therefore, less solute enters the permeate channels (ROY *et al.*, 2015). The effect of this is evident in Table 16, which shows the increase in the efficiency of solute retention at higher feed flow rates.

Higher cross-flow velocities reduce membrane fouling resulting in greater membrane retention. However, higher cross-flow velocities require pumps with greater power, which consume more energy. Accordingly, the cross-flow velocity of 0.63 cm s^{-1} is regarded to be the threshold cross-flow velocity. Above this velocity, the fouling mitigation did not change significantly.

Table 15: Water and permeate flux, flux decline, and hydraulic resistance (i.e. R_m, R_f, R_{fr}, R_{fir}, and R_{cc}) when applying NF at 20°C, 12 bar, and pH 8 under various cross-flow rates

Cross Flow velocity (cm s^{-1})	Jw (L m^{-2} h^{-1})	Jsd_0 [a] (L m^{-2} h^{-1})	Jsd_f [b] (L m^{-2} h^{-1})	Jw_{fc} [c] (L m^{-2} h^{-1})	Jw_{cc} [d] (L m^{-2} h^{-1})	Flux decline type			Hydraulic Resistance (x10^{13} m^{-1})					SEC
						Total	Fouling	CP[e]	R_m	R_f	R_{fr}	R_{fir}	R_{cc}	(kWh m^{-3} m^{-2})
0.21	28.29	25.53	21.17	27.69	30.73	25	9	17	15.24	9.20	4.45	4.75	0.00	7,556
0.42	30.73	24.15	23.37	29.50	29.85	24	4	20	14.03	8.11	4.60	3.51	0.41	13,691
0.63	29.85	23.84	23.37	29.51	29.84	22	1	21	14.45	8.22	5.13	3.09	0.01	21,027
0.84	29.84	23.84	22.83	29.51	29.84	23	1	22	14.45	8.22	5.13	3.08	0.00	28,036

[a]initial effluent permeate flux; [b]final effluent permeate flux; [c]water permeate flux after physical cleaning; [d]water permeate flux after chemical cleaning; [e]concentration polarization

Table 16: NF permeate characteristics

Parameter	MBR permeate	Permeate concentration				Observed rejection (%)			
		0.21 (cm s^{-1})	0.42 (cm s^{-1})	0.63 (cm s^{-1})	0.84 (cm s^{-1})	0.21 (cm s^{-1})	0.42 (cm s^{-1})	0.63 (cm s^{-1})	0.84 (cm s^{-1})
COD (mg L^{-1})	165.26	30.248±4.77	30.867±2.68	28.41±3.54	25.94±5.08	81.70±2.89	81.94±2.68	82.81±2.75	84.30±3.07
pH	8.64	7.44±0.08	7.25±0.07	7.36±0.08	7.45±0.09	-	-	-	-
EC (µS cm^{-1})	3796.10	81.89±9.08	81.90±12.31	82.81±7.22	88.23±4.46	97.84±0.24	97.84±0.32	97.82±.21	97.68±.012
Colour (HZ)	384.58	0	0	0	0	100	100	100	100
NH_3 (mg L^{-1})	0	0	0	0	0	-	-	-	-

-Not identified

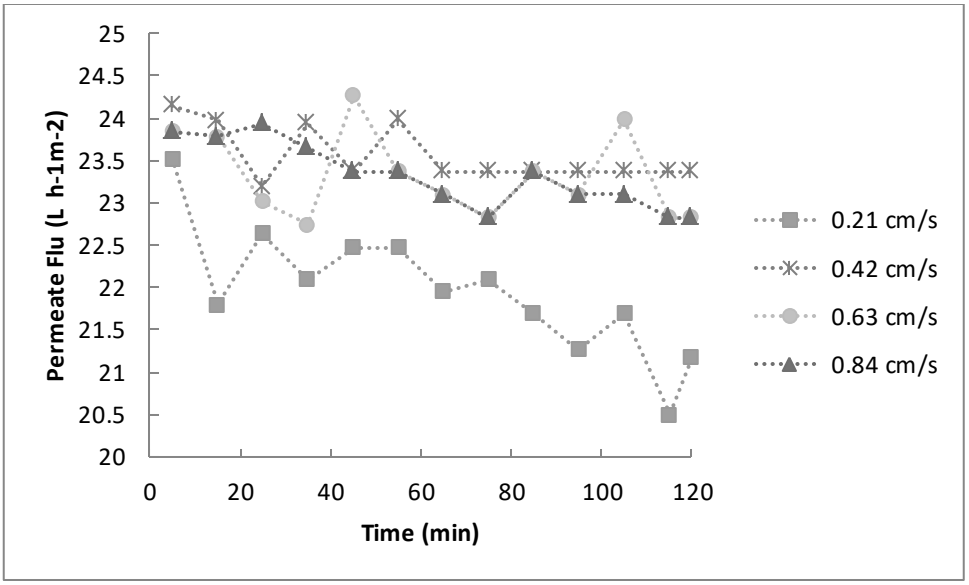

Figure 18: Time dependent flux decline as a function of cross flow velocities

3.3.5. Water Reuse in the Textile Industry

In the textile industry, the water quality for all processes must be sufficiently pure to avoid any problems with the process and quality of the final product. Although fresh softened water is used for all processes, water of lower quality can occasionally be used. As discussed in section 3.1., the water quality requirements depend on the process. Upon considering the quality restrictions shown in Table 10, it is evident that the NF permeate meets the quality requirements for all processes within the textile industry. Moreover, the NF concentrate has characteristics that meet the required water-quality standards for washing down equipment, screen washing for the print works, and general washing of print paste containers and floors (Table 17).

Table 17: Permeate and concentrate physicochemical characteristics

Parameters	MF permeate	BRM Permeate	NF concentrate	NF permeate
pH	8.68±0.29	8±0.26	8.54	8
EC ($\mu S\ cm^{-1}$)	2433±979	2461±504	8100	30.90±4.24
Colour (HZ)	0	288±96	0	0.00
Indigo Blue ($g\ L^{-1}$)	0	0	0	0.00
COD ($mg\ L^{-1}$)	612±170	164±54	515.77	34.35±5.38
Ammonia ($mg\ L^{-1}$)	6.60±9.76	0.11±0.18	0	0.00
Phosphorus ($mg\ L^{-1}$)	<2	<2	<2	<2
Alkalinity ($mg\ L^{-1}$)	573.33	498.52	1146.67	31.53
Calcium ($mg\ L^{-1}$)	32.69±1.53	25.21±1.15	66.64±1.73	<2.50
Magnesium ($mg\ L^{-1}$)	<1.25	<1.25	22.81±23.13	<1.25
Sulphate ($mg\ L^{-1}$)	259.32±84.82	228.13±1.45	291.52±0.35	<2.00
Hardness ($mg\ L^{-1}$)	30.1±2.29	26.46±3.03	58.27±4.23	<3.15
TS[a] ($g\ L^{-1}$)	3.62±2.09	2.48±0.93	6.28±1.25	nd[d]
TVS[b] ($g\ L^{-1}$)	0.99±1.21	0.73±1.02	1.82±0.98	nd[d]
Iron ($mg\ L^{-1}$)	0.16	nm[e]	0.26	nd[d]
Manganese ($mg\ L^{-1}$)	0.03	nm[e]	0.05	nd[d]
TSS[c] ($mg\ L^{-1}$)	nd[d]	nd[d]	nd[d]	nd[d]

[a]total solids; [b]total volatile solids; [c]total suspended solids; [d]not detected; [e]not measured

3.4. Conclusions

Treatment of textile effluent with a combination of MF and MBR processes is sufficient to meet the reuse criteria for some industry activities, such as floor cleaning; however, further polishing is required to achieve the quality needed for other steps in the dyeing process.

The principal cause of flux decline was determined to be concentration polarization; however, in most cases, chemical cleaning of the membrane was sufficient to regain the initial permeability, which demonstrates that the pre-treatment is effective.

The optimal TMP was determined to be 12 bar, at which good permeate characteristics were obtained with reasonable energy consumption; this is associated with a higher permeate flux. Feed pH values ranging from 7 to 11 were investigated and generated permeate with good characteristics; however, higher pH values of the NF feed resulted in increased membrane fouling. Higher cross-flow velocities led to decreased membrane fouling and higher membrane retention; however, they require increased energy. Accordingly, a cross-flow velocity of 0.63 cm s^{-1} was determined to be the threshold cross-flow velocity.

NF technology was successfully applied to polish textile effluent after filtration through MF and MBR processes. The NF permeate meets the quality requirements for all processes within the textile industry, while the NF concentrate can be used to wash equipment, screens in the printworks, print paste containers, and floors.

3.5. References

AMAR, N. B. KECHAOU, N.; PALMERI, J.; DERATANI, A.; SGHAIER, A. Comparison of tertiary treatment by nanofiltration and reverse osmosis for water reuse in denim textile industry. *Journal of Hazardous Materials*, v. 170, p. 111–117, 2009.

AOUNI, A.; FERSI, C; CUARTAS-URIBE, B; BES-PÍA, A.; ALCAINA-MIRANDA, M. I.; DHAHBI, M. Reactive dyes rejection and textile effluent treatment study using ultrafiltration and nanofiltration processes. *Desalinization*, v. 297, p. 87-96, 2012.

APHA. *Standard Methods for the Examination of Water and Wastewater*. 21 ed. Washington: American Public Health Association, 2005.

ARABI, S. & NAKHLA, G. Impact of molecular weight distribution of soluble microbial products on fouling in membrane bioreactors. *Separation and Purification Technology*. v. 73, n. 3, p. 391-396, 2010.

ASGHAR, A.; RAMAN, A. A. A.; DAUD, W. M. A. W. Advanced oxidation processes for in-situ production of hydrogen peroxide/hydroxyl radical for textile wastewater treatment: a review. *Journal of Cleaner Production*, v. 87, p. 826-838, 2015.

BELLONA, C.; DREWES, J. E. The role of membrane surface charge and solute physico-chemical properties in the rejection of organic acids by NF membranes. *Journal of Membrane Science*, v. 249, p. 227–234, 2005.

BLANCO, J.; TORRADES, F.; MORÓN, M.; BROUTA-AGNÉSA, M.; GARCÍA-MONTAÑO, J. Photo-Fenton and sequencing batch reactor coupled to photo-Fenton processes for textile wastewater reclamation: feasibility of reuse in dyeing processes. *Chem. Eng*, v. 240, p. 469-475, 2014.

BRIK, M.; SCHOEBERL, P.; CHAMAM, B.; BRAUN, R., FUCHS; W. Advanced treatment of textile wastewater towards reuse using a membrane bioreactor. *Process Biochemistry*, v. 41, p. 1751–1757, 2006.

BUSCIO, V.; MARÍN, M. J.; CRESPI, M.; GUTIÉRREZ-BOUZÁN, C.. Reuse of textile wastewater after homogenization–decantation treatment coupled to PVDF ultrafiltration membranes. *Chemical Engineering Journal*, v. 265,p. 122–128, 2015.

CHAKRABORTY, J. N. *Fundamentals and practices in colouration of textiles*. 1. ed. India: Woodhead Publishing, 2009. 400p.

CHEN, V.; YANGA, Y.; ZHOUA, M.;LIUA, M.; YUA,S.; GAOL, G. Comparative study on the treatment of raw and biological treated textile effluents through submerged nanofiltration. *Journal of Environmental Management*, v. 284, p. 121-129, 2015.

CHIDAMBARAM, T.; OREN, Y.; NOEL, M. Fouling of nanofiltration membranes by dyes during brine recovery from textile dye bath wastewater. *Chemical Engineering Journal*, v. 262, p. 156–168, 2015.

DALWANI, M.; BENES, N. E.; BARGEMAN, G.; STAMATIALIS, D.; WESSLING, M. Effect of pH on the performance of polyamide/polyacrylonitrile based thin film composite membranes. *Journal of Membrane Science*, v. 372, p. 228-238, 2011.

DASGUPTA, J.; SIKDER, J.; CHAKRABORTY, S.; CURCIO, S.; DRIOLI, E. Remediation of textile effluents by membrane based treatment techniques: A state of the art review. *Journal of Environmental Management*, v. 147, p. 55-72, 2015.

DE, S.; BHATTACHARYA, P. K. Prediction of mass-transfer coefficient with suction in the applications of reverse osmosis and ultrafiltration. *Journal of Membrane Science*, v. 128, p. 119-131, 1997.

ELLOUZE, E.; TAHRI, N.; AMAR, R. B. Enhancement of textile wastewater treatment process using Nanofiltration. *Desalination*, v. 286, p. 16–23, 2012.

Evironmental Protection Agency (EPA). *Guidelines for Water Reuse*. 1. Ed. Washington: U.S. Agency for International Development, 2004. 450p.

ERNST, M.; BISMARCK, A.; SPRINGER, J.; JEKEL, M. Zeta-potential and rejection rates of a polyethersulfone nanofiltration membrane in single salt solutions. *Journal of Membrane Science*, v. 165, p. 251-259, 2000.

FIESP/CIESP – *Conservação e Reúso de Água para a indústria, Manual de Orientações para o setor Industrial,* first ed., FIESP, São Paulo, 2004.

FRIHA, I.; BRADAI, M.; JOHNSON, D.; HILAL, N.; LOUKIL, S.; AMOR, F. B.; FEKI, F.; HAN, J.; ISODA, H.; SAYADI, S. Treatment of textile wastewater by submerged membrane bioreactor: *In vitro* bioassays for the assessment of stress response elicited by raw and reclaimed wastewater. *Journal of Environmental Management*, v. 160, p. 184-192, 2015.

GOZÁLVEZ-ZAFRILLA, J. M.; SANZ-ESCRIBANO, D.; LORA-GARCÍA, J.; LEÓN HIDALGO; M. C. Nanofiltration of secondary effluent for wastewater reuse in the textile industry. *Desalination*, v. 222, p. 272–279, 2008.

GERALDES, V.; SEMIAO, V.; PINHO, M. N. Flow management in nanofiltration spiral wound modules with ladder-type spacers. *Journal of Membrane Science*, v. 203, p. 87– 102, 2002.

LIU, M.; LÜ, Z.; CHEN, Z.; YU, S.; GAO, C. Comparison of reverse osmosis and nanofiltration membranes in the treatment of biologically treated textile effluent for water reuse. *Desalination*, v. 281, p. 372–378, 2011.

LIN, J.; TANG, C. Y.; YE, W. Y.; SUN, S.; HAMDAN, S. H.; VOLODIN, A.; HAESENDONCK, C. V.; SOTTO, A.; LUIS, P.; BRUGGEN, B. V. Unraveling flux behavior of superhydrophilic loose nanofiltration membranes during textile wastewater treatment. *Journal of Membrane Science*, v. 493, p. 690–702, 2015.

LYSTER; COHEN. Numerical study of concentration polarization in a rectangular reverse osmosis membrane channel: Permeate flux variation and hydrodynamic end effects. *Journal of Membrane Science*, v. 303, p. 140–153, 2007.

KAPDAN, I. K.; KARGIA, F.; MCMULLANB, G.; MARCHANT, R. Effect of environmental conditions on biological decolorization of textile dyestuff by C. *versicolor*. *Enzyme and Microbial Technology*, v. 26, p. 381–387, 2000.

MANU, B. Physico-chemical treatment of indigo dye wate-water. *Color. Technol.*, v. 123, p. 197-202, 2007.

MUKHERJEE, R.; MONDAL, M.; SINHA, A.; SARKAR, S.; DE, S. Application of nanofiltration membrane for treatment of chloride rich steel plant effluent. *Journal of Environmental Chemical Engineering*, v. 4, n. 1, p. 1-9, 2016.

ONG, Y. K.; LI, F. L.; SUN, S.; ZHAO, B.; LIANG, C.; CHUNG, T. Nanofiltration hollow fiber membranes for textile wastewater treatment: Lab-scale and pilot-scale studies. *Chemical Engineering Science*, v. 114, p. 51–57, 2014.

PASCHOAL, F. M. M.; TREMILIOSI-FILHO, G. Aplicação da tecnologia de eletrofloculação na recuperação do corante índigo blue a partir de efluentes industriais. *Quími. Nova*, v. 28, p. 766-772, 2005.

ROBINSON, T.; MCMULLAN, G.; MARCHANT, R.; NIGAM, P. Remediation of dyes in textile effluent: a critical review on current treatment technologies with a proposed alternative. *Bioresource Technology*, v. 77, p. 247-255, 2001.

ROY, Y.; SHARQAWY, M. H.; LIENHARD J. H. Modeling of flat-sheet and spiral-wound nanofiltration configurations and its application in seawater nanofiltration. *Journal of Membrane Science*, v. 493, p. 360–372, 2015.

SANROMAN, M. A.; PAZOS, M.; RICART, M. T.; CAMESELLE, C. Decolorization of textile indigo dye by DC electric current. *Eng. Geol.*, v. 77, p. 253-261, 2005.

SHAW, C. B.; CARLIELL, C. M.; WHEATLEY, A. D. Anaerobic/aerobic treatment of colored textile effluents using sequencing batch reactors. *Water Res.*, v. 36, p. 1993-2001, 2002.

SPAGNI, A.; CASU, S.; GRILLI, S. Decolourisation of textile wastewater in a submerged anaerobic membrane bioreactor. *Bioresource Technology*, v. 117, p. 180–185, 2012.

SULLINS, J. K.; KINGSPORT, T. Method of recovering oxidized dye from dye wash water. *United States Patent*. Nº 4.092.105, 1978.

UZAL, N.; YILMAZ, L.; YETIS, U. Microfiltration/ultrafiltration as pretreatment for reclamation of rinsing waters of indigo dyeing. *Desalination*, v. 240, p. 198-208, 2009.

VALH, J. V.; MARECHAL, A. M. L.; VAJNHANDL, S.; JERIC, T.; SIMON, E. *Treatise on Water Science:* Volume 4: Water-Quality Engineering. 1. ed. Slovenia: Elsevier, 2011. 22p.

VEDRENNE, M.; VASQUEZ-MEDRANOA, R.; PRATO-GARCIAA, D.; FRONTANA-URIBEC, B. A.; HERNANDEZ-ESPARZA, M.; ANDRÉS, J. M. A ferrous oxalate mediated photo-Fenton system: Toward an increased biodegradability of indigo dyed wastewaters. *Journal of Hazardous Materials*, v. 243, p. 292–301, 2012.

YIGIT, N. O.; UZAL, N.; KOSEOGLU, H.; HARMAN, I.; YUKSELER, H.; YETIS, U.; CIVELEKOGLU, G.; KITIS, M. Treatment of a denim producing textile industry wastewater using pilot-scale membrane bioreactor. *Desalination*, v. 240, p. 143-150, 2009.

ZHU, A; CHRISTOFIDES, P. D.; COHEN, Y. Energy consumption optimization of reverse osmosis membrane water desalinization subject to feed fluctuation. *Ind.eng. chem. Res*, v. 48, p. 9581-9589, 2009.

ZULAIKHA, S.; LAU, W J.; ISMAIL, A. F.; JAAFAR, J. Treatment of restaurant wastewater using ultrafiltration and nanofiltration membranes. *Journal of Water Process Engineering*, v. 2, p. 58-62, 2014.

4. INTEGRATION OF MICROFILTRATION AND NANOFILTRATION IN ORDER TO PROMOTE TEXTILE EFFLUENT REUSE

4.1. Introduction

Textile industries are one of the most significant manufacturing sectors that consume large amount of water in their processes. Subsequently, large amount of effluent is generated containing spent or unutilized resources used in different stages of textile process (DASGUPTA *et al.*, 2015). According to Kant (2012), the World Bank estimates that 17-20% if industrial water pollution is contributed by the textile industry. The discharged of textile effluent into the environment without an efficient treatment, it may cause severe damageThe textile effluent is characterized by high loads of chemical oxygen demand (COD), colour, inorganic salts, total dissolved solids (TDS), salinity, temperature, complex chemical, and consequently the water reuse may be a challenge.

Many treatment methods are applied to treat textile wastewater, such as, biological degradation, chemical coagulation and chemical oxidation (FRIHA *et al.*, 2015). Chemical treatment techniques, such as, adsorption, flocculation and coagulation, are efficient in colour removal, but these kind of technologies produce high amount of hazardous residues, requiring further treatment, making the technology costly (BLANCO *et al.*, 2012; BUSCIO *et al.*, 2015).

Thus, efficient and low cost treatment technologies in order to archive zero waste are required. For this, total decolourization and extended organic content removal is needed. In this context, membrane separation processes have been replacing the conventional biological processes in the treatment of industrial wastewater (FRIHA *et al.*, 2015), because it provides a realistic solution for pollution reduction in order to meet the increasingly strict discharged limits, promoting water reuse and recycling valuable components from the effluent (LIU *et al.*, 2011; ELLOUZE *et al.*, 2012; ZHENG *et al.*, 2013). Membrane separation process also offers various advantages, including: no additives, low energy intensive, high scalability, physical separation which doesn't produce hazardous by-product (MONDAL and DE, 2016).

Permeate flux can be pointed as one of the most important factors to be evaluated when membrane performance assessed. Also it directly impacts the economical feasible of membrane application in industrial scale. Permeate flux reflects the solute and solvent rate that pass through the membrane (LIU *et al.*, 2011). Reduction of permeate flux with time is

known as a major problem related to pressure-drive membrane application, since it represents a reduction in water production. Membrane fouling can be associated to deposition onto the membrane surface and sorption and pore block caused by organic and inorganic compounds, colloids, suspended solids, bacteria presented in the effluent, as well as an increase in osmotic pressure (ELLOUZE *et al*., 2012).

Since indigo blue molecule presents stable and insoluble in aqueous media, MF process may be used to recover this pigment and return it to the dyeing process. Microfiltration allows unconsumed auxiliary chemicals, dissolved organic pollutants, ions and other soluble contaminants to pass through the membrane with permeate (JUANG *et al*., 2013). Amaral *et al*. (2013) and Oliveira *et al*. (2013) evaluated the use of MF to recovery indigo blue from dyeing bath effluent. According to the authors, MF pre-treatment proves to be efficient on dye recovery (retention of 100%) and concentration (concentration factor (CF) ranging from 2.5 to 5.0), opening a possibility for dye reuse. MF permeate already has enough quality to attend certain activities in the textile industry, such as equipment and floor washing. However, it is needed a polishing step to reuse this effluent in more quality restringing steps, for instance, dye baths.

Nanofiltration is a technique that combines characteristics of ultrafiltration (UF) and reverse osmosis (RO). This unique feature allows high permeate fluxes in comparison to RO besides providing high retention of organic compound and multivalent salts (BAKER, 2004). Thus, NF membrane are found to be suitable as a polishing step to treat textile effluents generating a product with potential of reuse (BANERJEE and DE 2010; LIU *et al*., 2011; LIN *et al*, 2015). Chen *et al*. (2015) tested submerged NF membrane to treat raw and biological textile effluents. It was found that, in both cases, NF membrane is efficiently applied on the treatment of this effluent; however, better results in terms of COD, colour removal and flux decline were found when the wastewater was previously biologically treated. Gozalves-Zafrilla *et al*. (2008) assessed the application of three different NF membranes (NF90, NF 200 and NF270) to treat raw and UF treated textile effluent containing indigo blue. It was concluded that NF90 is the most suitable membrane, since it could meet the specification for water reuse in the textile effluent. Also, the application of UF as a pre-treatment is important to eliminate colloids and macromolecules responsible for most of the fouling. Ellouze *et al*. (2012), applying MF as a pre-treatment of NF processes, observed an enhancement of the

steady state flux from 14 L/h.m^2 to 34 L/h.m^2, if compared to coagulagtion/flocculation pre-treatment.

Evidently, nanofiltration shows high potential for textile effluent polishing, with high pollutants retention efficiencies. However, a thorough evaluation of textile treatment by nanofiltration in relation to all the main process characteristics was still needed. Therefore, the aim of this study was to optimize the nanofiltration process integrated to microfiltration applied to textile effluent treatment (indigo blue dye bath effluent) in relation to transmembrane pressure (TMP), pH, cross flow rate (CFR) and temperature; simultaneously evaluating the effects of each factor on the main pollutants retention and on membrane fouling potential. With these conditions optimized, a more realistic cost assessment was obtained.

4.2. Materials and methods

4.2.1. Analytical Methods

Analytical methods applied to characterization of raw effluent, MF and NF permeate and concentrate were carried out accordingly to section 3.2.2. Samples were also characterized by Fourier transform coupled total attenuated reflectance system (ATR-FTIR) using a spectrophotometer Shimadzu FTIR IRPrestige-21. The spectra were recorded in the range 4000-400 cm^{-1} with resolution of 4 cm^{-1}.

4.2.2. Effluent Source

Effluent source were accordingly to section 2.2.1.

Textile wastewater shows high variability in salinity (expressed here in terms of electrical conductivity), organic matter in terms of COD and colour due to different complex mixture of chemicals which their amount will depend on the jeans colours and fibres used in the processes (Table 18). Although it is known that the dyeing processes with indigo blue is taken in pH ranging from 10.5 to 11.5, it is possible to note that the raw effluent has neutral pH, confirming what is found on the literature (CHEN *et al*, 2015; GOZALVEZ-ZAFRILLA *et al*, 2008). It was possible to note approximately 100% of colour removal, as well a reduction on COD and conductivity, in about 65 and 26%, respectively in the MF process.

The indigo blue dye was efficiently retained by the MF membrane (100%) allowing its recovery in the concentrate stream.

Table 18: Characteristics of raw effluent and MF permeate

Parameter	Raw effluent	MF Concentrate	MF Permeate	% MF efficiency
pH	7.64±3.91	8.22±.3.91	8.68±0.29	-
EC (µS cm^{-1})	3275±1980	16375±1980	2433±979	25.71
Colour (HZ)	7129±3186	35644±3186	0	100
Indigo Blue (g L^{-1})	0.48±0.09	2.4±0.09	0	100
COD (mg L^{-1})	1771±396	6407±396	612±170	65.44
Ammonia (mg L^{-1})	10.16±9.33	24.37±9.33	6.60±9.76	
Phosphorus (mg L^{-1})	<2	<2	<2	-
Alkalinity (mg L^{-1})	530.33	430	573.33	
Calcium (mg L^{-1})	37.79±4.24	25.69±6.81	32.69±1.53	13.48
Magnesium (mg L^{-1})	<1.25	<1.25	<1.25	-
Sulphate (mg L^{-1})	178.67±2.02	223.56±0.47	259.32±84.82	6.87
Total solids (g L^{-1})	4.87±3.53	15.76±0.54	3.62±2.09	25.68
Total volatile solids (g L^{-1})	1.10±0.29	5.2±0.12	0.99±1.21	9.37

-Not identified

4.2.3. Experimental set-up and methods

Figure 19 shows the schematic of the laboratory-scale MF-NF hybrid system. The effluents were treated by MF in order to recovery the dye in the concentrated. MF was conducted on a commercial membrane module (PAM Membranas LTDA), polyetherimide-based polymer composition with average pore diameter of 0.4 µm, and a filtration area of 1 m^2. In all experiments, the pressure was measured by a manometer and was adjusted by a needle-type valve. MF was performed at concentrated mode filtration, where the permeates were collected in a separated tank and concentrates were returned to feed tank, constant pressure of 1 bar, cross flow rate of 2.4 L min^{-1} and up to a recovery rate of 80%. The permeate MF was further treated by the NF membranes. Nanofiltration was carried out with the membrane NF90 (Dow Filmtec). This membrane has a molar weight cut-off of 100 Da (ZULAIKHA *et al.*, 2014), average membrane hydraulic resistance of 5.8 x 1013 m-1, and rejection of NaCl (2,000 mg/L) and MgSO4 (2,000 mg/L) of 85-95% and 97%, respectively (DOWFILMTEC™). The NF unit had a maximum operating pressure of 15 bar, which was provided by a rotary vane pump equipped with a speed controller and maximum flow of 530

L/h. A needle-type valve was used to adjust the feed flow rate and the trans-membrane pressure. The pressure was measured by a nanometre. NF was conducted in a stainless steel membrane cell with 9 cm diameter and filtration area of 63.6 cm^2. The flat-sheet commercial membranes were properly cut to fit the membrane cell, and a feed spacer of 28 mil (25.4 μm) was placed over the membrane to promote flow distribution. The feed temperature was maintained at 20±5ºC by an immersed coil.

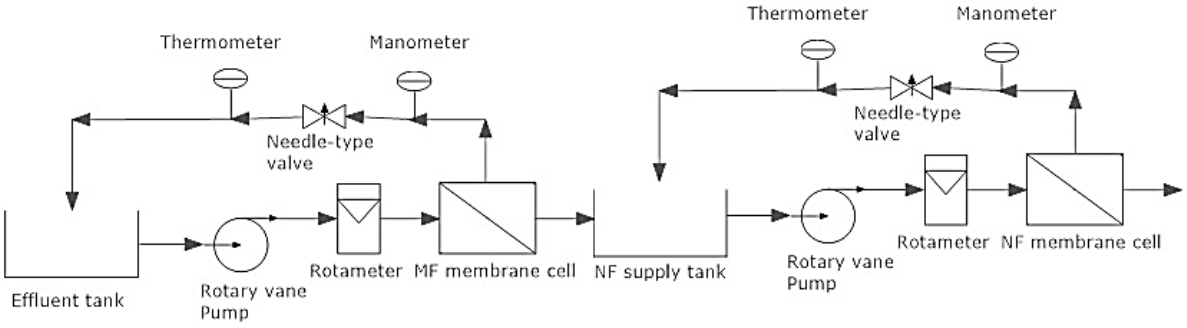

Figure 19: Schematic of the MF-NF bench scale units

4.2.4. Experimental procedure

The nanofiltration experiments were carried out with the MF permeate following the steps showed in section 3.2.4.

Recovery rate was also assessed. The procedure was similar to the tests used in order to select the best operating condition, however, the step (2) was carried out until it was obtained 60% of the initial volume of MF permeate.

4.2.5. Characterization of membrane and fouling layer

Scanning electron microscopy (SEM) and energy dispersive X-ray spectroscopy (EDX) analyses were performed using a Quanta 200 FEI system with EDX Bruker XFlach Detector 5010, with an acceleration voltage of 123 eV. The samples were prepared by coating with 5 nm gold-palladium.

4.2.6. Calculations

The volumetric permeate flux (J) in terms of litres per square meter per hour (L m^{-2} h^{-1}) was calculated using Eq. (1), as follows:

$$J = \frac{V}{A \times \Delta t}, \quad (1)$$

where A is the effective area of the membrane module for permeation and V is the volume of permeate collected over a time interval of Δt.

Flux normalization to 25 °C was accomplished by means of a correction factor related to the fluid viscosity, according to Eq. (2):

$$J = \frac{V}{A \cdot t} \cdot \frac{\mu(T)}{\mu(25°C)} \quad (2)$$

where J is the normalized permeate flux at 25 °C, $\mu(T)$ is the water viscosity at the process temperature, and $\mu(25\,°C)$ is the water temperature at 25 °C.

The membrane water permeability (K) for each test was obtained from the linearization of the ratio of normalized permeate flux of pure water (J) by applied pressure (ΔP) at 12.0, 10.0, 8.0, and 6.0 bar.

The observed rejection was calculated using Eq. (2), as follows:

$$R(\%) = \frac{C_f - C_p}{C_f} \times 100, \quad (3)$$

where C_f and C_p represent the solute content on the feed and permeate streams, respectively.

According to the simplified resistance-in-series model, the total filtration resistance could be divided into membrane resistance and fouling resistance. The membrane resistance to filtration (R_M) was determined from Eq. (4):

$$R_M = \frac{1}{K \cdot \mu(25°C)} \quad (4)$$

The total fouling resistance to filtration (R_f) was calculated based on the values of the normalized effluent permeate flux (J_{sd}) obtained near the end of each experiment (Eq. 5). This resistance includes the concentration polarization, the adsorption of components on the membrane surface and scaling.

$$R_f = \frac{\Delta P - \Delta\pi}{\mu(25°C) \cdot J_{sd}} - R_M \quad (5)$$

where ($\Delta P - \Delta\pi$) is the process effective pressure, i.e., applied pressure minus osmotic pressure. The osmotic pressure difference was calculated using the van't Hoff equation (Eq. 6):

$$\Delta\pi = \sum_{i=0}^{n} (C_r - C_p) \cdot R \cdot T \quad (6)$$

where C_r and C_p are the concentrations of solute "i" on the retentate and permeate, respectively, R is the universal gas constant, and T is the temperature in Kelvin.

The fouling resistance (R_f) is a combination of the resistance of the reversible fouling (R_{fr}) and irreversible fouling layer (R_{fir}), as follows [19]. R_{fr} is mostly due to the deposition of a cake layer on the membrane surface, which can be removed through physical cleaning, such as water washing; thus, it can be controlled by adjusting the feed flow conditions. R_{fir} is due to materials that adsorb onto the membrane surface and into the pores that can be removed by chemical cleaning.

The total flux decline (FD) was also calculated, as follows:

$$FD = \frac{(J_w - J_{sd})}{J_w}. \quad (7)$$

where J_w is the volumetric permeate flux of pure water of the membrane before effluent filtration.

Flux decline can be attributed to concentration polarization (CP) and fouling (F); thus, the flux decline due to CP was obtained using Eq. (8), as follows:

$$CP = \frac{(J_{pc} - J_{sd})}{J_{wc}}, \quad (8)$$

where J_{pc} is the volumetric water flux of the physically cleaned membrane after effluent filtration.

The flux decline due to fouling (F) was obtained using Eq. (9), as follows:

$$F = \frac{(J_w - J_{pc})}{J_w}. \quad (9)$$

The specific energy consumption (SEC) was calculated from the relation between the rate of work done by the pump (W_{pump}) and permeate flow rate (Q_p) using Eq. (10) [29], as follows:

$$SEC = \frac{W_{pump}}{Q_p}, \quad (10)$$

where

$$W_{Pump} = \Delta p \times Q_f, \quad (11)$$

where Q_f is the volumetric feed flow rate and Δp is assumed to be equivalent to the permeate pressure.

The permeate product water recovery for NF processes (Y) can be defined using Eq. (12), as follows:

$$Y = \frac{Q_p}{Q_f}. \quad (12)$$

By combining Eqs. (7), (8), and (9), the equation to determine SEC can be rewritten as follows:

$$SEC = \frac{\Delta P}{Y}. \quad (13)$$

Osmotic pressure ($\Delta\pi$) can be determined in terms of total dissolved solids by applying Eq. 26 (EPA, 2001), as follow:

$$\Delta\pi = \left[\frac{(TDS_a + TDS_c)}{2} - TDS_p\right] x 7.033.10^{-4} \quad (14)$$

Where TDS_a is the total dissolved salts in the feed stream, TDS_c is the total dissolved salts in the concentrate stream and TDS_p is the total dissolved salts in the permeate stream.

4.2.7. Statistic Evaluation

Statistical evaluation was according to section 3.2.6.

4.2.8. Preliminary Investment and Cost Estimate

A preliminary study was conducted to estimate the capital and operational expenses (CapEx and OpEx) of the optimized textile effluent treatment system. The following variables were considered: membrane unit cost, membrane replacement, acidifying agents, chemical cleaning agents, energy consumption, and system maintenance.

The capital cost of the MF-NF membrane unit was based on a price of 8,750.00 U$/m^3/h of effluent volumetric flow and was provided by a major supplier of commercial membranes in Brazil. It considered one filtration stage and a textile volumetric flow of 6.67 m³/h, which is the capacity of the designed system (Q_{des}). To estimate the capital cost per cubic meter of effluent, the capital cost was annualized by means of the amortization factor, as presented in Eq. 27 (SETHI; WIESNER, 2000).

$$A/P = \frac{i_c \cdot (1 + i_c)^{DL}}{(1 + i_c)^{DL} - 1} \quad (27)$$

where (A/P) is the amortization factor, i_c is the investment rate (in 2015 was equal to 10% in Brazil), and DL is the design life of the plant. The MF-NF system design life was considered to be 15 years. The capital cost per cubic meter was obtained from Eq. 28:

$$C_{cap/m^3} = \frac{C_{cap} \cdot A/P}{Q_{des}} \quad (28)$$

where C_{cap/m^3} is the capital cost per cubic meter of effluent, C_{cap} is the system capital cost, and Q_{des} is the capacity of the designed system.

Membrane replacement costs considered an average membrane lifespan of 5 years. To determine the cost for membrane replacement, the required membrane area for MF and NF was determined. The recovery rate was set at 90% and 40% for microfiltration and nanofiltration respectively. An average permeate flux of 13,23 L/h.m² was considered for NF, which was the lowest permeate flux obtained in the recovery rate experiment (40% RR). NF and MF membranes costs were 50.00 and 80.00 US$ per square meter, respectively. A large commercial membrane supplier provided these prices.

The energy cost estimate comprised the MF power requirement and the NF feed pump requirement. A once-through operation process was considered. The MF and NF power requirement was estimated from Eq. 16, 17, 18 and 19.

The energy tariff paid by this textile company in Brazil is 0.04 US$/kWh (considering an exchange rate of US$1 = R$0.25). The costs of chemicals for membrane cleaning and maintenance costs were estimated at 2 and 5% per year of the initial investment cost respectively (SHEN *et al*., 2014).

4.3. Results and discussion

4.3.1. Effect of TMP on flux and permeate characteristics

It is noted an increase in permeate flux with increasing TMP (from 8 bar to 15 bar), due to an increase of the driving force across the membrane (ELLOUZE *et al*., 2012; TANG and CHEN, 2002), which enhances the mass transfer coefficient (Table 5.2); changes on TMP leads to a small flux decline difference, ranging from 30 to 35% for TMP ranging from 8 to 15 bar.

The flux decline may be mainly associated with fouling and concentration polarization phenomena. The flux decline during operation at 8-12 bar occurred mainly due to

concentration polarization while during operation at 15 bar the flux decline can be associated to fouling. The increase in applied TMP leads to an increase in the initial flux values based on Darcy's law. However, the driving force enhanced at higher pressures, both solvent and solutes are more convected towards the membrane surface inducing more pollutants accumulate on it, leading to augmented concentration polarization and fouling and sharp flux decline (MUKHERJEE *et al.*, 2016). These mechanisms generally adds additional resistances to the permeation, both external (cake layer) and internal (adsorption and pore blocking) (CHEN *et al.*, 2015). The flux decay and increased flux resistance are related to salt precipitation/deposition on the membrane surface. This precipitation/deposition may happen when the critical limit of supersaturation is exceeded due to effluent concentration (RICCI *et al.*, 2016).

The membrane fouling resistance (R_f) increase with increasing the TMP, corroborating the flux decline results (Table 19). Furthermore, increasing pressure leads to increased irreversible resistance, suggesting that at high TMP the adsorption and pore blocking of materials onto the membrane surface and pores provides more contribution to the fouling resistance than the cake layer.

In addition, Hermia's model was used to explain the fouling mechanism. Table 20 summarizes k, J_0 and R^2 values under all the TMP applied. The higher values of R^2 correspond to a better fit of the model. It is observed that R^2 values at 8 and 10 bar (Table 20), the best fitting values has obtained for the cake mechanism. As TMP is increased, the pore blocking plays a major role to describe the fouling phenomenon. At TMP of 12 bar the best fitting values has obtained for the complete blocking filtration and standard blocking, and at TMP of 15 bar the complete blocking filtration plays a major role to describe the fouling phenomenon.

Also, by calculating the hydraulic membrane resistance after membrane chemical cleaning (R_{cc}), given by Eq. (21), it is possible to note that the chemical cleaning was efficient to all studied cases. Specific energy consumption (SEC) relates the permeate flux by area of membrane to the required energy. This factor is directly associated to operational costs. This analysis was also carried out to each test in order to achieve the energy-optimal process operation. It is observed a decrease in SEC with a decrease on TMP (Table 19).

Table 19: Water and Permeate flux, flux decline and hydraulic resistance (R_m, R_f, R_{fr}, R_{fir}, R_{cc}) and specific energy consumption when applying NF, under 20ºC, natural pH, flow rate of 2.4 $L.min^{-1}$ and different TMPs

TMP (bar)	Jw ($L/m^2.h$)	Jsd_0 [a] ($L/m^2.h$)	Jsd_f [b] ($L/m^2.h$)	Jw_{fc} [c] ($L/m^2.h$)	Jw_{cc} [d] ($L/m^2.h$)	Flux decline type			Hydraulic Resistance ($x10^{13} m^{-1}$)					SEC ($kWh\ m^{-3} m^{-2}$)	Cleaning efficiency (%)
						Total (%)	Fouling (%)	CP [e] (%)	R_m	R_f	R_{fr}	R_{fir}	R_{cc}		
15	62.03	54.13	40.39	47.56	62.60	35	23	12	8.87	4.48	0.95	3.52	0.00	14237	102.67
12	50.63	41.69	33.36	44.76	51.87	34	12	22	8.51	4.34	1.82	2.60	0.00	14186	107.17
10	42.44	35.29	29.11	38.64	47.16	31	9	22	8.47	3.88	1.35	2.52	0.00	13741	135.37
8	36.97	31.02	25.78	32.31	39.33	30	13	18	7.62	3.53	1.17	2.36	0.91	12414	121.11

[a] initial effluent permeate flux; [b] final effluent permeate flux; [c] water permeate flux after physical cleaning; [d] water permeate flux after chemical cleaning; [e] concentration polarization

Table 20: Hermia's model for the TMP test (k, J_0 and R^2 values)

Pressure (bar)	Model											
	Complete blocking filtration			Standard blocking filtration			Intermediate blocking filtration			Cake filtration		
	J_o ($L\ m^{-2}h^{-1}$)	k (m)	R^2	J_o ($L\ m^{-2}h^{-1}$)	k (m)	R^2	J_o ($L\ m^{-2}h^{-1}$)	k (m)	R^2	J_o ($L\ m^{-2}h^{-1}$)	k (m)	R^2
15	56.8	2.5×10^{-3}	0.97	57.2	1.8×10^{-4}	0.96	57.5	5.2×10^{-5}	0.94	58.5	2.2×10^{-6}	0.92
12	42.5	1.9×10^{-3}	0.98	42.6	1.6×10^{-4}	0.98	42.7	5.2×10^{-5}	0.97	43.0	2.8×10^{-6}	0.96
10	35.9	2.4×10^{-3}	0.95	35.8	2.1×10^{-4}	0.96	35.9	7.7×10^{-5}	0.97	36.2	4.9×10^{-6}	0.98
8	31.2	2.0×10^{-3}	0.94	31.3	1.9×10^{-4}	0.94	31.4	7.1×10^{-5}	0.94	31.5	5.1×10^{-6}	0.95

In general, NF rejection capacity decreases with increasing TMP (MONDAL and DE, 2016). In this study, it is also observed the decrease in COD rejection with increasing TMP values (Figure 20). According to Kruskal Wallis' statistical test, there is statistical difference in COD rejection, and applying multiple comparisons among groups it is noted difference between the tests at 12 and 15 bar and 8 and 10 bar for a p-value =0.05. However, it is observed statistical difference when compared both groups (12 and 15 bar and 8 and 10 bar). These results can be associated to different fouling mechanism observed. The cake filtration mechanism observed in the filtration at 8 and 10 bar maybe prevent the passage of organic solutes through the membrane. In relation to EC rejection, according to Kruskal Wallis' statistical test, there is statistical difference in EC rejection, and applying multiple comparisons among groups it is observed difference between 15 and 10 and 8 bar for a p-value =0.05. This result reinforces the hypothesis of occurrence of salts precipitation in NF at high TMP. However it is important to note that, even on the worst case scenario, i.e., under the TMP of 15 bar, the permeate quality satisfies the most exigent use in the textile industry (Figure 20).

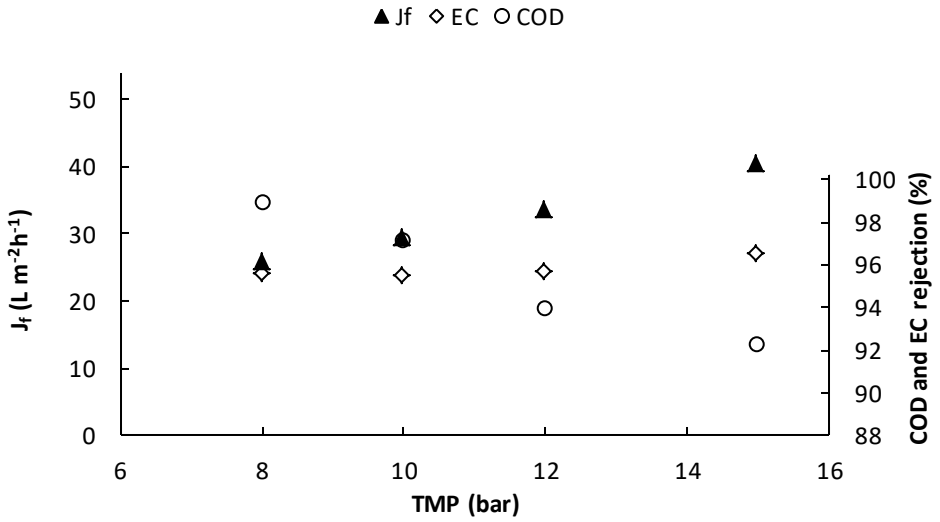

Figure 20: Permeate Flux, COD and EC rejection as a function of TMP values at 20ºC, natural pH, flow rate of 2.4 L.min^{-1}, feed COD 617 mg L^{-1} of and feed EC 1755 of µS cm^{-1}

Thus, considering flux decline, energy consumption, permeate production, permeate characteristics, and operational conditions, it was select the TMP of 12 bar.

4.3.2. Effect of pH on flux and permeate characteristics

pH is a very important factor to be assessed when the permeate flux of the NF membrane in salt mixtures is concerned, since attraction of molecule to the membrane surface may enhance the flux decline (KOYUNCU and TOPACIK, 2003). It is known that flux decline may be attributed to a combination of two factors: (1) molecular size that can be modified by the solution pH and (2) sorption phenomenon that can be enhanced electrostatic attraction, or even electrostatic repulsion of the molecules on the membrane surface (KOYUNCU and TOPACIK, 2003; BOUSSU *et al.*, 2006). Also, pH can influence the extend of some compounds' hydrophobicity in the feed solution, which may cause repulsion or attraction of molecules on the membrane surface (CHIDAMBARAM *et al.*, 2015).

It is observed higher flux decline at pH 9 and 11 (approximately 34% and 35%, respectively) (Table 21). The lowest flux values and COD and salinity rejection in terms of EC (90% and 95% respectively) were obtained at alkaline conditions (pH 11) (Figure 21). Under high pH (7-11), the membrane generally possess negative charge, and in alkaline conditions, interactions between the negative charged membrane and the positive molecule are very string, enhancing adsorption of compounds on the membrane and leading to pore blocking of the membrane. At pH7 and 8, it was noted that most flux decline was associated to CP, also being the highest CP (26%). Increasing the pH of the feed, both the contribution of the CP as the fouling in reducing the flux increases.

The pH may also change the size of the molecule, which may favour its passage through the membrane which negatively affects NF fouling (LIN *et al.*, 2013). Also, it has been reported on the literature that molecular weight cut-off of the membrane NF90 was practically constant in acidic and neutral conditions. Conversely, at extremely alkaline conditions (pH 11), the zeta potential of pores walls is highly negative, and the electrostatic repulsion may cause pore enlargement (DALWANI *et al.*, 2011). This would explain the results found in this study. According to Kruskal Wallis' statistical test there is statistical difference between the tests, and applying multiple comparisons among groups it is noted difference of NF rejection when operated with feed at pH 7 and 8 for COD and at 7, 8 and 9 for EC rejection (Figure 21), while the NF COD and EC rejection at pH 11 is statistical different from the NF COD and EC rejection at pH 7 and 8 for a p-value = 0.05.

Table 21: Water and Permeate flux, flux decline and hydraulic resistance (R_m, R_f, R_{fr}, R_{fir}, R_{cc}) when applying NF, under 20ºC, 12 bar, flow rate of 2.4 $L.min^{-1}$ and different pHs

pH	Jw ($L/m^2.h$)	Jsd_0 [a] ($L/m^2.h$)	Jsd_f [b] ($L/m^2.h$)	Jw_{fc} [c] ($L/m^2.h$)	Jw_{cc} [d] ($L/m^2.h$)	Flux decline type			Hydraulic Resistance ($x10^{13} m^{-1}$)					SEC	Cleaning efficiency (%)
						Total	Fouling	CP [e]	R_m	R_f	R_{fr}	R_{fir}	R_{cc}	(kWh $m^{-3} m^{-2}$)	
7	47.79	37.59	35.12	48.47	46.53	27	1	26	9.33	3.26	3.70	0.00	0.00	13334	90.12
8	46.53	35.43	32.22	44.24	45.89	31	5	26	9.11	4.28	3.64	0.64	0.00	13369	104.51
9	45.89	33.53	31.30	42.20	41.92	34	11	23	8.95	5.25	3.96	1.28	1.02	13369	76.00
11	41.92	31.27	27.87	39.77	42.89	35	11	24	9.97	5.14	3.84	1.30	0.00	15543	98.32

[a] initial effluent permeate flux; [b] final effluent permeate flux; [c] water permeate flux after physical cleaning; [d] water permeate flux after chemical cleaning; [e] concentration polarization

By calculating the hydraulic membrane resistance (Table 21), it is observed that the membrane fouling resistance (R_f) increase with increasing the feed pH, corroborating the flux decline results (Table 21). Furthermore, increasing pH leads to increased irreversible resistance, confirming the attraction interaction between the membrane surface and feed molecules.

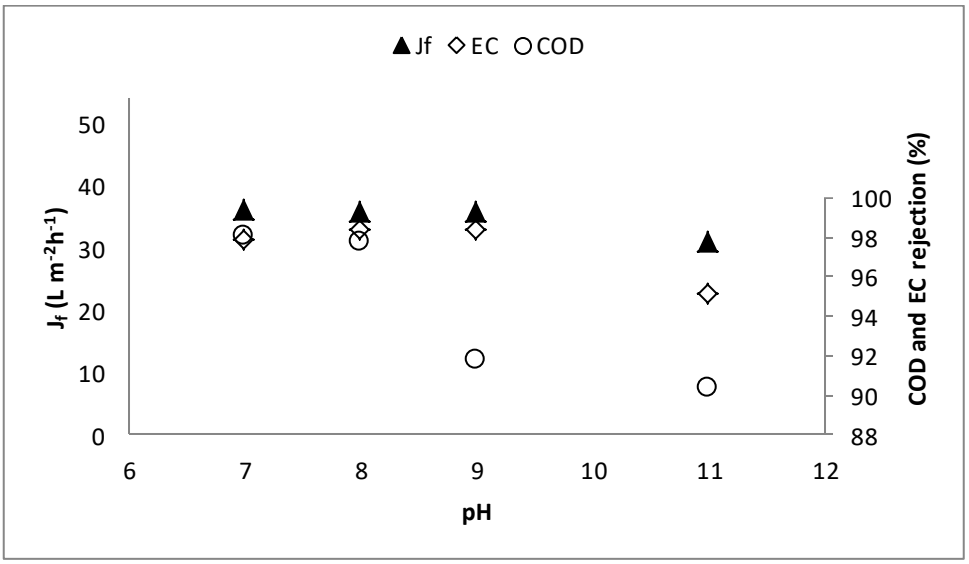

Figure 21: Permeate Flux, COD and EC rejection as a function of feed pH values at 20ºC, TMP of 12 bar and flow rate of 2.4 L.min^{-1} feed COD 439 mg L^{-1} of and feed EC 1989 of µS cm^{-1}

4.3.3. Effect of crossflow rate on flux and permeate characteristics

By increasing the feed flow rate, the cross-flow velocity grows and, consequently, the Reynolds number increases. This leads to a more turbulent flow and improves the mass transfer conditions, facilitating the back diffusion of solutes retained by the membrane to the bulk solution and reducing the concentration polarization phenomena. Consequently, the increase in permeate flux is attributed to two reasons: reduction of the membrane fouling and reduction of osmotic pressure on the membrane surface, which decreases the effective filtration pressure.

It was assessed four cross flow velocities of 0.21, 0.42, 0.63 and 0.84 cm.s^{-1} that correspond to Reynolds number of 280, 559, 839 and 1118, respectively. For rectangular channels, the transition between laminar and turbulent flow occurs at a Reynolds number between 150 and 300 in the presence of spacers. Then in this study it was evaluated one condition in laminar flow and three conditions in turbulent flow (GERALDES *et al.*, 2002).

Confirming what is found in the literature, permeate flux increases with cross flow velocity (Table 22) (LIU *et al*., 2011; ELLOUZE *et al*., 2012 and MONDAL and DE, 2016). The flux decline during operation at crossflow velocities of 0.21, 0.42, 0.63 and 0.84 $cm.s^{-1}$ occurred mainly due to concentration polarization. At higher cross-flow velocities, concentration polarization decreases, which reduce membrane fouling. There is a decrease of total flux decline with an increase in cross-flow velocities, however, when it is raised from 0.63 to 0.84 $cm\ s^{-1}$, this decline is much more subtle, showing that the cross flow velocity, above 0.63 $cm\ s^{-1}$ will not affect the permeate flux. Irreversible hydraulic fouling resistance is lower as the cross flow velocities increases, indicating that lower cross flow velocities may compromise the membrane life span (Table 22).

Apparently, it can be observed the increase in COD rejection with increasing crossflow velocity values (Figure 22). However, according to Kruskal Wallis' statistical test, there is no statistical difference between NF COD rejection at different crossflow velocity conditions for a p-value=0.05. When analysed the salinity rejection in terms of EC the test with 0.21 and 0.42 $cm\ s^{-1}$, showed a decrease in salinity rejection, being statistically different from the others for a p-value=0.05.

Table 22: Water and Permeate flux, flux decline and hydraulic resistance (R_m, R_f, R_{fr}, R_{fir}, R_{cc}) when applying NF, respectively, under 20ºC, 12 bar, pH 8 and different cross-flow rates

Cross Flow velocities (cm/s)	Jw ($L/m^2.h$)	Jsd_0[a] ($L/m^2.h$)	Jsd_f[b] ($L/m^2.h$)	Jw_{fc}[c] ($L/m^2.h$)	Jw_{cc}[d] ($L/m^2.h$)	Flux decline type			Hydraulic Resistance ($x10^{13} m^{-1}$)					SEC ($kWh\ m^{-3} m^{-2}$)	Cleaning efficiency (%)
						Total	Fouling	CP[e]	R_m	R_f	R_{fr}	R_{fir}	R_{cc}		
0.21	40.45	36.36	33.54	38.23	41.27	17	5	12	9.07	3.94	2.49	1.45	0.91	12421.98	111.79
0.42	41.27	40.64	36.88	39.34	41.36	11	5	6	9.98	2.30	0.78	1.51	0.27	12714	102.20
0.63	41.36	40.92	37.75	39.43	41.44	9	2	6	10.25	1.17	0.49	0.69	0.22	13016.72	102.24
0.84	41.44	40.75	38.64	40.70	41.92	7	2	5	10.47	1.08	0.41	0.68	0.55	14309.61	116.91

[a]initial effluent permeate flux; [b]final effluent permeate flux; [c]water permeate flux after physical cleaning; [d]water permeate flux after chemical cleaning; [e]concentration polarization

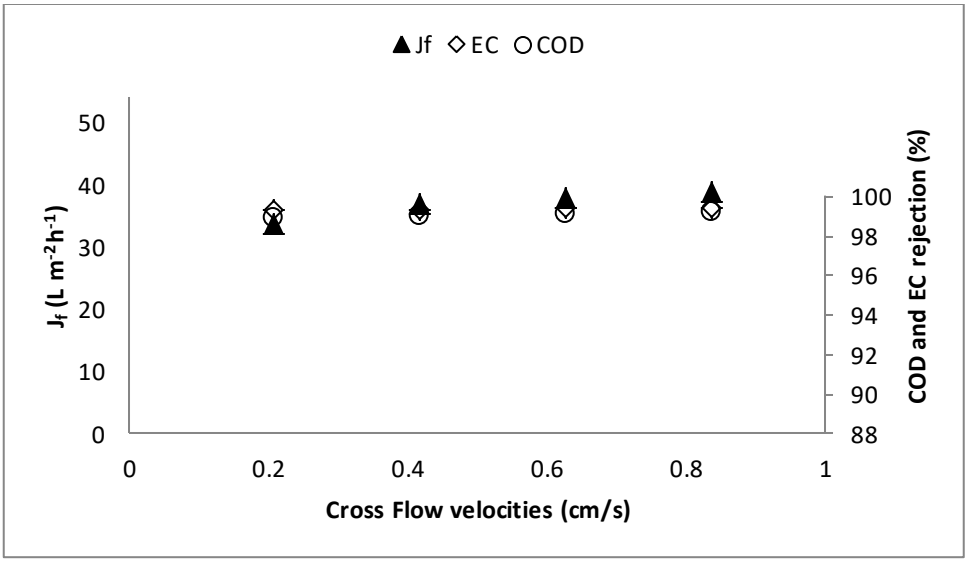

Figure 22: Permeate Flux and COD and EC rejection as a function of cross flow velocities values at 20ºC, pH 8 and TMP of 12 bar feed COD 1534 mg L^{-1} of and feed EC 12600 of µS cm^{-1}

Cross flow velocities are directly associated to flux and therefor, energy consumption, since there is an increase on flux with an increase on Reynolds number, it is observed a decrease on specific energy consumption (Table 22). Thus, it is considered more economical operate under higher cross flow velocities, however, higher cross flow velocities tend to heat up the solution much faster, which can affect the permeate quality if not properly cooled. Thus, 0.63 was selected to be the best cross-flow velocity.

4.3.4. Effect of temperature on flux and permeate characteristics

It is noted that permeate flux increases from 21 to 28 L/h.m^2 when the temperature increases from 27.5 ºC to 37.5ºC (Table 23). This behaviour may be explained by the decrease in the viscosity of the feed solution, which implies to the enhancement of the mass transfer coefficient (ELLOUZE *et al.*, 2012). Increasing temperature reduces the flux decline. Once again the flux decline occurred mainly due to concentration polarization. It can also be observed that the CP values decrease with the temperature increasing. The CP decrease can be associated to the improvement of the mass transfer near de membrane surface and the ions transport through the membrane. With temperature rising, it is expected to occur a dilatation in pore size facilitating ions transport through the membrane and reducing its concentration in the membrane pores and surfaces (SHARMA and CHELLAM, 2006). The reduction on COD and EC rejection with temperature rising also confirms an enhancement on mass transfer

coefficient and a dilatation of membrane pores (Figure 23). According to Kruskal Wallis' statistical test, there is statistical difference between NF COD and EC rejection at different temperature conditions for a p-value =0.05, however even the worst case, i.e., under the temperature of 37.5 ºC, NF90 is still able to attend the manufactory quality requirement. The R_{fr} values higher than R_{fir}, suggest that cake layer provides more contribution to the fouling resistance than the adsorption and pore blocking of materials onto the membrane surface and in the pores.

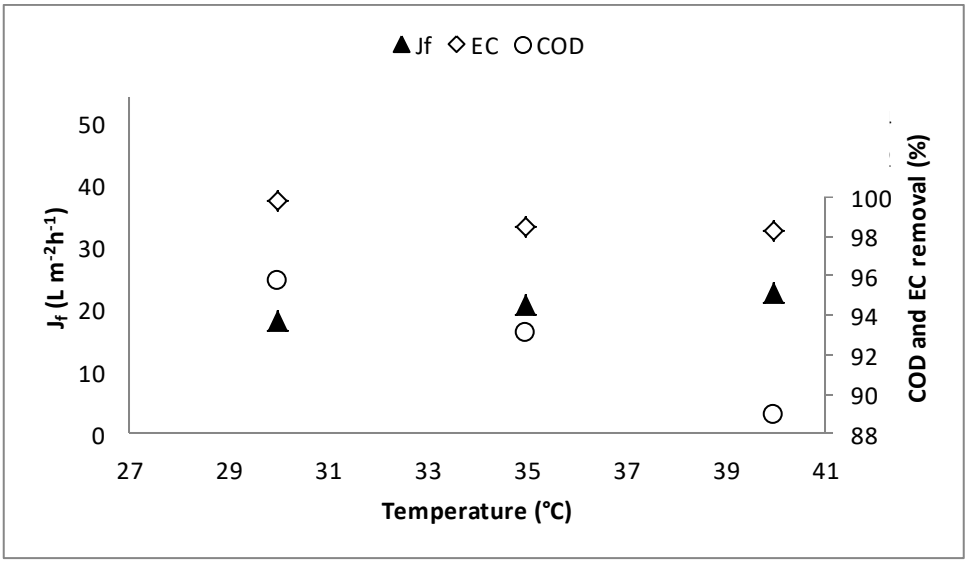

Figure 23: Permeate Flux and COD and EC rejection as a function of temperature values at 20ºC, pH 8, TMP of 12 bar and flow rate of 2.4 L.min^{-1} feed COD 1426 mg L^{-1} of and feed EC 11875 of µS cm^{-1}

Table 23: Water and Permeate flux, flux decline and hydraulic resistance (R_m, R_f, R_{fr}, R_{fir}, R_{cc}) when applying NF, under 20ºC, 12 bar, pH8, flow rate of 2.4 $L.min^{-1}$ and different temperature

Temperature (°C)	Jw ($L/m^2.h$)	Jsd_0 [a] ($L/m^2.h$)	Jsd_f [b] ($L/m^2.h$)	Jw_{fc} [c] ($L/m^2.h$)	Jw_{cc} [d] ($L/m^2.h$)	Flux decline type			Hydraulic Resistance ($x10^{13} m^{-1}$)					SEC ($kWh\ m^{-3} m^{-2}$)	Cleaning Efficiency (%)
						Total	Fouling	CP [e]	R_m	R_f	R_{fr}	R_{fir}	R_{cc}		
27.5	59.01	21.47	18.03	50.01	60.75	69	15	54	6.11	17.81	16.05	1.76	0.96	26623.23	104.24
32.5	60.75	24.54	20.71	51.31	60.36	66	16	50	7.07	13.08	12.09	0.98	0.95	22429.73	99.04
37.5	60.36	28.51	22.51	51.47	60.23	63	15	48	8.03	11.14	9.86	1.28	0.30	21327.58	99.65

[a] *initial effluent permeate flux;* [b] *final effluent permeate flux;* [c] *water permeate flux after physical cleaning;* [d] *water permeate flux after chemical cleaning;* [e] *concentration polarization*

4.3.5. Effect of dye concentration on flux and permeate characteristics

In an dyeing process is very usual to observe effluent load variations since the dyeing concentrate depend of denim type. The use of MF as a pre-treatment mitigates these fluctuations before NF process, but it is important to verify the effect of load variations on the NF performance. As expected, the higher the indigo concentration in the NF feed solution, lower is the permeate flux (51 to 34 L/h.m^2, when used 5% and 20% of raw effluent concentration, respectively) and higher is the flux decline (57 and 68%, respectively) (Table 24). The flux decline can be associated to concentration polarization phenomena and fouling. And when the indigo concentration increase, the flux decline becomes more influenced by the fouling (42%). Both fouling resistance, R_{fr} and R_{fir} increase with indigo blue concentration increasing. In this case, flux decline can occur by a combination molecular size and adsorption of molecules on the membrane surface. Furthermore, the NF COD and EC rejection increase as the dye concentration increases (Figure 24). Although cake formation enhances flux decline, it improves permeate quality due to reduction in pores size as well as electrostatic reactions on the cake layer (CHEN *et al.*, 2015).

The NF COD and EC rejection increase as the dye concentration increases (Figure 24). Although cake formation enhances flux decline, it improves permeate quality due to reduction in pores size as well as electrostatic reactions on the cake layer (CHEN *et al.*, 2015). The CP coefficient and mass transfer coefficient (K_i) was calculated using eq. 15. CP (0.805 g.s/m^4) was much lower than the one obtained by Chidambaram *et al.* (2015), maybe because of the favourable condition of mass transfer since the K_i value was higher 14.97 (10^{-5} m/s).

Table 24: Water and Permeate flux, flux decline and hydraulic resistance (R_m, R_f, R_{fr}, R_{fir}, R_{cc}) when applying NF, under 20ºC, 12 bar, pH8, flow rate of 2.4 $L.min^{-1}$ and different dye concentration

Indigo concentration (%)	Jw ($L/m^2.h$)	Jsd_0[a] ($L/m^2.h$)	Jsd_f[b] ($L/m^2.h$)	Jw_{fc}[c] ($L/m^2.h$)	Jw_{cc}[d] ($L/m^2.h$)	Flux decline type			Hydraulic Resistance ($x10^{13} m^{-1}$)					SEC ($kWh\ m^{-3} m^{-2}$)	Cleaning Efficiency (%)
						Total	Fouling	CP[e]	R_m	R_f	R_{fr}	R_{fir}	R_{cc}		
5	119.04	92.79	50.92	84.14	118.72	57	29	28	3.54	4.93	3.34	1.59	0.05	9425.90	99.52
10	118.72	84.69	46.71	82.61	113.18	61	30	30	3.59	6.02	4.39	1.63	0.31	10695.45	92.30
15	113.18	79.22	41.27	77.97	107.99	64	31	32	3.90	6.55	4.92	1.63	0.00	11631.96	92.79
20	107.99	73.32	34.98	65.32	109.75	68	40	28	3.90	8.73	6.02	2.70	0.00	14052.02	102.41

[a]initial effluent permeate flux; [b]final effluent permeate flux; [c]water permeate flux after physical cleaning; [d]water permeate flux after chemical cleaning; [e]concentration polarization

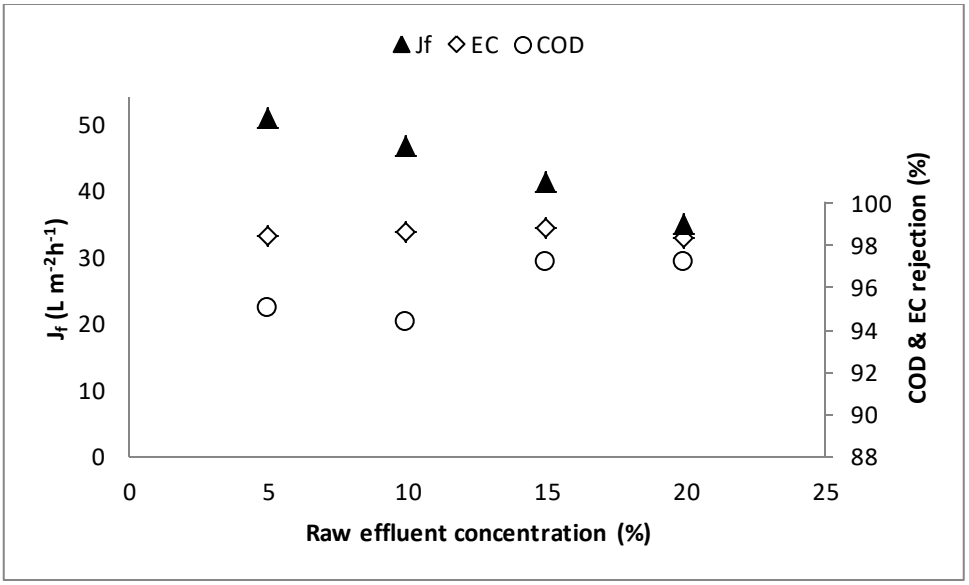

Figure 24: Permeate Flux and COD and EC rejection as a function of raw effluent concentration values at 20ºC, pH 8, TMP of 12 bar and flow rate of 2.4 L.min^{-1} feed COD 467 mg L^{-1} of and feed EC 2040 of µS cm^{-1}

4.4. Recovery rate of the water

The recovery rate is mostly restricted by membrane scaling and osmotic pressure increase. Figure 25 shows the permeate flux and osmotic pressure differential ($\Delta\pi$). The process effective pressure ($\Delta P_{effective}$) continuously decreased because of the increase in ionic concentration of the feed solution, which, consequently, increased the osmotic pressure (π_f) of the feed solution and the osmotic pressure differential ($\Delta\pi$). It is clear from figure 24 that permeate flux decay followed the effective pressure decay. This shows there was no severe membrane fouling. The initial normalized permeate flux was 29.87 L/m^2.h and reaching 1.97 L/m^2.h at the end of the experiment (RR = 60%). An increasing trend can be observed in the permeation of pollutants with the increase in the RR. Moreover, the permeate quality obtained up to 60% RR was enough to meet the quality required in many processes in textile industry. The continuous decline in the quality of the permeate is also clear from the increase in permeate EC and COD with recovery rate. A second sharp decline in EC and COD rejection efficiency was observed from the RR of 40%. In conclusion, the maximum water recovery rate obtained for a single NF step in the treatment of microfiltered textile effluent is 40%. Above this RR, the permeate flux decay would be sharper and permeate quality would decline.

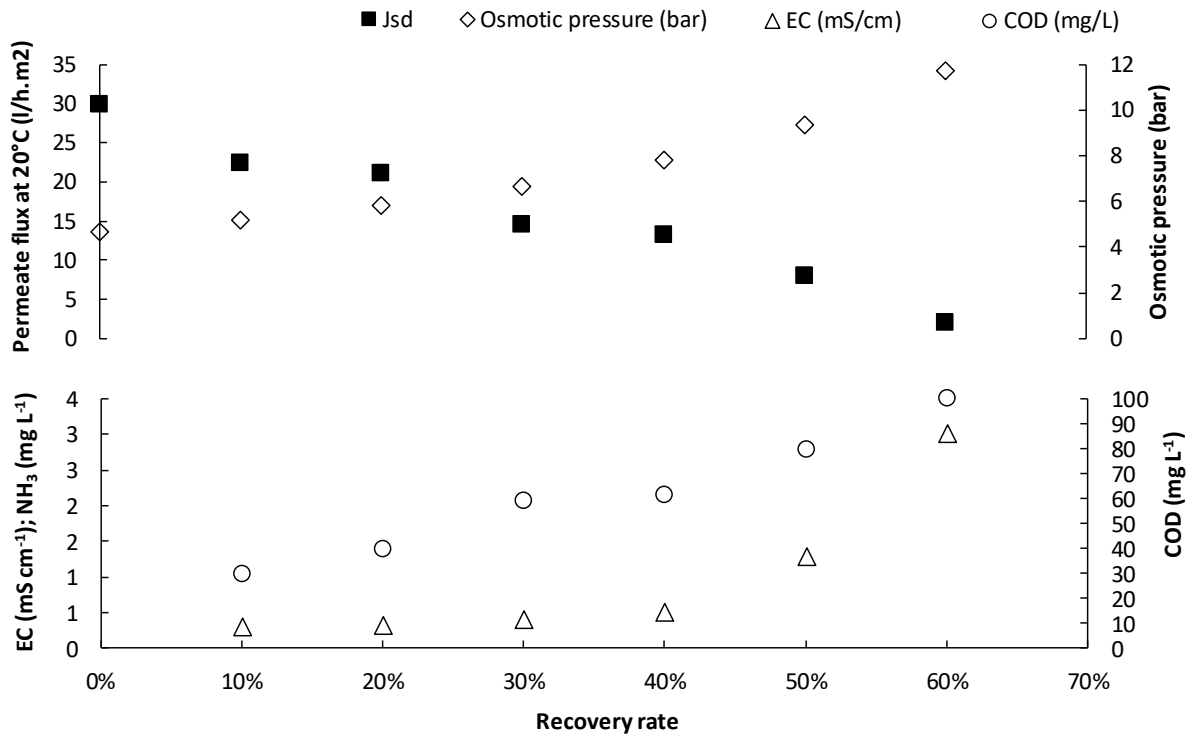

Figure 25: Permeate Flux and COD, EC, colour and ammonia permeate concentration as a function of recovery rate at 20ºC, pH 8, TMP of 12 bar and flow rate of 2.4 L.min^{-1}

The SEM image of NF membrane, after subjecting to membrane treatment of microfiltered textile effluent do not show any surface structural features comparing to the virgin membrane (Figure 26). It can also be observed solids deposits on the surface of the membrane after the effluent permeation due to salts precipitation. As can be seen on the Energy Dispersive Spectra (EDS) in Figure 27, this precipitate was predominantly composed of calcium and sodium sulphate.

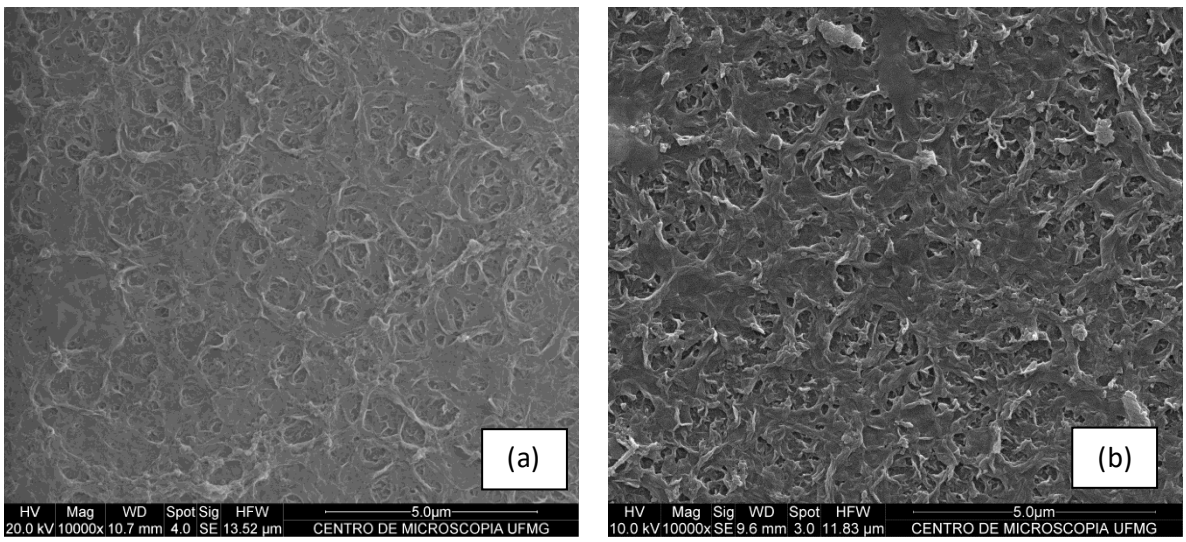

Figure 26: SEM observed surface of a virgin NF membrane (a), fouled membrane (b)

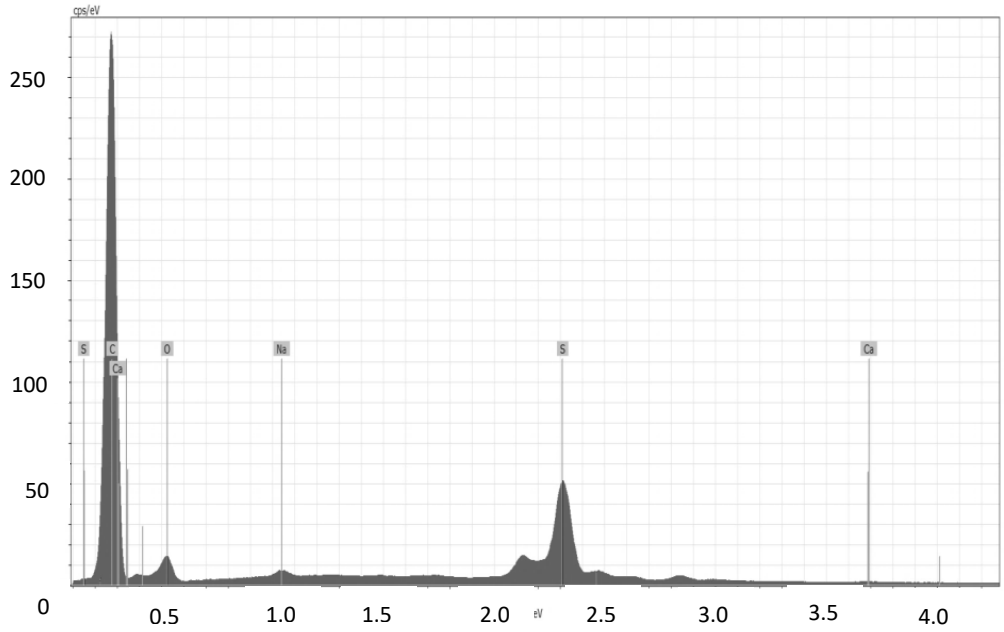

Figure 27: EDX from the surface of a fouled membrane

4.4.1. Water Reuse in the Textile Industry

In the textile industry, the water quality for all processes must be sufficiently pure to avoid any problems with the process and quality of the final product. Although fresh softened water is used for all processes, water of lower quality can occasionally be used. The water quality requirements depend on the process. It is evident that the NF permeate meets the quality requirements for all processes within the textile industry. Moreover, the NF concentrate has characteristics that meet the required water-quality standards for washing down equipment, screen washing for the print works, and general washing of print paste containers and floors (Table 25).

ATR-FTIR analysis was conducted for raw effluent, MF permeate and NF permeate. The spectrum of dry raw effluent sample where it can observe absorptions at 3290.5601 cm^{-1} (ν N-H) characteristic stretch of aromatic amine, 2976.1631 cm^{-1} (ν C-H), 1546.9104 cm^{-1} (ν C=O), 1404.1780 cm^{-1} (ν C=C) stretch aromatic ring, 1068.5641 cm^{-1} (δ C-H), 837.1061 cm^{-1} (δ C-H) angular deformation of the aromatic ring (Figure 27). The absorption values obtained for each of the functional groups are in, or near, the absorption band described in the literature for indigo blue dye (PASCHOAL *et al.*, 2005). By overlapping the bands of raw

effluent, MF and NF permeate the differences in intensity and width of the same band is due to interferents. It is possible to verify the efficiency of the microfiltration process to concentrate indigo blue in its insoluble form, since it is not observed all bands correspondent to indigo blue in the MF permeate. It can also be observed the NF process efficiency in the rejection of the remain contaminants.

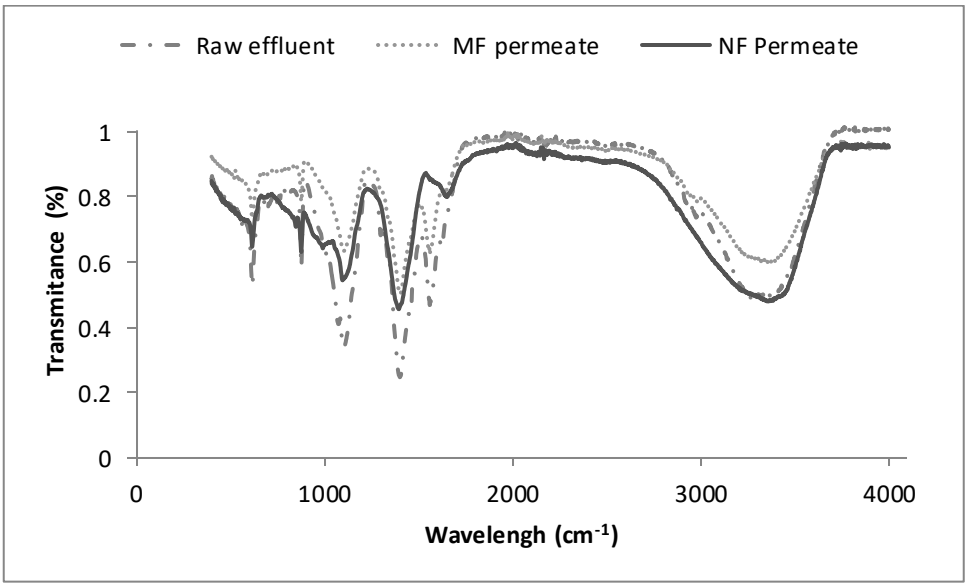

Figure 28: ATR-FTIR of the raw effluent, MF and NF permeate

Table 25: Permeate and concentrate physicochemical characteristics

Parameters	MF permeate	NF concentrate	NF permeate	Recycled Effluent[a]	Washing-off[a]	Equipment Washdown[a]
Colour (Hazen)	nv[b]	0.25	nv[b]	nv[b]	nv[b]	nv[b]
EC (µs cm^{-1})	9320 ±979	22348±220.43	380±88.17	-	-	-
COD (mg L^{-1} O_2)	2105.67±170	5146.27±38.31	47.22±1.94	20–50	200	500–2000
pH	9.39±0.29	8.64	8	6.5–7.5	7.0–8.0	6.5–8.0
Total hardness (mg L^{-1})	32.69±1.53	89.45±24.86	<2.50	90	100	100
Alkalinity (mg L^{-1})	573.33	1354.50	31.53	-	-	-
Chloride (mg L^{-1})	422.08±24.67	762.50±14.71	8.34±0.03	500	500–200	3000–4000
Sulfate (mg L^{-1})	259.32±84.82	1761.30±112.66	[c]nd	-	-	-
Fe (mg L^{-1})	0.16	0.4	[c]nd	0.1	0.1	0.1
Cu (mg L^{-1})	762	1905	[c]nd	0.005	0.05	0.05
Cr (mg L^{-1})	[d]nm	[d]nm	[d]nm	0.01	0.1	0.1
Mn (mg L^{-1})	1.58±0.03	22.81±0.45	<1.25	-	-	-

[a]VALH et al. 2011, [b]None visble, [c]not detected, [d]not measured

4.4.2. Preliminary Investment and Cost Estimate

The total capital cost (CapEx) of the NF system was estimated at 58,362.50 US dollars and the total operational cost (OpEx), at 0.31 US dollars per cubic meter of effluent (Table 26). These values are similar to those indicated in the literature. Gorenflo *et al*. (2002) reported that for the nanofiltration (NF200B – Filmtec/Dow) of 7,300,000 m^3/year of pretreated groundwater, with high hardness and NOM content, the CapEx and OpEx were 6,897,000€ and 0.23€/m^3, respectively. And Costa and De Pinho (2006) obtained for the nanofiltration (NF200B-400 – Filmtec/Dow) of 100,000 m^3/day of surface water for drinking water production a CapEx and OpEx of 17,610,716 € and 0.214€/m^3, respectively. In this cost estimate was not considered the cost of MF and NF concentrate treatment or disposal. The MF concentrate can be reused in the dye process. NF concentrate has characteristics that meet the required water-quality standards for washing down equipment, screen washing for the print works, and general washing of print paste containers and floors.

Table 26: Cost estimation of the MF-NF treatment system for textile effluent

	Description	**Values**	**Units**
System Characteristics	Annual System Capacity	57,629	m^3/year
	Average Permeate Flux	0.054	$m^3/h.m^2$
	Average Permeate Flux	0.013	$m^3/h.m^2$
	Required MF Membrane Area	118	m^2
	Required NF Membrane Area	191	m^2
	Design Plant Life	15	Years
	Membrane Lifespan	5	Years
	Brazil Investment Rate	10	%
	Energy Price	0.04	US$/kWh
CapEx	MF-NF Systems	58,362.50	US$
OpEx	MF-NF Membrane Replacement	0.07	US$/$m^3$
	Capital Cost Amortization	0.13	US$/$m^3$
	Cleaning Agent	0.02	US$/$m^3$
	MF-NF Energy Requirement	0.03	US$/$m^3$
	Maintenance	0.05	US$/$m^3$
	Total	0.31	US$/$m^3$

3.4. Conclusion

NF technology is found to be a successful applied on the textile effluent as a polishing step to MF process. The NF membrane at TMP of 12 bar and crossflow velocity of 0.63 cm s^{-1} was selected as the most promising for textile effluent treatment because it had the lowest fouling tendency, the highest permeate flux and high COD and EC retention. Although high temperature and pH reduces the NF rejection even the worst case evaluated (37.5 ºC and pH 11), NF90 is still able to attend the manufactory quality requirement.

The principal cause of flux decline observed in the study was attributed to concentration polarization.

The maximum water recovery rate obtained for a single NF step in the treatment of microfiltered textile effluent is 40%. Above this RR, the permeate flux decay would be sharper and permeate quality would decline.

The total capital cost (CapEx) of the NF treatment system was estimated at US$ 58,362.50, and the total operational cost (OpEx) was 0.31 US$/$m^3$ of effluent.

3.5. References

AMARAL, M. C. S.; NETA, L.F; Lima, M.S.; Barreto, N.C.; CARVALHO, R.B. evaluation of operational parameters from a microfiltration system for indigo blue dye recovery from textile dye effluent. *Desalination and Water Treatment* (Print), v. 52, p. 257-266, 2013.

APHA. *Standard Methods for the Examination of Water and Wastewater*. 21 ed. Washington: American Public Health Association, 2005.

BAKER, R.W. *Membrane technology and applications*, 2. Ed. John Wiley & Sons Ltd, England, 2004.

BANERJEE, P.; DE S. Coupled concentration polarization and pore flow modeling of nanofiltration of an industrial textile effluent. *Separation and Purification Technology*, v. 73, p. 355–362, 2010.

BI, F., ZHAO, H., ZHANG, L., YE, Q., CHEN, H. AND GAO, C. Discussion on calculation of maximum water recovery in nanofiltration system. *Desalination*, v. 332, p. 142-146, 2014.

BLANCO, J.; TORRADES, F.; MORÓN, M.; BROUTA-AGNÉSA, M.; GARCÍA-MONTAÑO, J. Photo-Fenton and sequencing batch reactor coupled to photo-Fenton

processes for textile wastewater reclamation: feasibility of reuse in dyeing processes. *Chem. Eng,* v. 240, p. 469-475, 2014.

BOUSSU, K.; BELPAIRE, A.; VOLODIN, A.; VAN HAESENDONCK, C.; VAN DER MEEREN, P.; VANDECASTEELE, C.; VAN DER BRUGGEN, C. Influence of membrane and colloid characteristics on fouling of nanofiltration membranes. Journal of Membrane Science, v. 289, p. 220–230, 2007.

BUSCIO, V.; MARÍN, M. J.; CRESPI, M.; GUTIÉRREZ-BOUZÁN, C.. Reuse of textile wastewater after homogenization–decantation treatment coupled to PVDF ultrafiltration membranes. *Chemical Engineering Journal*, v. 265,p. 122–128, 2015.

CHAKRABORTY, J. N. *Fundamentals and practices in colouration of textiles*. 1. ed. India: Woodhead Publishing, 2009. 400p.

CHEN, V.; YANGA, Y.; ZHOUA, M.;LIUA, M.; YUA,S.; GAOL, G. Comparative study on the treatment of raw and biological treated textile effluents through submerged nanofiltration. *Journal of Environmental Management*, v. 284, p. 121-129, 2015.

CHIDAMBARAM, T.; OREN, Y.; NOEL, M. Fouling of nanofiltration membranes by dyes during brine recovery from textile dye bath wastewater. *Chemical Engineering Journal*, v. 262, p. 156–168, 2015.

COSTA, A.R.; DE PINHO, M.N. Performance and cost estimation of nanofiltration for surface water treatment in drinking water production. *Desalination*, v. 196, p. 55-65, 2006.

DALWANI, M.; BENES, N. E.; BARGEMAN, G.; STAMATIALIS, D.; WESSLING, M. Effect of pH on the performance of polyamide/polyacrylonitrile based thin film composite membranes. *Journal of Membrane Science*, v. 372, p. 228-238, 2011.

DASGUPTA, J.; SIKDER, J.; CHAKRABORTY, S.; CURCIO, S.; DRIOLI, E. Remediation of textile effluents by membrane based treatment techniques: A state of the art review. *Journal of Environmental Management*, v. 147, p. 55-72, 2015.

DE, S.; BHATTACHARYA, P. K. Prediction of mass-transfer coefficient with suction in the applications of reverse osmosis and ultrafiltration. *Journal of Membrane Science*, v. 128, p. 119-131, 1997.

ELLOUZE, E.; TAHRI, N.; AMAR, R. B. Enhancement of textile wastewater treatment process using Nanofiltration. *Desalination*, v. 286, p. 16–23, 2012.

ERNST, M.; BISMARCK, A.; SPRINGER, J.; JEKEL, M. Zeta-potential and rejection rates of a polyethersulfone nanofiltration membrane in single salt solutions. *Journal of Membrane Science*, v. 165, p. 251-259, 2000.

Evironmental Protection Agency (EPA). *Guidelines for Water Reuse*. 1. Ed. Washington: U.S. Agency for International Development, 2004. 450p.

Evironmental Protection Agency (EPA). *Environmental technology report: Removal of arsenic in drinking water*. 1. Ed. Washington: U.S. Agency for International Development, 2001. 380p.

FRIHA, I.; BRADAI, M.; JOHNSON, D.; HILAL, N.; LOUKIL, S.; AMOR, F. B.; FEKI, F.; HAN, J.; ISODA, H.; SAYADI, S. Treatment of textile wastewater by submerged membrane bioreactor: *In vitro* bioassays for the assessment of stress response elicited by raw and reclaimed wastewater. *Journal of Environmental Management*, v. 160, p. 184-192, 2015.

GERALDES, V.; SEMIAO, V.; PINHO, M. N. Flow management in nanofiltration spiral wound modules with ladder-type spacers. *Journal of Membrane Science*, v. 203, p. 87– 102, 2002.

GORENFLO, A.; VELAZQUEZ-PADRON, D.; FRIMMEL, F.H. Nanofiltration of a German groundwater of high hardness and NOM content: performance and costs, *Desalination,* v. 151, p. 253-265, 2002.

GOZÁLVEZ-ZAFRILLA, J. M.; SANZ-ESCRIBANO, D.; LORA-GARCÍA, J.; LEÓN HIDALGO; M. C. Nanofiltration of secondary effluent for wastewater reuse in the textile industry. *Desalination*, v. 222, p. 272–279, 2008.

JAMALUDDIN, A.T.M.; FAROOQUE, A.M.; AL-RASHEED, R. A novel approach for prediction of osmotic pressure for plant design and performance normalization of seawater reverse osmosis (SWRO). In: 4th Annual Workshop on Water Conservation in the Kingdom, 2001, KFUPM.

JUANG, Y.; NURHAYATI, E.; HUANG, C.; PAN, J.R.; HUAN, S. A hybrid electrochemical advanced oxidation/microfiltration system using BDD/Ti anode for acid yellow 36 dye wastewater treatment. *Separation and Purification Technology*, v. 120, p. 289–295, 2013.

LIN, J.; TANG, C. Y.; YE, W. Y.; SUN, S.; HAMDAN, S. H.; VOLODIN, A.; HAESENDONCK, C. V.; SOTTO, A.; LUIS, P.; BRUGGEN, B. V. Unraveling flux behavior of superhydrophilic loose nanofiltration membranes during textile wastewater treatment. *Journal of Membrane Science*, v. 493, p. 690–702, 2015.

LIU, M.; LÜ, Z.; CHEN, Z.; YU, S.; GAO, C. Comparison of reverse osmosis and nanofiltration membranes in the treatment of biologically treated textile effluent for water reuse. *Desalination*, v. 281, p. 372–378, 2011.

KANT, R. Textile dyeing industry an environmental hazard. *Nat. sci.*, v. 4, p. 22-26, 2012.

KOYUNCU, I.; TOPACIK, D. Effects of operating conditions on the salt rejection of nanofiltration membranes in reactive dye/salt mixtures. *Separation and Purification Technology*, v. 33, p. 283-294, 2003.

MANU, B. Physico-chemical treatment of indigo dye wate-water. *Color. Technol.*, v. 123, p. 197-202, 2007.

MONDAL, M.; DE, S. Treatment of textile plant effluent by hollow fiber nanofiltration membrane and multi-component steady state modelling. *Chemical Engineering Journal*, v.285, p. 304-3018, 2016

MUKHERJEE, R.; MONDAL, M.; SINHA, A.; SARKAR, S.; DE, S. Application of nanofiltration membrane for treatment of chloride rich steel plant effluent. *Journal of Environmental Chemical Engineering*, v. 4, n. 1, p. 1-9, 2016.

PASCHOAL, F. M. M.; TREMILIOSI-FILHO, G. Aplicação da tecnologia de eletrofloculação na recuperação do corante índigo blue a partir de efluentes industriais. *Quími. Nova*, v. 28, p. 766-772, 2005.

OLIVEIRA, I.B.; ANDRADE, L. H.; NETA, L.F.; AMARAL, M. C. S. Textile wastewater treatment by microfiltration aiming at indigo blue dye recovery. In: 7th IWA Specialised Membrane Technology Conference and Exhibition for Water and Wastewater Treatment and Reuse, 2013, Toronto.

RICCI, B.C.; AGUIAR, A.O.; ANDRADE, L.H.; PIRES, W,L.; MIRANDA, G.A.; AMARAL, M.C.S. Gold acid mine drainage treatment by membrane separation processes: An evaluation of the main operational conditions. *Separation and Purification Technology*, v. 170, p. 360-369, 2016.

ROBINSON, T.; MCMULLAN, G.; MARCHANT, R.; NIGAM, P. Remediation of dyes in textile effluent: a critical review on current treatment technologies with a proposed alternative. *Bioresource Technology*, v. 77, p. 247-255, 2001.

SANROMAN, M. A.; PAZOS, M.; RICART, M. T.; CAMESELLE, C. Decolorization of textile indigo dye by DC electric current. *Eng. Geol.*, v. 77, p. 253-261, 2005.

SETHI, S.; WIESNER, M.R. Cost modeling and estimation of crossflow membrane filtration processes. *Environmental engineering science*, v. 17, p. 61-79, 2000.

SHARMA, R.R.; CHELLAM, S. Solute rejection by porous thin film composite nanofiltration membranes at high feed water recoveries. *Journal of Colloid and Interface Science*, v. 328, p. 353-366, 2008.

SHAW, C. B.; CARLIELL, C. M.; WHEATLEY, A. D. Anaerobic/aerobic treatment of colored textile effluents using sequencing batch reactors. *Water Res.*, v. 36, p. 1993-2001, 2002.

SHEN, J.; HUANG, J.; RUAN, H.; WANG, J.; VAN DER BRUGGEN, B. Techno-economic analysis of resource recovery of glyphosate liquor by membrane technology. *Desalination*, v. 342, p. 118-125, 2014.

SULLINS, J. K.; KINGSPORT, T. Method of recovering oxidized dye from dye wash water. *United States Patent*. Nº 4.092.105, 1978.

TANG, C.; CHEN,V. Nanofiltration of textile wastewater for water reuse. *Desalination*, v. 143, p. 11-20, 2002.

VALH, J. V.; MARECHAL, A. M. L.; VAJNHANDL, S.; JERIC, T.; SIMON, E. *Treatise on Water Science:* Volume 4: Water-Quality Engineering. 1. ed. Slovenia: Elsevier, 2011. 22p.

VEDRENNE, M.; VASQUEZ-MEDRANOA, R.; PRATO-GARCIAA, D.; FRONTANA-URIBEC, B. A.; HERNANDEZ-ESPARZA, M.; ANDRÉS, J. M. A ferrous oxalate mediated photo-Fenton system: Toward an increased biodegradability of indigo dyed wastewaters. *Journal of Hazardous Materials*, v. 243, p. 292–301, 2012.

ZHENG, Y.; YU, S.; SHUAI, S.; ZHOU, Q.; CHENG, Q.; LIU, M; GA, C. Color removal and COD reduction of biologically treated textile effluent through submerged filtration using hollow fiber nanofiltration membrane. *Desalination*, v. 314, p. 89–95, 2013.

ZULAIKHA, S.; LAU, W J.; ISMAIL, A. F.; JAAFAR, J. Treatment of restaurant wastewater using ultrafiltration and nanofiltration membranes. *Journal of Water Process Engineering*, v. 2, p. 58-62, 2014.

ZHU, A; CHRISTOFIDES, P. D.; COHEN, Y. Energy consumption optimization of reverse osmosis membrane water desalinization subject to feed fluctuation. *Ind.eng. chem. Res*, v. 48, p. 9581-9589, 2009.

5. FINAL CONSIDERATIONS

Microfiltration (MF) showed to be completely efficient in separating and concentrating indigo blue. The best operation condition in terms of applied pressure and pH, provided almost 60% and 99.5% of COD and colour removal, respectively. Also, the flux decline was mostly attributed to concentration polarization and the chemical cleaning was efficient enough to recover initial hydraulic resistance.

Raw textile effluent is not biodegradable due to dye chemical complexity, however MF permeate is much more biodegradable since the molecules weight are much smaller, being readily assimilated by the microorganisms.

Treatment of textile effluent with a combination of MF and MBR processes is sufficient to meet the reuse criteria for some industry activities, such as floor cleaning; however, further polishing is required to achieve the quality needed for other steps in the dyeing process.

MBR process provides a stable process, showing great efficiency in removing organic load in the MF permeate in about 77%, muffling such impacts, maintaining its permeate COD concentration and COD removal efficiency mostly constant throughout the time. Also, showing good efficiency in ammonia removal.

BRM treatment served to remove all the molecular weight fractions efficiently specially compounds with higher molecular weight (greater than 1 kDa) confirming the biodegradability of MF permeate, also, this is probably due to less membrane fouling, which leaves the pores free for the passage of these substances.

The principal cause of flux decline in the NF process in both treatment routs was determined to be concentration polarization; however, in most cases, chemical cleaning of the membrane was sufficient to regain the initial permeability, which demonstrates that the both assessed pre-treatments are effective.

For both cases, the optimal TMP was determined to be 12 bar, at which good permeate characteristics were obtained with reasonable energy consumption; this is associated with a higher permeate flux. Feed pH values ranging from 7 to 11 were investigated and generated permeate with good characteristics; however, higher pH values of the NF feed resulted in

increased membrane fouling. Higher cross-flow velocities led to decreased membrane fouling and higher membrane retention; however, they require increased energy. Accordingly, a cross-flow velocity of 0.63 cm s^{-1} was determined to be the threshold cross-flow velocity. High temperature and pH reduces the NF rejection even the worst case evaluated (37.5 ºC and pH 11), NF90 is still able to attend the manufactory quality requirement.

For the MF-NF treatment rout COD and EC permeate content and final flux ranged about 47.22±1.94 mg/L, 380±88.17µs/cm and 37.75 L/m^2h respectively. Whereas MF-MBR-NF treatment rout showed COD and EC permeate content and final flux about 34.35±5.38 mg/L, 30.90±4.24 µs/cm and 23.37 L/m^2h.

Thus, both treatment routs are considered to have good performances. NF technology was successfully applied to polish textile effluent after filtration through MF and MBR processes. Even in the worst case scenarios, NF permeate meets the quality requirements for all processes within the textile industry, while the NF concentrate can be used to wash equipment, screens in the printworks, print paste containers, and floors.

The maximum water recovery rate obtained for a single MF-NF step in the treatment of microfiltered textile effluent is 40%. Above this RR, the permeate flux decay would be sharper and permeate quality would decline.

The total capital cost (CapEx) of the MF-NF treatment system was estimated at US$ 58,362.50, and the total operational cost (OpEx) was 0.31 US$/$m^3$ of effluent.

Considering area requirements, energy and equipment consumption, as well as system complexity, the MF-NF rout was chosen to be applied to the treatment of textile industries. The NF concentrate has the potential to be applied in coarse activities, such as floor washing, however, in case of critical situation of organic overload, it is possible to apply other treatments such as advanced oxidation processes, or even activate sludge, since it has proven that MF permeate is biodegradable.

However since many textile industries already have activated sludge as the main treatment technology in the industry plant, there is a possibility of BRM using. Also, this treatment rout, although it requires more area, energy and it is more complex, this system appears to be more stable, prevent organic overload, reassuring the possibility of NF concentrate reuse.